MODELING AND SIMULATION OF LIQUID-LIQUID EXTRACTION COLUMN

A Thesis Submitted in Partial
Fulfilment of the Requirements
for the Degree of
Master of Technology

by

RAJEEV KUMAR

Department of Chemical Engineering
Indian Institute of Technology, Kanpur

April 1996

CERTIFICATE

It is certified that the work contained in the thesis titled **Modeling and Simulation of Liquid-Liquid Extraction Column**, by *RAJEEV KUMAR*, has been carried out under my supervision and that this work has not been submitted elsewhere for a degree.

Ashok Khanna

Dr. Ashok Khanna
Associate Professor
Department of Chemical Engg.
IIT Kanpur [INDIA]

April, 1996

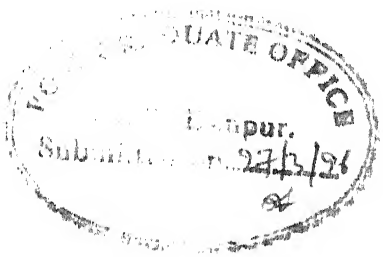

Acknowledgements

I express my deep gratitude to my thesis supervisor **Dr. Ashok Khanna** for his valuable suggestions, critical discussions and incessant encouragement throughout this work.

I am very much indebted to the faculty and staff for providing a creative academic environment at I.I.T.Kanpur to carry out my M.Tech thesis work effectively. Computational facilities available at ITTK and especially maintained in our lab will ever remain in my memory as a positive facets of my educational experience. I gratefully acknowledge the contribution of all these factors in my work.

Friends have always been a source of encouragement for me. I take this opportunity to thank all my friends and in particular Ritwik Bhatia who shared some unforgettable moments of my life during our M.Tech tenure. I also extend my thankfulness to other friends — Desh Raj, Akshay Kant, Alok, B.C.Rao, Abhijit, Gandhi, Saurav, Bansi, Surendra Verma and others for giving their *time, love and affection* in making my stay at IITK thrilling and full of joy.

Lastly I would like to thank Dr. S.J.Chopra, Mr Jain, Mr. Sheoraj Singh, Mr. Vohra and Mr. Deepak Sarkar of *R & D Centre, Engineers India Limited, Gurgaon* providing me an opportunity to visit EIL for discussions and shared pilot plant data for testing the simulator. I am also thankful to *AICTE* for providing partial financial support.

RAJEEV KUMAR

Contents

Abstract

A non-equilibrium stage model has been developed for the steady state and dynamic simulation of a countercurrent multicomponent liquid-liquid extraction column. Dispersed phase behavior described by means of drop population model, allows to split the drop spectrum into different drop classes interacting with bulk continuous phase. Mass balances are then written for each drop class and bulk continuous phase in a stage. Rigorous transport relations using interactive mass transfer coefficients have been used to explain interphase mass transfer in extraction column. This model to incorporates effects such as reverse and osmotic diffusion which remain unaccounted for by simple transport relations. Drop breakage and coalescence have been considered with mass transfer in this study; generation term Π_{ijk} accounts for these in mass balance equations.

Newton-Raphson (N-R) method has been used to solve the set of non-linear equations for steady state. DASSL (Differential Algebraic System SoLver) with N-R method has been implemented to solve differential-algebraic equations (DAE) for dynamic simulation. DASSL has various advantages over other methods such as Runge-Kutte and Gear's method apart from being simple and easy to understand. Computer program (simulation package) of about 12,000 lines of "C" code divided into 19 files has also been developed as a part of this thesis. Model developed in this thesis is general and applicable to all types of multicomponent counter-current extraction column. In this work the model has been tested for unagitated sieve tray column. Two extraction system, Aromatic extraction by Sulfolane and Acetone extraction by Toluene have been taken for this study. Voluminous results generated by the simulator have been thus analyzed this covers study of concentration profile, dynamic holdup, flow and velocity profiles under various feed conditions and perturbations.

List of Figures

List of Tables

Nomenclature

a	interfacial area, m^2
$A(v)$	probability density of the droplet size.
c	mixture molar density, $moles/m^3$
$\overline{c^d_{jk}[v']}$	molar density of drop class having drops of volume v', $moles/m^3$
d	drop diameter, m
d_n	sieve tray perforation diameter, m
d_{vs}	Sauter mean diameter, m
$\mathbf{D}$	axial dispersion coefficient, m^2/s
$\mathcal{D}$	Maxwell binary diffusion coefficient, m^2/s
$\mathcal{D}^\circ$	infinite dilution diffusivity, m^2/s
F	sidestream feed flow, $moles/s$
Δh	effective mass transfer height of real stage, m
$h(v_i, v_j),\ h(d_i, d_j)$	collision frequency, m^3/s
$\overline{J^*}$	diffusive flux, $moles/m^2 - s$
k	binary mass transfer coefficient, $moles/m^2 - s$
$K^\bullet$	distribution coefficient.
M	molecular weight.
$n(v)$	number of drops in drop class corresponding to drop diameter v.
N	interphase mass transfer rate, $moles/s$
N_0	number of drops in column feed.
NC	number of components.
ND	number of drop classes.
NS	number of stages.
p	number fraction of each drop class in column feed.
P	volume fraction of each drop class in a stage.
P_{j0}	volume fraction of drop class j in feed.
Re	Reynolds number.
S	column cross section area, m^2

Sh	Sherwood number.
Sc	Schmidt number.
T	temperature, K
u	velocity, m/s
u_r^*	characterstic velocity of drop. m/s
$\overline{u^2}$	mean velocity of drop in a stage, m/s
U_{in}	column feed (continuous phase), $moles/s$
U_n	jet velocity, m/s
v	volume of drop, m^3
$\overline{v_0}$	mean drop volume. m^3
V (without subscript)	effective volume for mass transfer in each stage, m^3
V_{in}	column feed (dispersed phase) , $moles/s$
V_{j0}	molar flow of drop class j in column feed. $moles/s$
Δv	discrete space for drop volume, m^3
x	mole fraction of dispersed phase.
$x_{ijk}(v')$	mole fraction of component i in drop class corresponding to v'.
y	mole fraction of continuous phase.

Greek letters

$\beta(v_i, v_j)$, $\beta(d_i, d_j)$	probality density of drops v_i produced by breakage of drops v_j.
γ	interfacial tension, N/m
ϵ	energy dissipation, m^2/s^3
$\lambda(v_i, v_j)$	coalescence efficiency of collision.
μ	viscosity, $kg/m-s$
ν	type of drop breakage (binary,tertiary,...)
Π	generation term due to drop breakage and coalescence, $moles/s$
ρ	density, kg/m^3
ρ_m	mixture molar density. $moles/m^3$
$\Delta\rho$	density difference, kg/m^3
σ	standard deviation.
ϕ	dynamic holdup.
ϕ_0	dyanmic holdup for feed as initial guess.

Subscripts

av	average
c	continuous phase
d	dispersed phase
i, m	component (specie)
in	inlet
j	drop class
k	stage
max	maximum
min	minimum
t	total

Superscripts

c	continuous phase
d	dispersed phase
DB	drop breakage
DC	drop coalescence
f	feed
I	interface
r	relative
$+, -$	material gained or lost respectively in phase.

Chapter 1

Introduction

1.1 General

Chemical process industries, often need to separate the components of homogeneous liquid mixture. Out of several approaches, liquid-liquid extraction (LLX) commonly known as solvent extraction, is a technique for separating liquid components of a solution by distribution between two liquid phases. With the recent emphasis on energy conservation in process industries, extraction today is a choice preferred over distillation especially for separation of dilute liquid mixture in which distillation requires enormous amount of energy. Mixtures of heat sensitive components can be separated at low temperature using suitable solvent by LLX.

Solvent used in the extraction process should be immiscible or partially miscible with one of the component of mixture in order to facilitate the separation of liquid phase. Liquid-liquid extraction is now being adopted as a more economic alternative to other separation processes and has found immense application in the separation of :

- Solution of components having low relative volatility, especially when vacuum distillation is expensive.
- Solution of close boiling point and azeotrope forming components.
- Separation of solute from mixture when evaporation is impractical.
- Solutes of heat sensitive components such as antibiotics.

Over a period of time organic, inorganic and nuclear industries developed interest in LLX operation. Various processes such as *aromatic extraction, acetic acid extraction from water, Uranium and other hydrometallurgical extraction* developed commercially

have been in operation for a long time. In order to understand these processes thoroughly and generalize results from one process to another, theoretical research is necessary. Modeling of separation processes has now become an integral part of chemical process development and scale up process. With the help of theoretical models, process behavior could be visualized a priori and important decisions can be arrived at before erecting actual equipment at site. This not only saves money but provides better insight of the process also. Even though much of the work with which chemical engineers are involved, concerns the steady state behavior of process (which are quite useful in equipment design decisions) the unsteady state characteristics of a process are also important in a certain class of problems such as :

Startup problem in which it is desired to predict the rate at which a process proceeds to steady state with given initial state.

Control problem in which information is desired on the open loop response of the controlled variables in process due to uncontrolled disturbances in certain input stream. With the advent of fast computing machines, these models can be tailored for on line process simulation and control (such as feed forward control). Prior study could be carried out on process simulator to design control system for the process plant which is yet to be erected.

Training simulator Training of operators for process, without having recourse to real equipments, could be facilitated by a simulation model, which imitates the real process.

Present thesis is devoted to the development of both steady-state and dynamic simulation model for multicomponent countercurrent liquid-liquid extraction process.

1.2 Literature review

Modeling of extraction process

One of the simplest way to model any chemical separation process such as extraction, distillation, absorption for a staged process is to assume equilibrium state at each stage. Such an approach is rather impractical, especially in extraction process where extraction efficiency may be as low as 20-25%, Laddha [1]. Hence an alternate, rate based approach is proposed to model the mass transfer behavior of an extraction process. Several attempts have been made in this direction such as by Ricker [2], Spencer [3] and others. Apart from non-equilibrium, staged processes also experience the phenomena of *backmixing or axial dispersion.* Baird [4], Ricker [2], Spencer [3] have dealt with this phenomena by assuming some fraction of main flow as the backmixing flow. Recent success of rigorous models based on coupled fluxes in distillation (Krishnamurthy [5, 6]), encourages the use of such models for extraction process modeling. Zimmermann's [7] proposed model for extraction allows rigorous calculation

of mass transfer coefficients incorporating interaction effect. Zimmermann extended the non-equilibrium approach with drop population balance and rigorous mass transfer coefficient calculation. Earlier work by Khani [8] using the population balance approach has been formulated as set of partial differential equations. However mass transfer aspects were not discussed in detail.

Modeling of drop breakage and coalescence

Extraction involves two distinct phases – Continuous and Dispersed. Dispersed phase is described by the droplets formed in the process. During the past three decades a need has been felt to incorporate drop population approach. Review article by Ramakrishna [9] described the status of population balance vis a vis other aspects of modeling of liquid dispersion. In the direction of liquid-liquid dispersion one of the pioneering work was by Coulaloglou and Tavlarides [10]. Tavlarides proposed a phenomenological model to describe drop breakage and coalescence in a turbulently agitated liquid-liquid dispersion.In last 3 decades several workers have extended this approach to modeling of extraction process. Sovová [11] worked out the same model for batch stirred extraction process and discretized it based on the real stages. Sovová [12] used the same discrete model and applied drop population approach for a vibrating plate extractor Hsia and Tavlarides [13] used a similar approach for stirred tank. Hsia and Tavlarides [14] described drop breakage, coalescence and micromixing in stirred tank.Rubio [15] discusses about the various possible theoretical drop spectrum distribution in a Wirz extraction column and fits them to a real extraction operation. Recent work by Tsouris and Tavlarides [16, 17, 18] further discusses in great deal about the model development for drop breakage and coalescence based on earlier work of Coulaloglou [10].The model has been analyzed for drop breakage and coalescence behavior and control of dynamic holdup along the multistage extraction column.

Mass transfer and axial dispersion

Above works on drop population behavior, incorporate only drop population model and say very little about mass transfer effect on extraction process. Zimmermann [7] synthesized both drop population and non-equilibrium approach and proposed a detailed mathematical model for extraction column at steady state. The approach relies a *Polydispersed phase* model of Jiřičný [19] according to which dispersed phase having a drop spectrum is assumed as several separate phases (plugs of dispersed phase – each plug contains drops of same volume), interacting with continuous bulk phase. Backmixing is assumed in form of axial dispersion between adjacent stages, which is represented by axial dispersion coefficients $\mathbf{D^c}, \mathbf{D^d}$. Rigorous transport relations as used by Krishnamurthy [5, 6] for distillation and absorption are used for extraction process also. These transport relations have been independently solved by linearizing relationships Stewart and Prober [20], utlizing the film theory of Taylor [21] and Smith [22]. In this thesis these relations are the part of a simulation model thus solved simultaneously with other equations.

Equilibrium relations

Every extraction model uses equilibrium relations in form of $y_i = K_i x_i$, where distribution ratio K_i is one of the tedious factors in modeling of extraction column. For organic systems especially used in refinery and petrochemical complexes, UNIFAC method is one of the most relied and easy to use method available in literature. The method based on group contribution has been proposed by Fredenslund and Prausnitz [23] for non-ideal liquid mixtures. Pioneering work by Magnussen [24], reports UNIFAC LLE parameters for 32 main groups and 57 sub-groups in the temperature range of $10 - 40°C$. LLE data for specific systems has been reported in *DECHEMA*, Chemistry Data Series part I,II,III [25].

A modified UNIFAC group contribution model Larsen [26] also allows to incorporate temperature effect, but published data on this model is scarce. Several other papers published on specific systems such as LLE phase equilibrium for dearomatization of ATF(Aviation turbine fuel) fraction by Mehrotra, Garg and Chopra [27]. Mukhopadhyay [28] published UNIFAC parameters for aromatic extraction system for high temperature also. Hooper [29] published UNIFAC data in the temperature range of $20 - 250°C$ for some water organic liquid system.

Empirical correlations

Several correlations used for extraction columns such as characteristics velocity and binary mass transfer coefficient have been refered to from the design book by Laddha [1] and handbooks by Baird [4] and Rousseau [30].

Solution of algebraic and differential-algebraic equations system

For steady state simulation Block-tridiagonal equations sets are solved by Newton-Raphson (N-R) method and Block-thomas algorithm. However for dynamic simulation a set of Differential-Algebraic Equation (DAE) is formed. Review paper by Gani [31] and Gani [32, 33] applied the solution for DAE system. Several DAE system solver are proposed by authors such as by Gear's [34, 35] and variety of Runge-Kutta methods which are popular for solving DAE. In recent years DAE solver DASSL *(Differential Algebraic System SoLver)* proposed by Petzold [36] has been found to be very robust and easy to use. This method is very suitable for semi-implicit DAE (Brenan [37]) such as formed for staged separation process. DASSL is based on backward difference formula (BDF) which changes its order and step size of integration as per the need. The details are described in Brenan [37].

Chapter 2

Non-Equilibrium Model Incorporating Drop Population Balance

2.1 Introduction

Rigorous simulation of multistage separation processes such as extraction, distillation and absorption is,more often than not ,based upon the equilibrium approach Henley [38].These models assume that streams leaving stages are in equilibrium with each other. Material and energy Balance equations along with constraints such as equilibrium relations and normalization equations. are then solved for such models. These models are easy to use but predict poor results in practice.

In actual operation, stages rarely, if ever, are operated at equilibrium despite attempts to approach this condition by proper design and choice of operating conditions. The usual way of dealing with departure from equilibrium is by incorporating a stage efficiency into the equilibrium relations. However despite the presence of several definitions of efficiencies, as yet no consensus has been arrived at to prove which is best.

In the present work, use of empirical correction factors such as efficiencies or HETP is completely avoided; and a non-equilibrium model has been developed for the simulation of a counter-current multicomponent extraction process. Since dynamics and mass transfer in a liquid-liquid dispersion are correctly determined by the behavior of the dispersed phase, the change in the characteristics (holdup,mean drop size d_{32} ...) of the drop population along the column have to be considered in order to describe conveniently the hydrodynamics of column.

Continuous contact column such as extraction column can be simulated by two ways :

1. The column hydrodynamics can be represented by plug flow model in which dispersed phase (droplets) is considered as plugs of phase moving along the height.(Polydispersed model, Jiřičný [19]).

2. Model relying on a drop population balance that leads to the drop size distribution at every level of the column. Such works have been proposed by Khani and Cassamatta [8] for dynamic and steady state simulation of liquid-liquid extraction (llx) column and Tsouris and Tavlarides for describing dispersion [17], holdup profile dynamics and control [16].

The above two approaches have been coupled by developing a detailed mathematical model for steady state by Zimmermann [7].In this model, mass-transfer is described by adopting rate based approach such as proposed earlier by Spencer [3] and Ricker [2]. A rigorous non-equilibrium stage model as developed by Krishnamurthy and Taylor [5, 6] (for distillation column), which has been adopted by Zimmermann and his co-workers.

In present work the basic mathematical formulation of Zimmermann 1992 [7] has been adopted to simulate extraction column, both for dynamics and steady state both. Drop breakage and coalescence term Π_{ijk} is modified from the work by Tsouris [16, 17] to facilitate mass transfer. In Tsouris work it was used in drop population balance equations for the control of extraction column (such as holdup etc.). Dynamic simulation has been worked out by including accumulation term in the balance equations of above approach.

Mathematical formulation for steady state simulation is divided into following four sections :

- FLUID DYNAMICS.
- TRANSPORT RELATIONS.
- INTERPHASE MODEL.
- NORMALIZATION EQUATION.

The model is based on following major assumptions :

1. Extraction column is operating isothermally.

2. Stages are assumed to be in mechanical equilibrium i.e. pressure of both phases in a stage are equal ($p^c = p^d$).

3. Trays are numbered in the direction of dispersed phase flow. This is for convenience in representation of variables. Variables are defined accordingly so that exactly same model formulation can be used whether the dispersed phase is heavier or lighter with respect to continuous phase.

4. Mixture molar densities are assumed uniform for all drops in the same drop class j at any stage k.

5. No mass transfer resistance at interface between the two phases.

2.2 Fluid Dynamics

As with any other model of chemical process, the analysis of the non-equilibrium stage starts with the construction of the material balance. Here process is considered isothermal[1] . The model as proposed by Khani and Cassamatta [8] is discretized on the basis of real stages along column height.

2.2.1 Conservation relationships

A schematic representation of non-equilibrium stage is shown in Figures 2.1(a,b). Both figures are similar except the flow direction of both phase is reversed. On each stage two phases are brought into contact from adjacent stages.The whole drop spectrum is discretized in different drop class say 1,2,...,ND based on their drop volumes (see section 2.8). Drops of same volume (diameters) are considered as one drop class moving as a plug in contact with bulk continuous phase, and the interface area is the area between bulk and the drops of that drop class, shown by wavy line in Figures 2.1. So in each stage the corresponding two phases are separated by interface – thin film of corresponding phases on either side of interface. These films offer resistance for mass transfer. Continuous phase is also described as plug flow[2]. Each drop class is described by basic variable P_{jk}which is the volume fraction of drop class j. Summation over all drop classes at any stage k, yields the dynamic holdup (referred to as holdup) ϕ_k of the dispersed phase at any stage k.

$$\phi_k = \sum_{j=1}^{ND} P_{jk} \tag{2.1}$$

The mass balance at any stage k for any drop class j and component (species) i are as follows :

MBD_{ijk} :Mass balance for Dispersed phase

$$V^+_{jk-1}x_{ijk-1} - (V^+_{jk} + V^-_{jk})x_{ijk} + V^-_{jk+1}x_{ijk+1} + N_{ijk} + F^d_{jk}x^f_{ik} + \Pi_{ijk} = 0 \tag{2.2}$$

[1]The model can be applied for a column in which at least every stage is considered at uniform temperature and temperature gradient along the column may be considered without energy balance

[2]which is interacting with ND plugs of drop classes

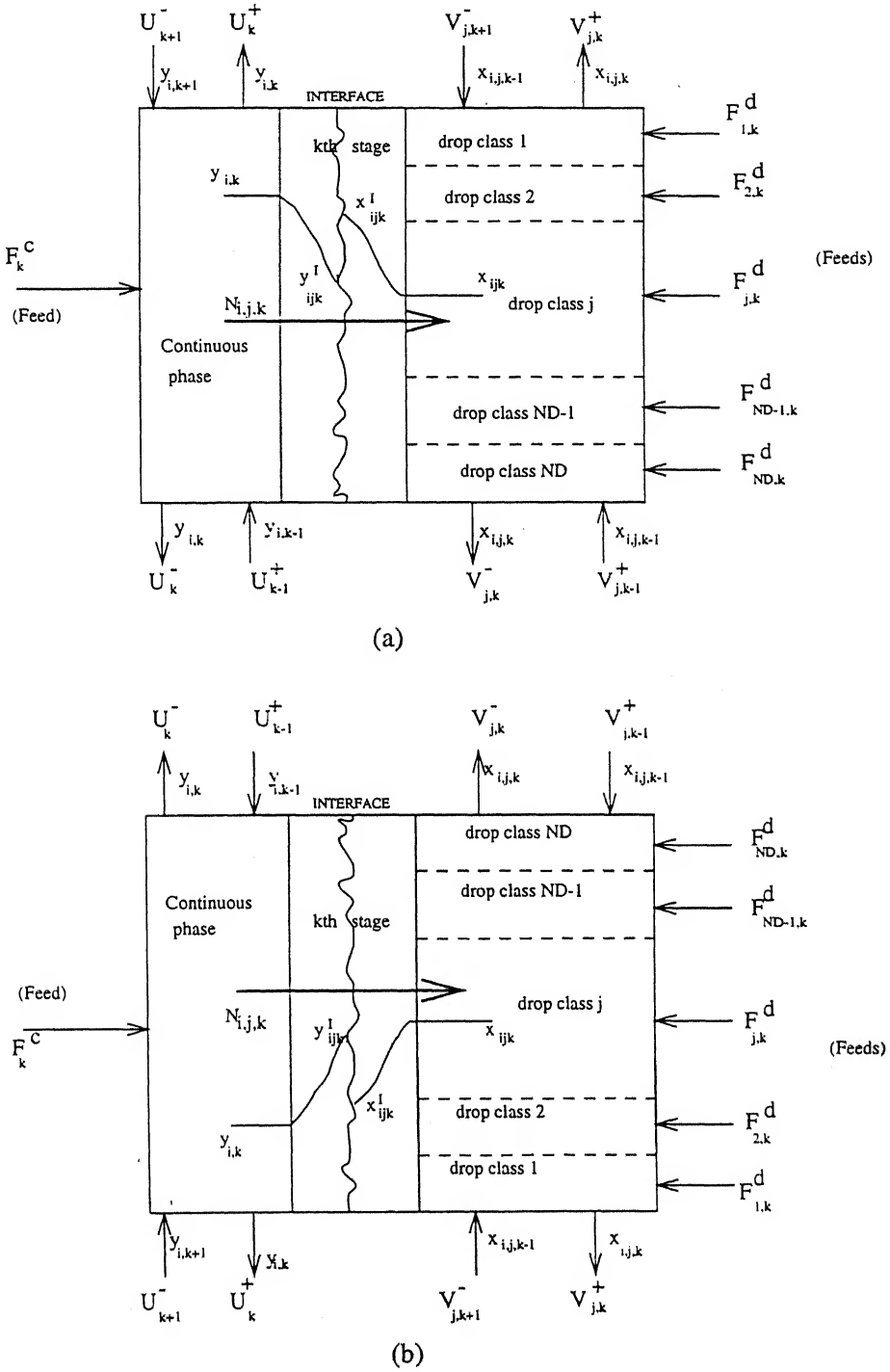

(a)

(b)

Figure 2.1: Schematic representation of a non-equilibrium stage: (a)Light dispersed phase. (b) Heavy dispersed phase.

MBC_{ik} :*Mass balance for Continuous phase*

$$U_{k-1}^{+}y_{ik-1} - (U_k^{+} + U_k^{-})y_{ik} + U_{k+1}^{-}y_{ik+1} - \sum_{j=1}^{ND} N_{ijk} + F_k^c y_{ik}^f = 0 \qquad (2.3)$$

where subscripts i,j,k takes on value
i=1,2,...,NC; j=1,2,...,ND; k=1,2,...,NS;

N_{ijk} represents the interface mass transfer rate (moles/s) in a stage from continuous to dispersed phase, N_{ijk} will be negative if transfer takes place from dispersed to continuous phase. Π_{ijk} is a generation term due to drop breakage and coalescence, which is described in detail in section 2.8.

2.2.2 Flow relationships

Flow streams V_{jk}^{+},V_{jk}^{-},U_k^{+} and U_k^{-} departing from k^{th} stage to the adjacent stage are described as a combination of convective and diffusive contribution of flows. Main flow direction will contain both convective and dispersion flow; however only dispersion flow will exist against the main flow, causing backmixing in extraction column. Axial dispersion coefficient $\mathbf{D^c}_k$ and $\mathbf{D^d}_k$ are used to represent axial dispersion in continuous and dispersed phase respectively at any stage k.

Flow VP_{jk} :*Forward flow for Dispersed phase*

$$V_{jk}^{+} = \left(u_{jk}^{d} + \frac{\mathbf{D^d}_k}{\triangle h_k}\right) P_{jk} c_{jk}^{d} S = 0 \qquad (2.4)$$

Flow VM_{jk} :*Backward flow for Dispersed phase*

$$V_{jk}^{-} = \left(\frac{\mathbf{D^d}_{k-1}}{\triangle h_{k-1}}\right) P_{jk} c_{jk}^{d} S = 0 \qquad (2.5)$$

Flow UP_k :*Backward flow for Continuous phase*

$$U_k^{+} = \left(\frac{\mathbf{D^c}_k}{\triangle h_k}\right) (1 - \phi_k) c_k^{c} S = 0 \qquad (2.6)$$

Flow UM_k :*Forward flow for Continuous phase*

$$U_k^{-} = \left(u_k^{c} + \frac{\mathbf{D^d}_{k-1}}{\triangle h_{k-1}}\right) (1 - \phi_k) c_k^{c} S = 0 \qquad (2.7)$$

Mixture molar densities c_k^c and c_{jk}^d are assumed uniform in k^{th} stage for continuous bulk phase and all drops of same drop class for dispersed phase respectively. Convective contributions are described by the velocity of two phases u_k^c and u_{jk}^d respectively and diffusive contribution are defined by axial dispersion coefficient. Mixture molar densities are given by following relationships.

$$c_{jk}^d = \frac{\rho_{jk}^d}{\sum_{i=1}^{NC}(x_{ijk}M_i)} \tag{2.8}$$

$$c_k^c = \frac{\rho_k^c}{\sum_{i=1}^{NC}(y_{ik}M_i)} \tag{2.9}$$

Velocity of dispersed phase u_{jk}^d is expressed by the following kinematic relationship.

$$u_{jk}^d = -u_k^c + u_{jk}^r \tag{2.10}$$

$$u_{jk}^r = (1-\phi_k)^m u_{jk}^{r*} \tag{2.11}$$

where u_{jk}^r is a relative velocity and u_{jk}^{r*} is a characteristic velocity usually available as an empirical correlation (· Laddha [1]). Exponent m (usually 0-1) is a function of the hydrodynamics condition, particularly of the *Re* relative to the drops. In present work this is assumed as model parameter and kept unity. However this must be evaluated independently by carrying out optimization of model parameter against real data for any specific column.

2.2.3 Transport relationships

A more rigorous approach is adopted here to represent transport relationships (see section 2.9 for details).

$MBIC_{ijk}$: *Interphase flow balance, based on continuous phase*

$$N_{ijk} = y_{ik}\sum_{i=1}^{NC} N_{ijk} + a_{jk}\sum_{m=1}^{NC-1} K_{imjk}^c(y_{mk} - y_{mjk}^I) \tag{2.12}$$

$MBID_{ijk}$: *Interphase flow balance,based on dispersed phase*

$$N_{ijk} = x_{ijk}\sum_{i=1}^{NC} N_{ijk} + a_{jk}\sum_{m=1}^{NC-1} K_{imjk}^d(x_{mjk}^I - x_{mjk}) \tag{2.13}$$

K^c_{imjk} and K^d_{imjk} are mass transfer coefficients due to interaction effect in multi-component mixture. Evaluation of these coefficients is described in section 2.9.1.

It should be noted that only (NC-1) independent diffusion fluxes (Taylor [21]) exist, since the diffusion flux $\overline{J_i^*}$ as well as composition gradient must sum to zero over the NC species. Interfacial area a_{jk} is directly given by the drop size distribution at each stage of the column :

$$a_{jk} = 6.0 \left(\frac{V_k}{d_{jk}} \right) P_{jk} \tag{2.14}$$

2.3 Interface model

In present model equilibrium between two phases is assumed at the interface with no resistance to mass transfer. Equilibrium relation relates the interfacial concentration due to both phases by following relation:

$$y^I_{ijk} = K^*_{ijk} x^I_{ijk} \tag{2.15}$$

values of K_{ijk}. distribution ratio are calculated by means of ratio between the activity coefficients of both phases. In general K_{ijk} depends upon pressure ,temperature and composition of both phases at interface. Various standard and reliable methods based on group contribution such as UNIFAC, UNIQUAC, NRTL methods can be used for evaluating activity coefficients of phases. In present work the simulation is carried out with the UNIFAC model (Fredenslund [23]). Various references are also mentioned in Bibliography about UNIFAC method and its applicability.

2.4 Normalization relations

In order to complete the set of equations corresponding to independent variables, normalization equations are written for each phase:

NDI_{jk} :

$$\sum_{i=1}^{NC} x^I_{ijk} = 1.0 \tag{2.16}$$

NCI_{jk} :

$$\sum_{i=1}^{NC} y^I_{ijk} = 1.0 \tag{2.17}$$

ND_{jk} :

$$\sum_{i=1}^{NC} x_{ijk} = 1.0 \tag{2.18}$$

NC_k :

$$\sum_{i=1}^{NC} y_{ik} = 1.0 \tag{2.19}$$

where (j=1,2,...,ND) and (k=1,2,...,NS)

2.5 Overall simulation model

Section 2.2 to 2.4 described the model for any general multistage counter-current extraction column which is summarized in Table 2.1. The model is discretized in such a way that it can be applied for any type of extraction column (agitated and non-agitated) such as sieve tray, pulsed sieve tray, RDC etc., without any major modification. However correlations used in model may be different for diffrent types of columns. In present work the model is analyzed for unagitated sieve tray column (counter-current). In such a column there exist two types of holdup – dynamic holdup and static holdup. Static holdup has no major relevance in mass transfer except that its surface in contact with bulk continuous phase provides mass transfer area between the two phases. Further, static holdup causes retardation in the flow of dispersed phase, which can be accounted for by velocity correlation of the dispersed phase such as proposed by Khani and Cassamatta [8] with the introduction of K_v factor in u^{r*} correlation. In case of unagitated sieve tray column only dynamic holdup will be considered and height caused by the static holdup (beneath or above each sieve tray, as the case may be, see Figure 2.2) is deducted from the total compartment height of the actual column. The difference is then considered as the active height for mass transfer and will be accounted in the volume of stage (V_k) used for model. Further correction in the height may be introduced by the fact that interface area between the static holdup and bulk continuous phase also provides area for mass transfer. For this area extra height may be added up and used in the volume of stage V_k calculation.

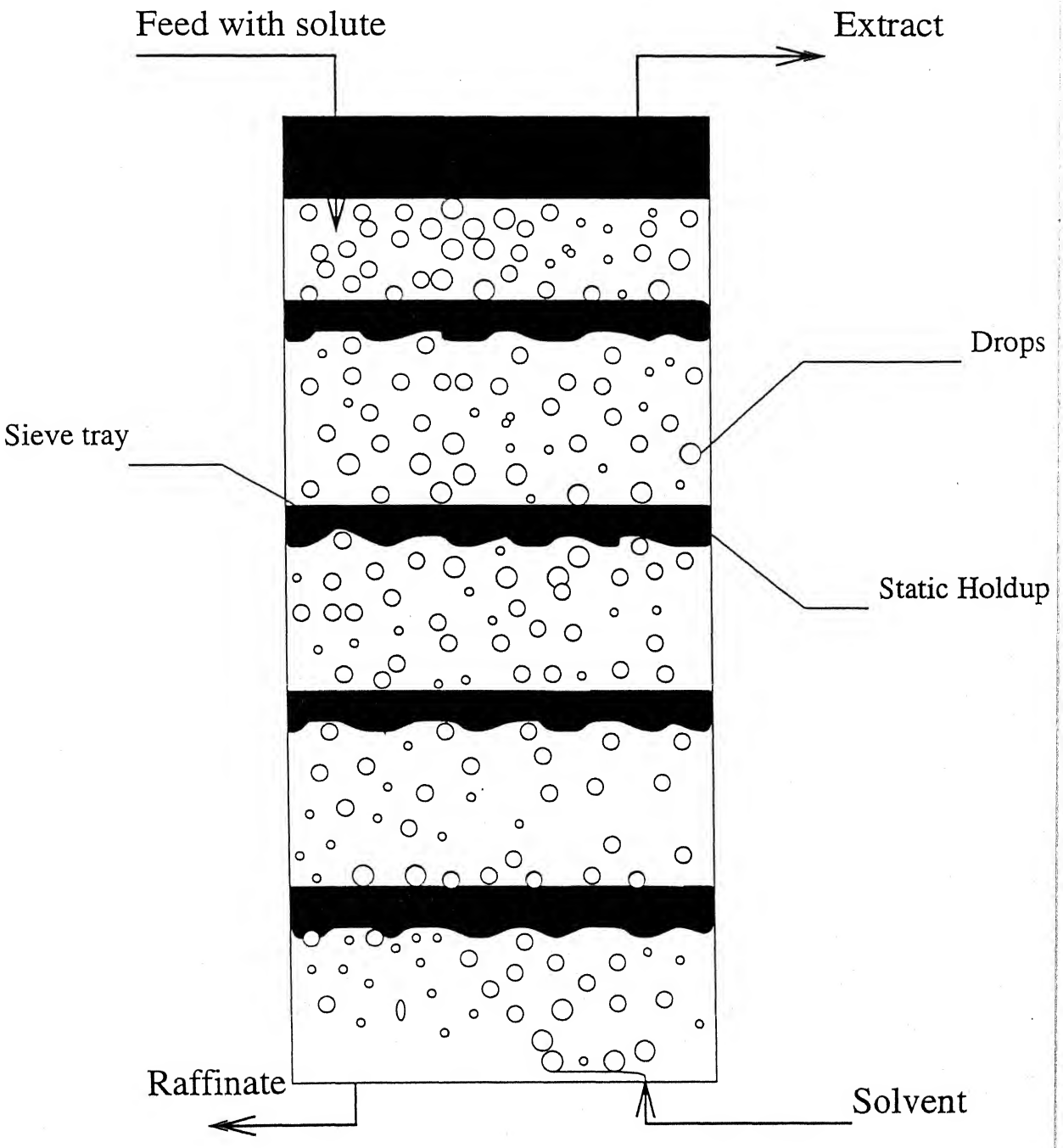

Figure 2.2: Schematic representation of extraction column (Light dispersed phase)

Table 2.1: Simulation model summary

$V^+_{jk-1}x_{ijk-1}$ - $(V^+_{jk} + V^-_{jk})x_{ijk} + V^-_{jk+1}x_{ijk+1} + N_{ijk} + F^d_{jk}x^f_{ik} + \Pi_{ijk} = 0$ $U^+_{k-1}y_{ik-1}$ - $(U^+_k + U^-_k)y_{ik} + U^-_{k+1}y_{ik+1}$ - $\sum_{j=1}^{ND} N_{ijk} + F^c_k y^f_{ik} = 0$
V^+_{jk} - $(u^d_{jk} + \frac{D^d_k}{\Delta h_k})P_{jk}c^d_{jk}S = 0$ V^-_{jk} - $(\frac{D^d_{k-1}}{\Delta h_{k-1}})P_{jk}c^d_{jk}S = 0$ U^+_k - $(\frac{D^c_k}{\Delta h_k})(1\text{-}\phi_k)c^c_k S = 0$ U^-_k - $(u^c_k + \frac{D^c_{k-1}}{\Delta h_{k-1}})(1\text{-}\phi_k)c^c_k S = 0$
N_{ijk} - $y_{ik}\sum_{i=1}^{NC} N_{ijk}$ - $a_{jk}\sum_{m=1}^{NC-1} K^c_{imjk}(y_{mk} - y^I_{mjk}) = 0$ N_{ijk} - $x_{ijk}\sum_{i=1}^{NC} N_{ijk}$ - $a_{jk}\sum_{m=1}^{NC-1} K^d_{imjk}(x^I_{mjk} - x_{mjk}) = 0$
y^I_{ijk} - $K_{ijk}x^I_{ijk} = 0$
$\sum_{i=1}^{NC} x^I_{ijk}$ - $1.0 = 0$ $\sum_{i=1}^{NC} y^I_{ijk}$ - $1.0 = 0$ $\sum_{i=1}^{NC} x_{ijk}$ - $1.0 = 0$ $\sum_{i=1}^{NC} y_{ik}$ - $1.0 = 0$
where (j=1,2,...,ND) and (k=1,2,...,NS)

2.6 Degree of freedom analysis

Table 2.1 lists the set of equations for single stage, similar sets of equations can also be written for other stages, which constitutes the complete problem to be solved.

For any stage k, following independent variables exist

Independent variables	Total No. of variables
Flow rates of each drop class (V^+_{jk},V^-_{jk})	2ND
Flow rates of continuous phase (U^+_k,U^-_k)	2
Bulk mole fractions (x_{ijk},y_{ik})	(NDxNC)+NC
Interface mole fractions (x^I_{ijk},y^I_{ijk})	2(NDxNC)
Mass transfer rate (N_{ijk})	(NDxNC)
Drop class volume fractions (P_{jk})	ND
Velocity of continuous phase (u^c_k)	1
Total no. of variables/stage	4(NDxNC)+3ND+NC+3

Similarly for any stage following are the number of equations :

Independent equations	Total No. of equations
Material balance equation MBD_{ijk}	(NDxNC)
Material balance equation MBC_{ik}	NC
Flow Equations $VP_{jk}, VM_{jk}, UP_k, UM_k$	2(ND+1)
Transport relation $MBID_{ijk}, MBIC_{ijk}$	2ND(NC-1)
Equilibrium relations EQ_{ijk}	(NDxNC)
Normalization relations NDI_{jk}, NCI_{jk}	2ND
Normalization relations ND_{jk}, NC_k	ND+1
Total no. of equations/stage	4(NDxNC)+3ND+NC+3

The above problem becomes a set of non-linear algebraic equation for steady state ans a set of Differential-Algebraic equations for dynamic state. , which are to be solved by any non-linear equation solver ,such as multivariable Newton-Raphson method. Solution strategy is described in chapter 3 each dynamic and steady state simulation. Providing reasonable initial guess, this method is very robust and converge well even for very large equation system.

2.7 Dynamic model

Dynamic model is formulated by adding accumulation term in the material balance equation sets of steady state model. All other relations in section 2.5 are constraints, so they remain same for the dynamic model formulation. Extension of material balance sets are given below.

- $\underline{DMBD_{ijk}}$

$$\underbrace{\frac{d}{dt}[V_k P_{jk} c^d_{jk} x_{ijk}]}_{DY_d} = \underbrace{V^+_{jk-1} x_{ijk-1} - (V^+_{jk} + V^-_{jk}) x_{ijk} + V^-_{jk+1} x_{ijk+1} + N_{ijk} + F^d_{jk} x^f_{ik} + \Pi_{ijk}}_{SS_d} \tag{2.20}$$

where DY_d (left hand side) term denotes molar accumulation of component i of drop class j at stage k.This term is further simplified as :

$$-V_k \left[P_{jk} c^d_{jk} \frac{d}{dt} x_{ijk} - \frac{P_{jk} c^d_{jk} x_{ijk}}{(Mav)^d_{jk}} \sum_{i'=1}^{NC} \left(M_{i'} \frac{d}{dt} x_{i'jk} \right) + c^d_{jk} x_{ijk} \frac{d}{dt} P_{jk} \right] + SS_d = 0 \tag{2.21}$$

- $\underline{DMBC_{ik}}$

$$\underbrace{\frac{d}{dt}[V_k(1-\phi_k)c_k^c y_{ik}]}_{DY_c} = \underbrace{U_{k-1}^{+}y_{ik-1} - (U_k^{+}+U_k^{-})y_{ik} + U_{k+1}^{-}y_{ik+1} - \sum_{j=1}^{ND} N_{ijk} + F_k^c y_{ik}^f}_{SS_c} \tag{2.22}$$

where DY_c (left hand side) term denotes molar accumulation of component i at stage k in continuous phase. This term is further simplified as :

$$-V_k\left[(1-\phi_k)c_k^c\frac{d}{dt}y_{ik} - \frac{(1-\phi_k)c_k^c y_{ik}}{(Mav)_k^c}\sum_{i'=1}^{NC}\left(M_{i'}\frac{d}{dt}y_{i'k}\right) + c_k^c y_{ik}\sum_{J=1}^{ND}\frac{d}{dt}P_{Jk}\right] + SS_c = 0 \tag{2.23}$$

All other equation sets described in section 2.5 will remain same for dynamic modeling also. These relations act like constraints at any instant of time. Degree of freedom analysis discussed in section 2.6 is still valid since number of equations and number of independent variables remained unaltered.

2.8 Drop Breakage and Coalescence

Smooth flow of dispersed phase in form of droplets in extraction column can be described by the simple transport relations. Abrupt changes in drop distribution due to drop breakage and coalescence cannot be handled by the transport relations alone satisfactorily, instead population balance approach is introduced for such situations. Especially in case of extraction where large transport area is created by agitation, accompanied by high drop breakage and coalescence, need of such model is immense. Because of breakage and coalescence phenomena dispersed phase droplets continually forgo their individual identities. The material domain for which the transport equations are applicable is thus subject to discontinuous changes in an apparently random manner.

Ramakrishna [9] gives an excellent review of the several works that have been published on drop breakage and coalescence during past 2-3 decades. Among the first published works in the field, Coulaloglou [10] proposed a phenomenological model to describe drop breakage and coalescence in a turbulently agitated liquid-liquid dispersion. It was a theoretical model based on fundamental concepts. The same model has been worked out by several other workers Sovavă [11, 12], Rubio [15], Hsia and Tavlarides [13, 14] and Tsouris [16, 17]. These works utilized the drop population balance ignoring mass transfer aspects. Such a model has been well applied by Tsouris [17] for drop-breakage analysis, holdup profile and holdup control of the column. The work presented here incorporates the concept of these models (based on number of drops balance) into the mass transfer model in this work. Drop breakage rate Π_{ijk}^{DB} and coalescence rate Π_{ijk}^{DC} terms are modified as described in the next paragraph.

Earlier drop breakage and coalescence rates were written for population balance in which balance over number of drops was used. In present model number of drops and

their concentration (of each drop class) are easily calculable as simulation variables. So these rate terms in form of number of drops per time as described in Tsouris [16, 17] are simply multiplied by the volume, molar density and concentration of respective drop (drop class) to get corresponding mass transfer rate (moles/s) due to drop breakage and coalescence. These transfer terms in all are called as generation term Π_{ijk} due to drop breakage Π_{ijk}^{DB} and coalescence Π_{ijk}^{DC} and thus included in material balance equation set MBD_{ijk} see section 2.2. However for non-agitated columns generation term may not be very much significant at any stage of extraction column.

Following sections describe the dichotomy of Π_{ijk} term and its derivation from population balance model. Various correlations were also used in the original works, some of them still need detailed research, in fact drop breakage and coalescence is still a topic of intense research at present in the field of liquid-liquid dispersion.

2.8.1 Generation due to drop-breakage and coalescence: Π_{ijk}

In dispersion drop spectrum is discretized on the basis of volume of drops (say 0 to v_{max}) and each discretized part is assigned a number as 1,2,...,ND. Diameters are than calculated for each drop class. The generation term Π_{ijk} (negative for loss) in material balance equation MBD_{ijk} is divided in two parts as below. DB and DC refer to drop breakage and drop coalescence respectively.

$$\Pi_{ijk} = \Pi_{ijk}^{DB} + \Pi_{ijk}^{DC} \tag{2.24}$$

Each of two terms on the right hand side of above equation is further divided into two parts as actual loss and actual gain of material from any drop class at any stage. Subscripts i,j,k are used for component, drop class and stage respectively. For all terms base formulation are referred from Tsouris [16], Coulaloglou [10] and Sovová [11]. They are modified for mass transfer here.

Generation due to drop breakage : Π_{ijk}^{DB}

In present formulation sometimes only drop class is referred (by j), but in actual calculation either drop volume or drop diameter is used whichever is convenient. The term Π_{ijk}^{DB} is divided as :

$$\Pi_{ijk}^{DB} = -\Pi_{ijk}^{DB^-} + \Pi_{ijk}^{DB^+} \tag{2.25}$$

- $\Pi_{ijk}^{DB^-}$ *(Material lost from jth drop class due to breakage of drops of jth class)*

This material will be distributed in lower[3] drop class. For lowest drop class this term is not applicable.

$$\Pi_{ijk}^{DB^-} = [g_k(j)n_k(j,t)]v_j c_{jk}^d x_{ijk} \tag{2.26}$$

Correlations for $g_k(j)$ (breakage frequency) can be referred from Appendix B. $n_k(j,t)$ is a number of drops in drop class j, at any time t. v_j is a volume of single drop of drop class j.

- $\Pi_{ijk}^{DB^+}$ (*Material gained by jth drop class due to breakage of higher*[4] *drop class*

This material is gained by the drop classes (except highest drop class) due to breakage of other drops.

$$\Pi_{ijk}^{DB^+} = \int_{v_j}^{vmax} [\beta(v_j, v')\nu(v')g(v')n(v',t)]v_j c_{jk}^d(v')x_{ijk}dv' \tag{2.27}$$

Breakage type ν is assumed as *binary breakage* for present study. A daughter probability density function $\beta(j,j')$ is used to obtain probability of breakage for drops of volume v' into v_j, which must satisfy some conditions, Ramkrihshna [9, page 58] such as

$$\int_0^{v'} \beta(v,v')dv = 1.0 \tag{2.28}$$

$$\beta(d_i, dj) = 0.0, \quad if i = j (or d_j < d_i) \tag{2.29}$$

where j= father drop class i= daughter drop class

Appendix B can be seen for $\beta(v_j, v')$ correlations.

Generation due to drop coalescence : Π_{ijk}^{DC}

Similarly this term is divided into two parts.

$$\Pi_{ijk}^{DC} = -\Pi_{ijk}^{DC^-} + \Pi_{ijk}^{DC^+} \tag{2.30}$$

- $\Pi_{ijk}^{DC^-}$ (*Material lost from jth drop class due to its coalescence with other drops*)

[3]means drop class having less diameter of jth drop class
[4]means, drop class having large diameter than jth drop class

This material will go to other possible higher drop classes.

$$\Pi_{ijk}^{DC^-} = n(v_j,t)v_j c_{jk}^d x_{ijk} \int_{v_{min}}^{v_{max}-v_j} \lambda(v_j,v')h(v_j,v')n(v')dv' \tag{2.31}$$

Since after coalescence drop volume is not expected greater than v_{max} hence upper limit of integration is set as $(v_{max} - v_j)$.

- $\Pi_{ijk}^{DC^+}$ *(Material gained by jth drop class due to coalescence of other small drops)*

This material is gained by the drop class (except lowest drop class), due to coalescence of other smaller drops.

$$\Pi_{ijk}^{DC^+} = \int_{v_{min}}^{v_j/2} [\lambda(v_j-v',v')h(v_j-v',v')n(v_j-v',t)n(v',t)]\ v_j(c_{jk}^d)'(x_{ijk})'dv' \tag{2.32}$$

where drop molar density of the new drop formed by coalescence

$$(c_{jk}^d)' = \frac{\overline{c_{jk}^d[v']}\ v' + \overline{c_{jk}^d[v_j-v']}\ (v_j-v')}{v' + (v_j-v')} \tag{2.33}$$

and its molar fraction

$$(x_{ijk})' = \frac{\overline{c_{jk}^d[v']}\ v'\ \overline{x_{ijk}[v']} + \overline{c_{jk}^d[v_j-v']}\ (v_j-v')\ \overline{x_{ijk}[v_j-v']}}{\overline{c_{jk}^d[v']}\ v' + \overline{c_{jk}^d[v_j-v']}\ (v_j-v')} \tag{2.34}$$

NOTE : Drop volume enclosed in brackets [ ] in above equations represents the corresponding drop class for that variable. For example $\overline{c_{jk}^d[v']}$ represents the molar density of drop class corrosponding to drop volume v'.

$h(v_i,v_j)$ is the collision frequency of two drops and $\lambda(v_i,v_j)$ is the coalescence efficiency between two drops. The efficiency $\lambda(v_i,v_j)$ term is not well understood in liquid-liquid dispersions and various correlations are proposed by different authors. Some favor high efficiency for larger drops and some for smaller drops. $h(v_i,v_j)$ term, originally derived from kinetic thery of gases (Kennard [39, pp 103-104], has been further modified by other authors. These correlations are listed in Appendix B.

The integration terms in above formulation are evaluated by using trapezoidal rule, since discrete points are already known in form of distinct drop class (drop diameter or volume) from 0 to v_{max}, hence no separate discretization is necessary for trapezoidal rule. Similar formulation based on trapezoidal rule for drop population model can also be seen from Sovová [11], which also described explained discretization errors.

In general drop generation term Π_{ijk},is function of :

$$\Pi_{ijk} = f(x_{ijk}, P_{jk}) \tag{2.35}$$

where bold subscript **j** represents the general functionality valid over j=1,2,...,ND , whereas i,k are same in both right and left hand side of above functionality relation.

2.8.2 Discretization and drop size distribution at inlet

For simulation either a single drop class is assumed with average drop diameter (sauter mean diameter) in dispersion calculated by suitable correlation (Laddha [1],Baird [4]) or a discretized drop spectrum is taken. For dynamic simulation a single drop class approach is advisable computationally. However for a broader analysis of extraction, one needs to include more than one drop class in simulation. More number of drop classes means less discretization error but at the cost of higher computational time. Optimal number of drop classes are used for simulation based on these two factors. Usually about 8 drop classes are enough to avoid any siginificant discretization error.

As described earlier discretization is made on the basis of drop volume usually between $v_{min}(=0)$ to v_{max}; where v_{max} is calculated by a suitable correlation such as Baird [4, 1983,pp 129,eqn 17]. Let's say v_{min} and $\overline{v_0}$ are the minimum and mean volume of drops respectively in a given dispersion, then a discrete point for n^{th} drop class is given by:

$$v(n) = v_{min} + n * \Delta v \tag{2.36}$$

The feed distribution can be assumed as a Gaussian probability density distribution function which suggests that the probability of drops falling with in range v to $v + \Delta v$ is given by.

$$A(v) = \frac{1}{\sqrt{2\pi}\,\sigma} \exp\left[-\frac{1}{2}\left(\frac{v - \overline{v_0}}{\sigma}\right)^2\right] \tag{2.37}$$

where $-\infty < v < \infty$
here σ is the standard deviation.

So the number fraction of drops that may lie from (j-1) to j^{th} drop class but accounted in j^{th} drop class is given by

$$p_j = \int_{v_{j-1}}^{v_j} A(v_j)dv_j \tag{2.38}$$

which must satisfy for real problem,

$$\int_0^{vmax} A(v_j)dv_j = 1.0 \tag{2.39}$$

if above is not satisfied then normalize to give.

$$p_j = \frac{\int_{v_{j-1}}^{v_j} A(v_j)dv_j}{\int_0^{vmax} A(v_j)dv_j} \tag{2.40}$$

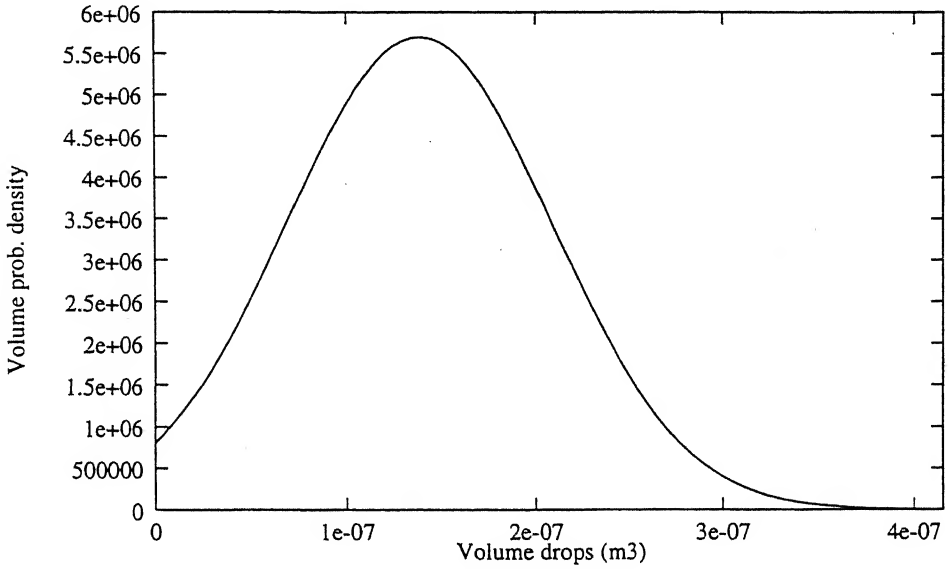

Figure 2.3: Normal distribution for inlet drop spectrum *(Volume probabilty density vs volume of drops)*

N_0 the total number drops at inlet is calulated on the basis of mean drop volume,

$$N_0 = \frac{V_1\ \phi_0}{\overline{v_0}} \tag{2.41}$$

here ϕ_0 the holdup is assumed for initial calculations. Volume fraction of drop class j for inlet is calculated as :

$$P_{j0} = \frac{(N_0 p_j) v_j}{V_1} \tag{2.42}$$

substituting N_0, we get

$$P_{j0} = \frac{\phi_0 p_j v_j}{\overline{v_0}} \tag{2.43}$$

In order to avoid any anomaly due to discritization this can be normalized again for getting $\sum_{j=0}^{ND} P_{j0} = \phi_0$
Further inlet distribution of dispersed phase flow rate is decided as

$$V_{j0} = V_{in} \frac{P_{j0}}{\phi_0} \tag{2.44}$$

for all j=1,2,....ND

This way discretization and inlet distribution of flows are fixed. Usually inlet distribution depends upon the way inlet is introduced to column, i.e. by using nozzle, sparger etc. If somehow, actual distribution is known that can be used instead of theoretical distribution suggested above. For other stages 1 to NS , the variable P_{jk} is calculated and simulation results are used to find out drop distribution at any stage.

2.9 Estimation of Mass Transfer Coefficient Matrix

Recent developments and success of rigorous simulation model, using coupling between various species present in separation processes such as distillation and absorption Krishnamurthy [5, 6], encourage the use of such rigour in modeling of extraction also.

Mass transfer in multicomponent mixture is more complicated than in binary system because of possible coupling between the individual concentration gradients. Phenomena such as reverse diffusion[5] or osmotic diffusion[6] are possible in multicomponent system (Taylor [21]). Models of mass transfer that are able to account for interaction effect are described here.

Mass transfer is a rate process driven by gradients in concentration. The rate of mass transfer in the continuous and the dispersed phase depends upon the concentration gradient across the film. Here bulk concentrations are assumed uniform and equilibrium is assumed at interface. Many other factors such as temperature, concentration, physical properties of the fluids (density, density difference, viscosity, interfacial tension etc.), system geometry and hydrodynamics , influence the rates that are achieved. Current practice is to lump the effects of most of these variables into mass transfer coefficient. Mass transfer in a multicomponent mixture is descibed $[N_i = y_i \sum_{i'} N_{i'} + \overline{J_i^*}]$ as in Bird [40] and Taylor [21]. On right hand side of this expression, first term represents the convective mass transfer and second term represents the diffusive mass transfer.

2.9.1 Estimation approach

A more rigorous approach is used to write transport relationships $MBID_{ijk}$ and $MBIC_{ijk}$. Resistance to mass transfer (offered by both phases) can be accounted for by using separate rate equation incorporating *interactive mass transfer coefficients.* Interfacial area between bulk continuous phase and any drop class is easily calculated by equation 2.14 as a_{jk}.

Methods that take interaction effects into account, but are implicit in fluxes or transfer rate[7], are proposed by Krishnamurthy [5, 6] for distillation and absorption. Same philosophy is used here, but variables are tailored for extraction. In general, transfer rate for continuous phase is written as (similar development is true for dispersed phase):

[5] diffusion of species against its own concentration gradient

[6] diffusion of species even though no concentration gradient for that species exist

[7] Here transfer rate as $N_{ijk}$is used directly,since in material balance actual transfer rate is used instead of flux

$$N_{ijk} = y_{ik} \sum_{i'=1}^{NC} N_{i'jk} + a_{jk}\overline{J^*_{ijk}} \tag{2.45}$$

Flux $\overline{J^*_{ijk}}$ can be written by incorporating interaction effect into account, by using generalized Fick's law, Taylor [21], based on mass transfer coefficient instead of diffusivity. Equation 2.45 can be rewritten as :

$$N_{ijk} = y_{ik} \sum_{i'=1}^{NC} N_{i'jk} + a_{jk} \sum_{m=1}^{NC-1} K^c_{imjk}(y_{mk} - y^I_{mjk}) \tag{2.46}$$

In matrix form above equation can be written for each drop class "j" and in stage k^{th} as:

$$(N)_{jk} = (y)_{jk}N_t + a_{jk}[K^c]_{jk}(y - y^I)_{jk} \tag{2.47}$$

Where $Nt = \sum_{i'=1}^{NC} N_{i'jk}$
() represents vector
[] represents matrix in equation 2.47

Equation 2.47 consists of (NC-1) equations for any drop class j at stage k ,since $\sum_{i=1}^{NC} \overline{J^*_{ijk}} = 0.0$. hence only (NC-1) independent equation will exist.

In general *mass transfer coefficient* **k** is dependent on
$\mathbf{k} = \{(bulk\ conc.,\ Interfacial\ conc.,\ flux\ or\ transfer\ rate)$
. Mass transfer coefficient matrix of size (NC-1) by (NC-1) are then evaluated as :

$$[K^c]_{jk}.a_{jk} = [B]^{-1}_{jk} a_{jk} [\Phi]_{jk} \{\exp[\Phi]_{jk} - [I]\}^{-1} \tag{2.48}$$

This expression is then evaluated by following one of the procedures.

- Krishna and Standart method This method is used in present study.

$$\frac{[B]_{jk}}{a_{jk}} = [M]_{jk} \qquad with\ m_{ijk} = y_{ik} \tag{2.49}$$

$$[\Phi]_{jk} = [M]_{jk} \qquad with\ m_{ijk} = N_{ijk} \tag{2.50}$$

- In linearized theory due to Toor(1964)

$$\frac{[B]_{jk}}{a_{jk}} = [M]_{jk} \quad with\ m_{ijk} = \overline{y_{ik}} \equiv \frac{1}{2}(y_{ik} + y^I_{ijk}) \tag{2.51}$$

Where general matrix $[M]_{jk}$ components are evaluated as given below :

$$M_{iijk} = \frac{m_{ijk}}{\mathbf{k}_{iNCjk}\ a_{jk}} + \sum_{\substack{m'=1 \\ m' \neq i}}^{NC} \frac{m_{m'jk}}{\mathbf{k}_{im'jk}} \quad i = 1, 2, \ldots, (NC-1) \tag{2.52}$$

$$M_{im'jk} = -m_{ijk}\left(\frac{1}{\mathbf{k}_{im'jk}\ a_{jk}} - \frac{1}{\mathbf{k}_{iNCjk}\ a_{jk}}\right) \quad i \neq m' \quad i = 1, 2, \ldots, (NC-1) \tag{2.53}$$

Above method is described in full detail by Taylor [21, Chap. 7,8] and is based on film theory. General solution of Krishna and Standartis is applicable to mixture with any number of species. Some limiting cases are also described there. Zimmermann [7] used *linearized theory* of Toor(1964), whereas *Krishna and Standart* is used here. This method is general and gives exact solution.

2.9.2 Evaluation of binary pair $\mathbf{k}_{imjk}$ from correlation

The binary local mass transfer coefficient $\mathbf{k}_{imjk}$ for any drop class j and stage k, can be calculated by various empirical correlations (see Appendix B) available in literature [4], Rousseau [30],Treybal [41]. Usually these correlations are available in form of Sherwood number (Sh) relationship, such as :

$$Sh = c_1\ Re^{c_2}\ Sc^{c_3} \tag{2.54}$$

Where c_1, c_2, c_3 are empirical constants.

$$Sh = \frac{\mathbf{k}_{im}}{\rho_m \mathcal{D}_{im}} \tag{2.55}$$

where $k_{im} = binary\ mass\ transfer\ coefficient$
$\rho_m = molar\ density\ \equiv c^d_{jk}\ or\ c^c_k$
$\mathcal{D}_{im} = Diffusion\ coefficient(Maxwell)\ of\ binary\ pair\ i-m$

In multicomponent mixture diffusion coefficient $\mathcal{D}_{im}$ is given by (see equation 4.2.18;Taylor [21,:pp 91, is rewritten here)

$$\mathcal{D}_{im} = (\mathcal{D}^\circ_{im})^{\frac{(1+x_m-x_i)}{2}} (\mathcal{D}^\circ_{mi})^{\frac{(1+x_i-x_m)}{2}} \tag{2.56}$$

Where *infinite dilution diffusivity* $\mathcal{D}^\circ$ is evaluated by Wilke – Chang (1955) correlation see Taylor [21, pp 73] or Reid & Sherwood [42, pp 549].Only mutual diffusivity $\mathcal{D}^\circ_{im}(i \neq m)$ needs to be evaluated here. However for self diffusion coefficient $\mathcal{D}^\circ_{ii}$ separate correlations are used, though these are not required in section 2.9.1 calculations. *Binary mass transfer coefficients* calculated here are used in section 2.9.1.

Chapter 3

Steady State and Dynamic Simulation

3.1 General

Section 2.5 desribes the overall simulation model to be solved for independent simulation variables listed in section 2.6. The simulation model described is a set of non-linear equations which has to be solved by using multivariable Newton-Raphson method. A computer code is written in "C" langauage for this purpose, both to solve steady state and dynamic simulation of multicomponent unagitated sieve tray column. However with the replacement of correlations, the same model as well as computer program can be used for other types of extraction columns (agitated columns) also. Newton-Raphson method for solving set of non-linear equation is found to be very stable. Extension of steady state simulation is used for dynamic simulation by using DASSL (Differential Algebraic System SoLver). In dynamic simulation some elements (related to balance equations) of Jacobian is evaluated by using DASSL and all Jacobian elements used for steady state are used without alteration. The system is again solved using Newton-Raphson(N-R) method at any instant of time.

3.2 Steady state simulation

Let $(f_{s.s}(X))$ denotes the a vector of non-linear equations to be solved (as simulation model listed in Table 2.1) for collection of independent simulation variables $X \equiv (X_1, X_2, \ldots, X_n)$, with solution $(f_{s.s}(X)) \equiv (0)$. Then N-R method suggests the solution improvement X^{p+1} by the following relation.

$$[J^p]_{s.s}(X^{p+1} - X^p) = -(f_{s.s}(X^p)) \tag{3.1}$$

Where $[J^p]_{s.s}$ is the Jacobian matrix with elements :

$$J_{ij} = \frac{\partial f_i(X)}{\partial X_j} \quad \textit{at any iteration "p"} \tag{3.2}$$

where $J_{ij} \in [J^p]_{s.s}$ and $f_i(X) \in (f_{s.s}(X))$. This method is very robust and versatile except that it requires the calculation of the Jacobian which involves derivatives of equations to be solved with respect to independent variables. These independent variables are listed in section 2.6 and here denoted by single vector X.

3.2.1 Jacobian evaluation for steady state simulation

The analytical derivatives are evaluated by partial differentiating the model equations (as in Table 2.1) with respect to independent variables as denoted by X. Derivatives of some complicated terms (such as such as K_{ijk}(distribution ratio), mass transfer coefficient K^d_{imjk},K^c_{imjk}, drop breakage and coalescence generation term Π_{ijk}) with respect to independent variables (X), which are difficult to derive analytically are evaluated numerically. Since calculation of numerical derivative is a time consuming process, good bookkeeping is necessary during simulation to avoid duplicate calculations and to save simulation time. In order to improve simulation time further, some other hybrid techniques are proposed (Krishnamurthy [5, 6]) in literature. Sometimes however these methods may cause an instability problem due to less accurate update of Jacobian elements. Since in this work accuracy is stressed more, derivatives are evaluated analytically to the extent one can evaluate comfortably and the remaining derivatives are evaluated numerically. For storage and calculation variables double precision arithmetic is used on Unix based machines (DEC α 2000, HP9000-850 m/c).

As for any other staged separation process, a Block-Tridiagonal Jacobian matrix (see Figure 3.1) is formed. Where block "A" represents the interaction from previous stage, block "C" represents the interaction due to to next stage and block "B" is the main block for any stage in Jacobian $[J_{s.s}]$. Apart from blocks A,B and C remaining Jacobian matrix is full of zeros. Vector D contains the residuals of the equations to be solved by Newton-Raphson method.

The extent of sparsity increases with number of stages. Hence a linearized simulation model equation 3.1 is solved by some suitable linear equation solver such as Block-Thomas algorithm [43]. Block-Thomas algorithm requires only storage of blocks A.B,C and function vector D for every stage. The size of all A,B and C blocks is same as the square matrix $(m \times m)$,where *m=number of independent simulation variables per stage* (see section 2.5). Residual vector D will be having size of $(m \times 1)$.

In order to make evaluation and coding of computer program easier each block (A,B or C) is further divided into subblocks or minors (M_{ij}). Selection of rows and columns of Jacobian for each minor is shown in Figure 3.2. The rows of minors are marked (by the type of equation sets, as described in section 2.5 and column of

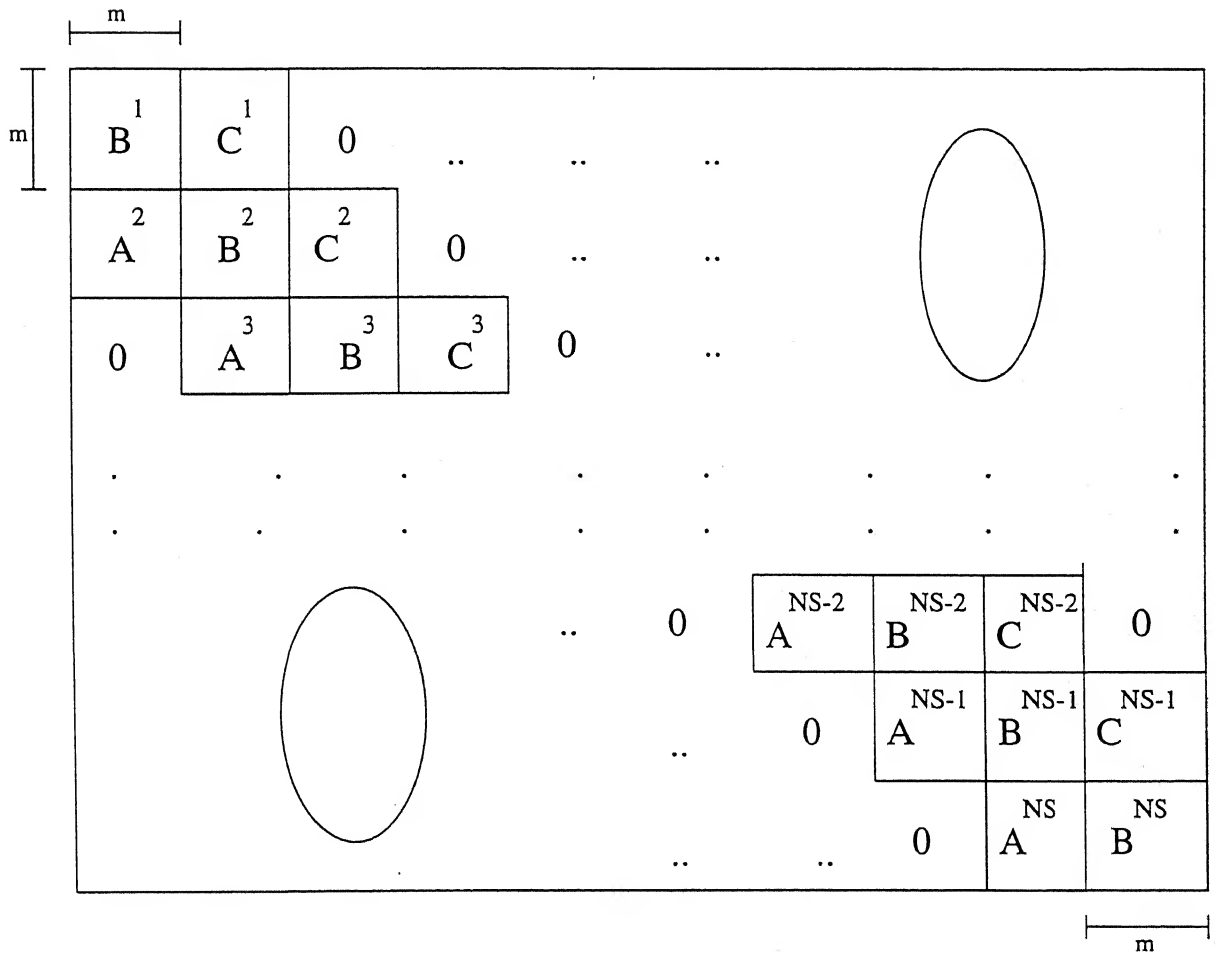

Figure 3.1: Block Tridiagonal Jacobian matrix (superscript represents stage number)

minor matrix is marked by class of independent variables described by section 2.6. A general block containing 30 minors is then represented as in Figure 3.2. These minors contains partial derivative of equations (listed as row heads) with respect to independent variables (listed as column heads).

As per "C" language convention minors subscripts are starts from (0,0) intead of (1,1). Similarly vector D is divided into 5 (5×1) parts. These minors and vector D are then calculated separately for one stage and finally synthesized as A,B,C blocks and D vector respectively for that stage.

Steady state simulation strategy is then summarized as below :

NOTE: Stages are numbered along the direction of dispersed phase flow.

 # 1 : Read data (Computer file : simulfun02.c (Table C.1)
→ Column specific (design parameters) as in Table C.2
→ System specific (Physical properties, molecular weight etc. as in Table C.3)
→ Operating condition (P,T,flow etc. as in Table C.4) → Read UNIFAC parameters as in Table C.

 # 2 : Condition input data (simulfun02.c Table C.1) as per the simulation variables used for column simulation, i.e. feeds are represented in terms of variables used in simulator. Carry out discretization of drop spectrum based on the drop volumes. This discretization (ND) and number of stages (NS) along with number of components (NC) decides the total number of independent equations and variables to be solved.

 # 3 : Set iteration number, p ← 0 .
Suggest initial condition as :
For main flows (V^+, U^-) → Take same as total feed flow up to that stage for respective phase.
(x_{ijk}, y_{ik}) → same as feed concentration.
(x^I_{ijk}, y^I_{ijk}) → same as feed concentration.
(N_{ijk}) → very low value such as 10^{-06}.
(P_{jk}) → Assume some value between 5–15%
(u^c_k) → depends upon column and flows ,typical value is (3mm/sec).

 # 4 : Increment p ← p+1.
Solve set of simulation equations (step.c Table C.1) for independent simulation variables by Newton-Raphson method, at step "p" and update simulation variables as

$$X^{p+1} = X^p - \lambda [J^p]^{-1}_{s.s} (f_{s.s}(X^p)) \tag{3.3}$$

Where λ is calculated by single variable optimization (Golden section search) of objective function (i.e. sum of square of residuals of model equations).

Figure 3.2: Minors of Block (A,B or C) and corresponding D vector

5 : If termination condition satisfied then stop simulation else go to step # 4.

6 : Report solution at steady state.

3.3 Dynamic simulation

In order to distinguish between steady state and dynamic simulation formulation "Y" is used for independent variable vector at any instant of time in place of "X" used for steady state. By modified material balance for dynamic modeling $DMBD_{ijk}$, $DMBC_{ik}$ (as in section 2.7 the new set of equations can be written as :

$$f_{d.s}(t_{n+1}, Y_{n+1}, Y'_{n+1}) = 0 \tag{3.4}$$

were Y' is a derivative vector containing time derivative of independent variables. Equation 3.4 represents the Differential-Algebraic Equation (DAE) system of index more than 1 (using terminology of Brenan [37]).

In order to solve equation 3.4 one can use *backward difference* (BDF) technique such as *Euler's method.* For Euler's method time derivatives Y' vector elements (y') are represented as :

$$y'_{n+1} = \left(\frac{y_{n+1} - y_n}{h}\right) \tag{3.5}$$

"h" is current time step and y is the element of vector (Y), thus DAE becomes at any instant t_{n+1}

$$f_{d.s}\left(t_{n+1}, y_{n+1}, \frac{y_{n+1} - y_n}{h}\right) \equiv 0 \tag{3.6}$$

This equation could be solved for Y_{n+1} at any instant of time t_{n+1} by using previous known value Y_n. with starting Y_0 as initial guess. Other techniques such as Gear's algorithm, Runge-kutta method could also be applied to solve DAE problem.

Since, steady state model has been solved by N-R method, it was found convenient to use any BDF technique which could be solved by N-R method with little modification. Euler's method is very inefficient to solve such a problem. A new robust BDF technique known as DASSL (Differential Algebraic System SoLver) is used as proposed by Petzold [36, 1982]. This method is quite robust for DAE system for index 1 or lower and works efficiently for semi-implicit DAE such as present dynamic model formulated for LLX column. For using DASSL formulation initial condition Y_0 and Y'_0 are required. It is assumed that DASSL is applied from one steady state to other steady state. Hence, when first DASSL is applied $Y'_0 = (0)$ is assumed; if not, then either these values have to be supplied or calculated (as in Brenan [37]).

By using DASSL formulation (as given in Appendix A

$$y'_{n+1} = y'^{(0)}_{n+1} - \frac{\alpha_s}{h_{n+1}}(y_{n+1} - y^{(0)}_{n-1}) \tag{3.7}$$

This is substituted in equation 3.6 and solved for vector Y_{n+1} by using N-R method at any instant of time.

The N-R problem at any instant of time t_{n+1} is given by:

$$[J^p]_{d.s}(Y^p_{n+1} - Y^p_n) = -(f_{d.s}(Y^p)) \tag{3.8}$$

The elements of new Jacobian $[J^p]_{d.s}$ are given by

$$J_{ij} = \frac{\partial f_i(Y)}{\partial Y_j} \quad \textit{at any iteration "p"} \tag{3.9}$$

where $f_i(Y) \in f_{d.s}$ and $J_{ij} \in [J^p]_{d.s}$. The Jacobian for dynamic simulation problem is then given as :

$$[J^p]_{d.s} = \left[\frac{\partial f_{d.s}}{\partial Y}\right] = \left[\frac{\partial f_{s.s}}{\partial Y}\right] + \left[\frac{\partial f_{d.s}}{\partial Y}\right]^* + \alpha\left[\frac{\partial f_{d.s}}{\partial Y'}\right] \tag{3.10}$$

Here independent variable vector (Y) is exactly similar to vector (X), desribed in steady state formulation except (Y) is at any instant of time t_{n-1}. Where matrix $\left[\frac{\partial f_{d.s}}{\partial Y}\right]^*$ contains derivative of accumulation terms only, which includes derivatives of DY_d and DY_c with respect to elements of vector (Y) only. Derivatives of these accumulation terms with respect to time derivative (Y') are included in $\left[\frac{\partial f_{d.s}}{\partial Y'}\right]$ matrix. Derivative of remaining terms are already included by matrix $\left[\frac{\partial f_{s.s}}{\partial Y}\right]$. So,

$$[J^p]_{d.s} = \left[\frac{\partial f_{d.s}}{\partial Y}\right] + \alpha\left[\frac{\partial f_{d.s}}{\partial Y'}\right] \tag{3.11}$$

where

$$\left[\frac{\partial f_{d.s}}{\partial Y}\right] = \left[\frac{\partial f_{s.s}}{\partial Y}\right] + \left[\frac{\partial f_{d.s}}{\partial Y}\right]^* \tag{3.12}$$

For dynamic simulation only elements of $\left[\frac{\partial f_{d.s}}{\partial Y}\right]^*$ and $\alpha\left[\frac{\partial f_{d.s}}{\partial Y'}\right]$ have to be evaluated extra and will be appended to the formulation of Jacobian for steady state.

DASSL is a variable order and variable step size algorithm which makes it robust. When system tends towards steady state, step size increases automatically and at perturbation it reduces the step appropriately. Formulation of DASSL, step size and order selection strategy can be seen in Appendix A.

Chapter 4

Results and Discussion

4.1 Application of the model

In principle the model described in previous chapters can be applied for any type of multicomponent, staged countercurrent extraction column. In this thesis the validity of such a model is tested for unagitated sieve tray extraction column. Two extraction systems have been tested in detail; results of which are presented here.

System 1 n-Heptane(1),cyl-Hexane(2),Benzene(3),Toluene(4),o-Xylene(5) and Sulfolane(6).

This is an industrial extraction system commonly known as aromatics extraction. Here sulfolane as a solvent, extracts BTX (Benzene,Toluene,Xylene) from naphtha feed, which contains n-heptane, cyclo-hexane along with BTX. Sulfolane, as a solvent is kept in dispersed phase and fed from the top(first tray) of the 40 staged column see Appendix C; whereas light naphtha feed in continuous phase enters from the bottom (40th tray) of the column. Products leaving the column are — Raffinate phase (purified naphtha) from the top of the column and Extract phase (which contains solvent sulfolane and BTX extracted from naphtha) from bottom of the column. In real operation this extract phase is further washed with steam, BTX is separated out and purified sulfolane recirculated to the extraction column. Data for a 30 cm diameter and 40 stage unagitated sieve tray column in this study have been obtained from *Engineers India Limited (EIL), Gurgoan.* Column design parameters, system properties and operating conditions obtained from EIL are listed in Appendix C. These data are then fed to the simulator program developed as a part of this thesis and results obtained. Naphtha as a continuous phase feed enters with composition (0.37.0.37, 0.05,0.16,0.05,0.0) [1]; BTX in feed is extracted by pure sulfolane in dispersed phase having feed composition (0.0,0.0,0.0.0.0,0.0,1.0). Extrac-

[1] 6 components. described as System 1

tion operation has been considered isothermal at $95°C$, thus physical properties are evaluated at this temperature. However, UNIFAC parameters available at $25°C$ in literature are used in the absence of any other reliable data. UNIFAC parameters reported by Mukhopadhyaya [28] have been tried out also in this work. These parameters have been evaluated at $100°C$ for some organic compound, however use of these parameters only favors the extraction of Benzene and Toluene and Xylene remained unextracted which is not true for practical column consodered in this study. The reason of such failure may be that these parameters are evaluated based on binary or tertiary mixtures of limited components whereas data reported in Magnussen [24] (used finally in this work) have been evaluated based on binary or tertiary mixtures of thousands of componets.

System 2 Water(1),Acetone(2),Toluene(3).

This is a test system recommended for the lab experiments. Toluene as a solvent (dispersed phase) enters from bottom of the 4 tray unagitated sieve tray column, which extracts, Acetone from the continuous aqueous phase entering from top of the column. Data are listed in Appendix D and results are also included therein.

4.2 Steady state results

Test SYSTEM 1

For the ease of simulation a single drop class having an average drop diameter is considered initially with no breakage and coalescence effects. A total of 1440 (36 equations per stage) equations are solved by using Newton-Raphson (N-R) method, with convergence criteria as sum of squares of residuals of equations being less than the given tolerance 10^{-10}. N-R method converges normally in 4-5 steps for all simulation runs described here. Data for all simulation runs are listed in Appendix C (Table C.2 to C). Here 5 simulations runs (run 1 to 5) for steady state are presented. Feed conditions for each of these simulation run are listed in Table 4.1.

Simulation run 1(Figures 4.1 to 4.7)

Figures 4.1 and 4.2 show the concentration profiles of all 6 components in continuous and dispersed phase respectively. From theses profiles it is clear that sulfolane extracts almost all BTX contents from the naphtha feed. Naphtha product as a raffinate phase leaves with 50.5 % n-heptane and 47.6 % cyl-hexane. Extract phase is leaving with 87.4 % sulfolane, remaining being BTX with negligible amounts of cyl-hexane and n-heptane. Solutes BTX concentration profiles are further enlarged in figures 4.3(a,b).Sulfolane selectivity is highest for Benzene then Toluene and lowest for o-Xylene. Hence all benzene is extracted up to 30^{th} stage (i.e only in 10 stages from

Table 4.1: Feed conditions for steady state simulation runs

Run no.	*S* (moles/s)	*F* (moles/s)	*S/F* (w/w)	*Naphta feed concentration* (mole fraction)	*Remarks*
1.	4.5	2.0	2.7	0.37,0.37,0.05,0.16,0.05,0.0	Base case
2.	4.5	3.0	1.8	0.37,0.37,0.05,0.16,0.05,0.0	S/F decreased
3.	5.5	2.0	3.3	0.37,0.37,0.05,0.16,0.05,0.0	S/F increased
4.	6.75	3.0	2.7	0.37,0.37,0.05,0.16,0.05,0.0	Throughput increased
5.	4.5	2.0	2.7	0.37,0.37,0.09,0.10,0.07,0.0	BTX conc. changed
10.	4.5	2.0	2.7	0.37,0.37,0.05,0.16,0.05,0.0	With two values of axial dispersion coefficients $\mathbf{D^c} = 3.0$ and 35 cm^2/s.

S=Solvent feed rate (Average molecular weight = 120)
F=Naphtha feed rate (Average molecular weight = 100)
S/F= Solvent to feed ratio

feed inlet), whereas toluene and o-xylene require full column height to be extracted fully.

One of the key variable in the simulation of extraction process is a dynamic holdup, which is found in the range of 5.2 % to 5.8 % throughout the column see figure 4.4.Forward (main) flows of both phases are also plotted in figures ??. For present case continuous phase axial dispersion coefficient $\mathbf{D^c} = 3.0cm^2/s$ is assumed, whereas no axial dispersion between stages is assumed for dispersed phase i.e. $\mathbf{D^d} = 0.0cm^2/s$. Effect of this dispersion is clearly seen in figure 4.6, which shows higher forward flow in the intermediate stages as compared to inlet and outlet flow rates. Continuous phase velocity which is one of the independent variable is also plotted against stage number in Figure 4.7, ranging from 2.6 to 3.8 mm/s.

Profiles shown and described above are in agreement of real aromatic extraction process. However exact value may not match at this point of time, since model is not fine tuned against real plant data.In the absence of any real plant data, against which model could be tested, some logical tests can be performed over simulation package to check its validity. Simulation run no. 2,3,4 and 5 are devised for this purpose. Simulation runs are performed with the data set corresponding to these runs and each of these runs are then compared independently against results obtained in simulation run 1 (base case).

Simulation run 2(S/F ratio decreased, Figures 4.8,4.12,4.13)

In this continuous phase inlet flow rate (Uin) is increased from 2.0 moles/s (0.20 kg/s) to 3.0 moles/s (0.3 kg/s), keeping solvent (dispersed phase) flow rate as constant at 4.5 moles/s (0.54 kg/s), thus decreasing S/F ratio [2] from 2.7 w/w to 1.8 w/w. Figures 4.8(a,b), show the concentration profiles of BTX (solutes) in continuous and dispersed phase respectively. Since S/F ratio is decreased it should cause less extraction. This is clear from figure 4.8(a), which shows naphtha product leaves as a raffinate with higher aromatic contents (B=0.0%, T=3.1%, X=2.7%) as compared to in figure 4.3(a). On the other side extract phase also leaves with higher content of extracted aromatics (since feed contents of BTX has increased) as compared to figure 4.3(b). Dynamic holdup ranges from 5.3% to 6.0%, (as seen in figure 4.12) not much change is expected, because there is no change in the flow rate of dispersed phase. However continuous phase velocity registers a change, which peaks up to 6.0 mm/s as seen in figure 4.13 compared to 3.8 mm/s in Run 1.

Simulation run 3(S/F ratio increased)(Figures 4.9,4.12,4.13)

In this set, dispersed phase feed flow rate is increased from 4.5 moles/s (0.54 kg/s) to 5.5 moles/s (0.66 kg/s), keeping continuous phase flow rate constant correspond to

[2]Solvent to feed ratio

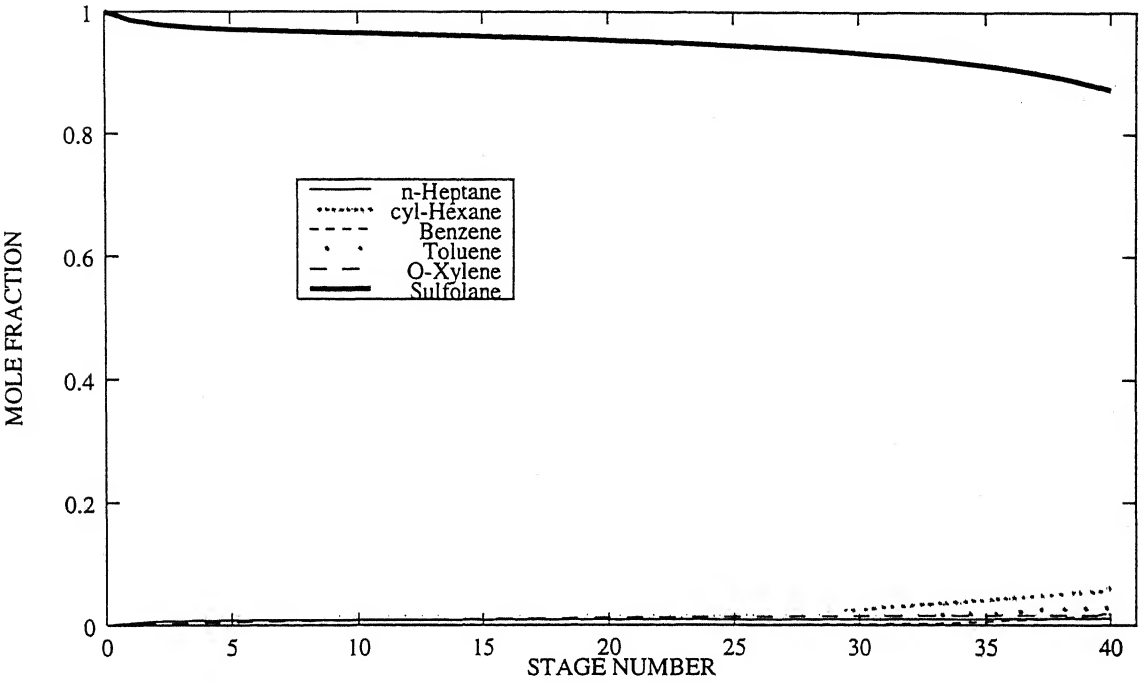

Figure 4.1: Concentration profile for dispersed (Sulfolane) phase (Run 1)

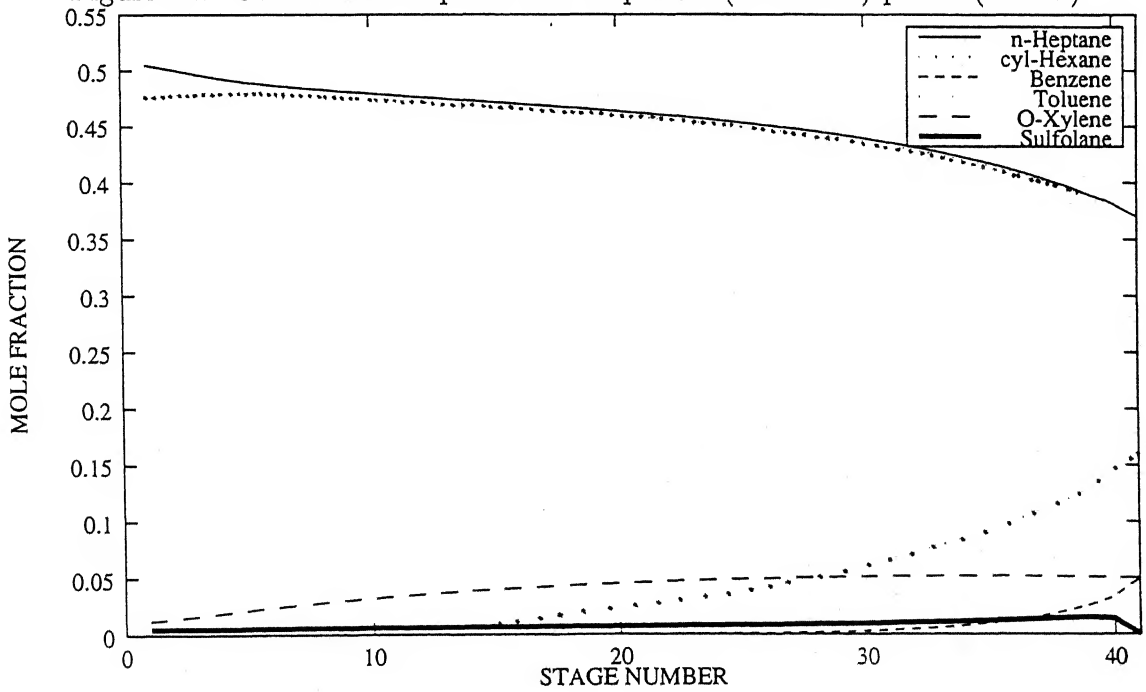

Figure 4.2: Concentration profile for continuous (Naphtha) phase (Run 1)

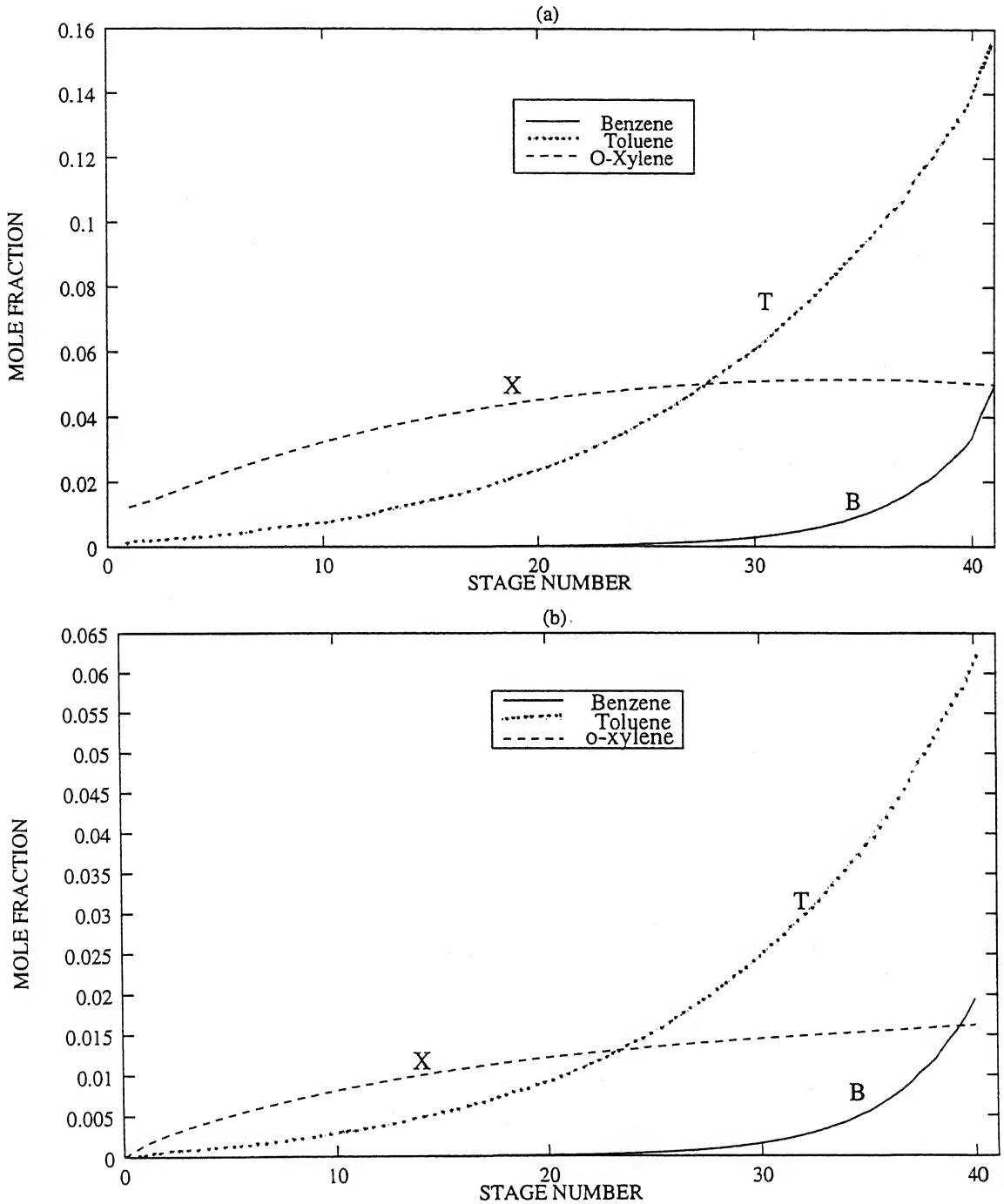

Figure 4.3: Solutes (BTX) concentration profile (a)Continuous naphtha phase (b) Dispersed sulfolane phase (Run1)

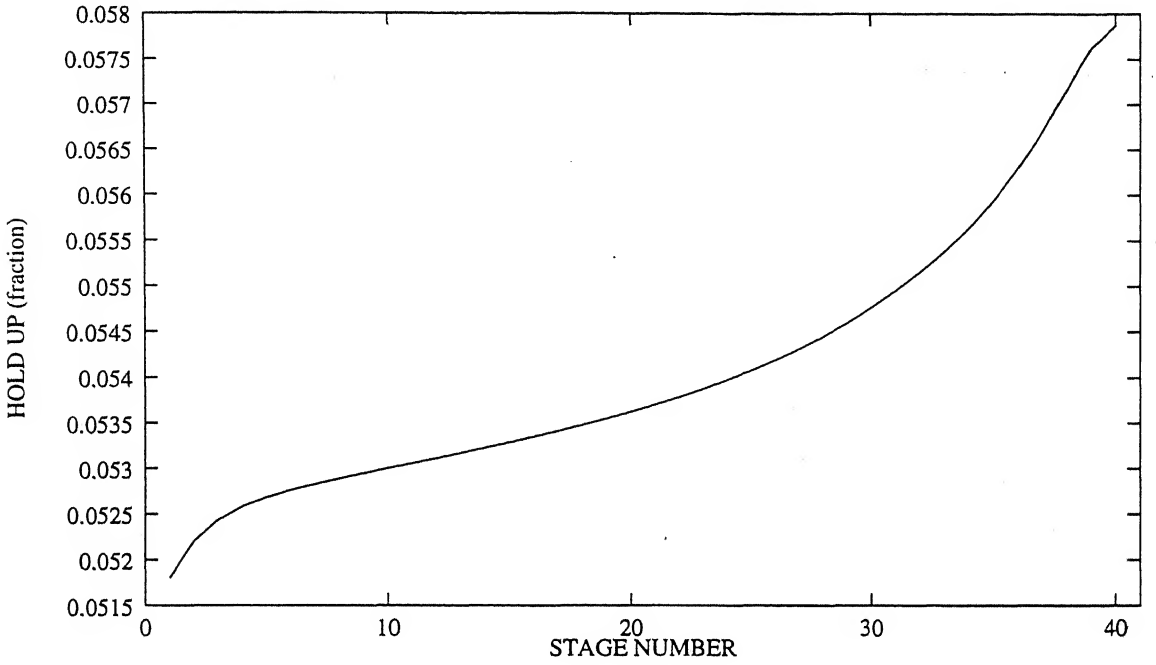

Figure 4.4: Dynamic holdup profile(run 1)

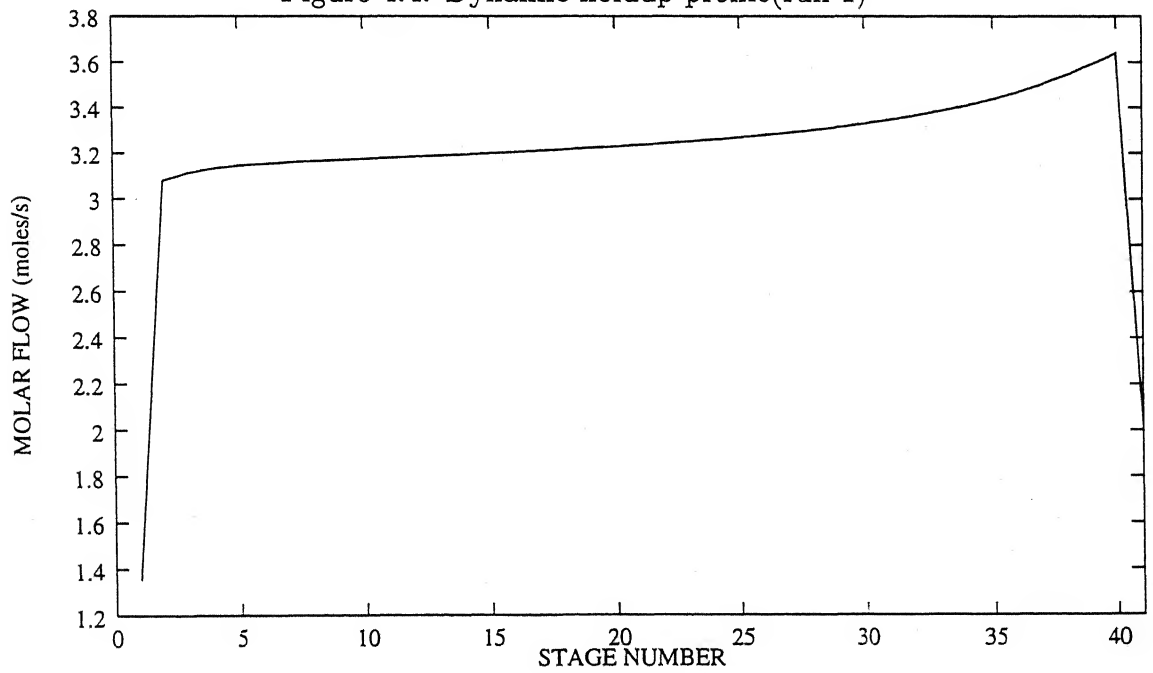

Figure 4.5: Forward flow (continuous phase)(Run 1)

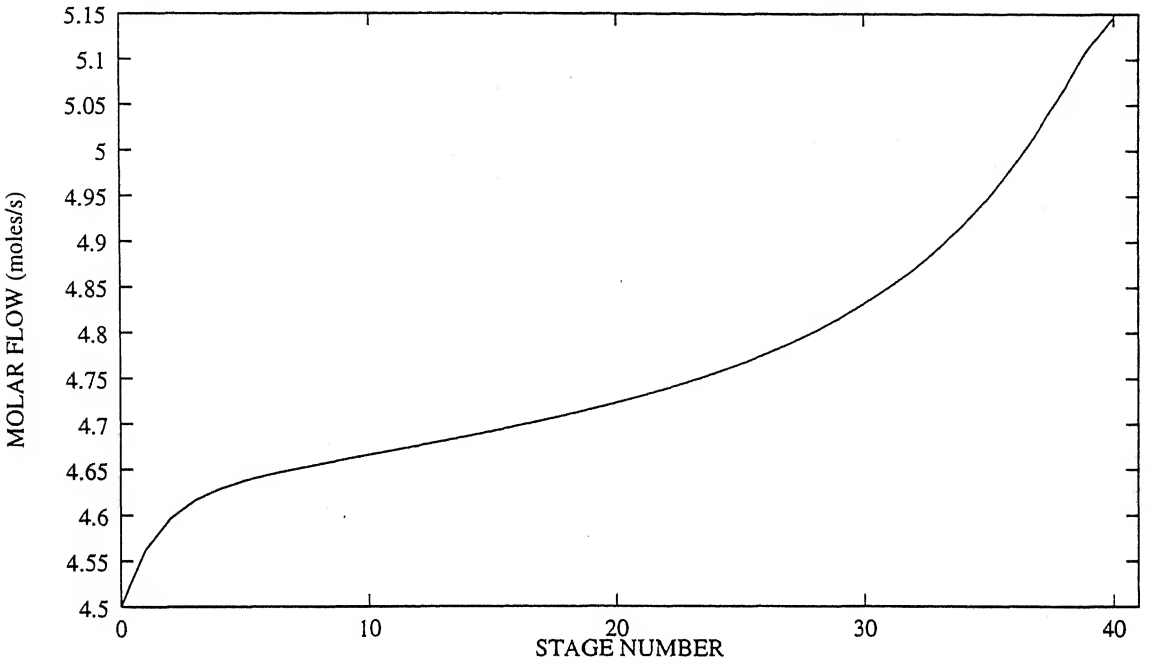

Figure 4.6: Forward flow (dispersed phase)(Run 1)

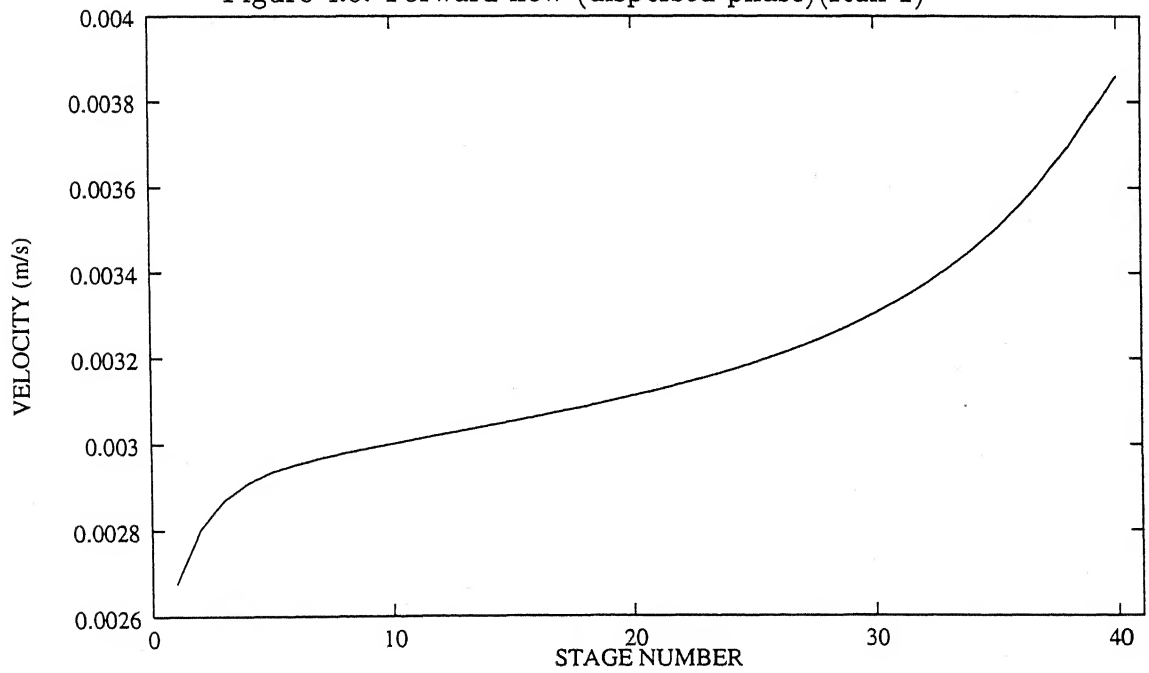

Figure 4.7: Continuous phase velocity(Run 1)

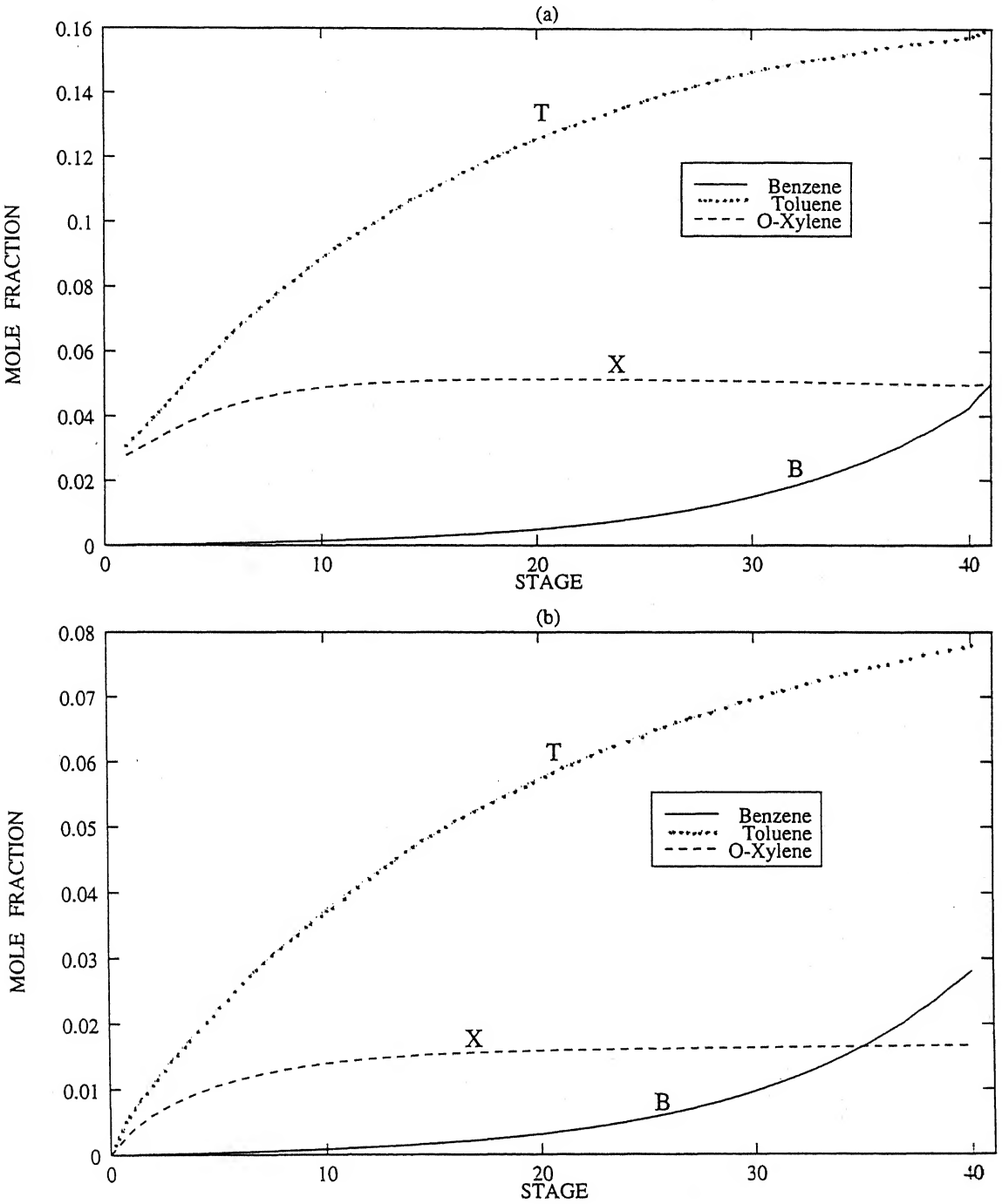

Figure 4.8: Solutes (BTX) concentration profiles (a) Continuous naphtha phase (b) Dispersed sulfolane phase. (Run 2) S/F decreased

simulation run 1 as 2.0 moles/s (0.20 kg/s), thus increasing S/F ration from 2.7 w/w to 3.3 w/w. Again Figures 4.9(a,b) show concentration profiles of solutes (BTX) in continuous and dispersed phase respectively. As per expectation increased S/F ratio causes early extraction of solutes thus reverting concentration profiles for toluene and xylene in continuous phase. Solvent phase even after full extraction carries lower percentage (although high amount) of BTX, as compared to in figure 4.3(b). Dynamic holdup ranges from 6.4% to 7.1%; it is up by 2.0% approximately, mainly due to increase in solvent flow rate as seen in figure 4.12. Continuous phase velocity doesn't register any significant change as seen in figure 4.13.

Simulation run 4(S/F constant, throughput increased)(Figures 4.10,4.12,4.13)

For this run, both continuous and dispersed phase feed flow rates are increased as :

Continuous phase — from 2.0 moles/s (0.20 kg/s) to 3.0 moles/s (0.30 kg/s).
Dispersed phase — from 4.5 moles/s (0.54 kg/s) to 6.75 moles/s (0.81 kg/s).
So flow rates are increased but S/F ratio is kept same at 2.7 w/w. Since column throughput is increased, solute concentration profiles do not change as is clear from comparison of Figures 4.10(a,b) to Figures 4.3(a,b). However both dynamic holdup and continuous phase velocity register an upward change in their values. Dynamic holdup (Figure 4.12) peaks to 9.2% and velocity to 6 mm/s (Figure 4.12).

Simulation run 5(BTX concentration changed)(Figures 4.11,4.12,4.13)

In this set, concentration of naphtha feed is changed from (0.37,0.37,0.05,0.16,0.05,0.0) to (0.37,0.37,0.09.0.10,0.07,0.0) i.e in continuous feed – only BTX concentration is disturbed (overall BTX concentartion is not changed). Benzene is extracted up to 25th stage (see figure 4.11[a]) from naphtha feed. BTX concentration profiles are seen with appropriate changes in figures 4.11(a,b) with change in feed contents of BTX. Dynamic holdup does not change since no feed flow rates have been changed as seen in figure 4.12.

The above four logical tests (Run 2,3,4 and 5) have been performed to validate the model as well as computer program written for this purpose. Results obtained in above 4 sets support the validity of the model for the extraction column using the test system 1 chosen for study. Again it must be noted that, these may not tally with the exact values obtained from real plant as model parameters have not been fine tuned against real data. Similar runs have been performed on Test System 2 (water-acetone-toluene) and found satisfactory. Results have been presented in Appendix D.

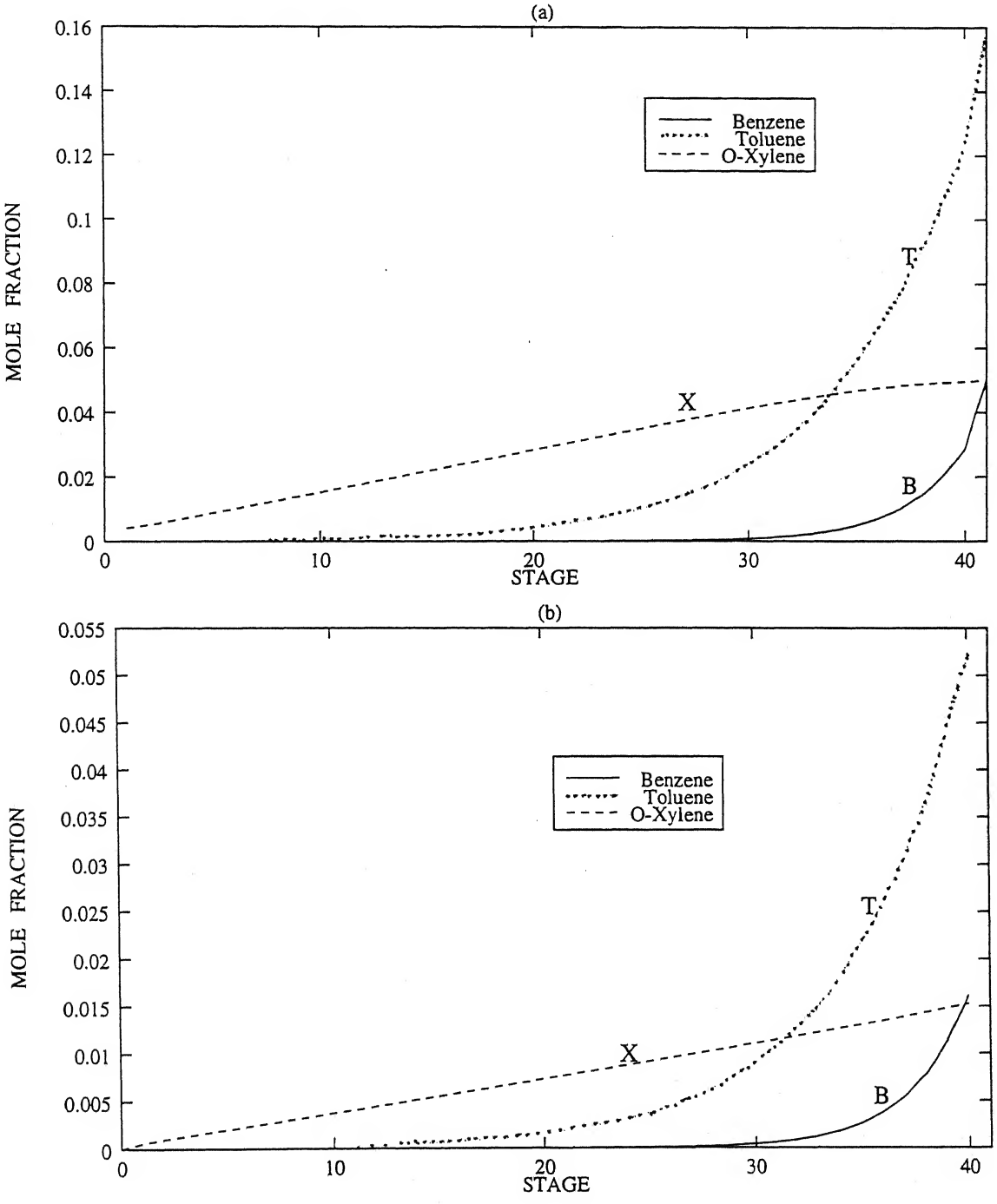

Figure 4.9: Solutes (BTX) concentration profiles (a) Continuous naphtha phase (b) Dispersed sulfolane phase. (Run 3) S/F increased

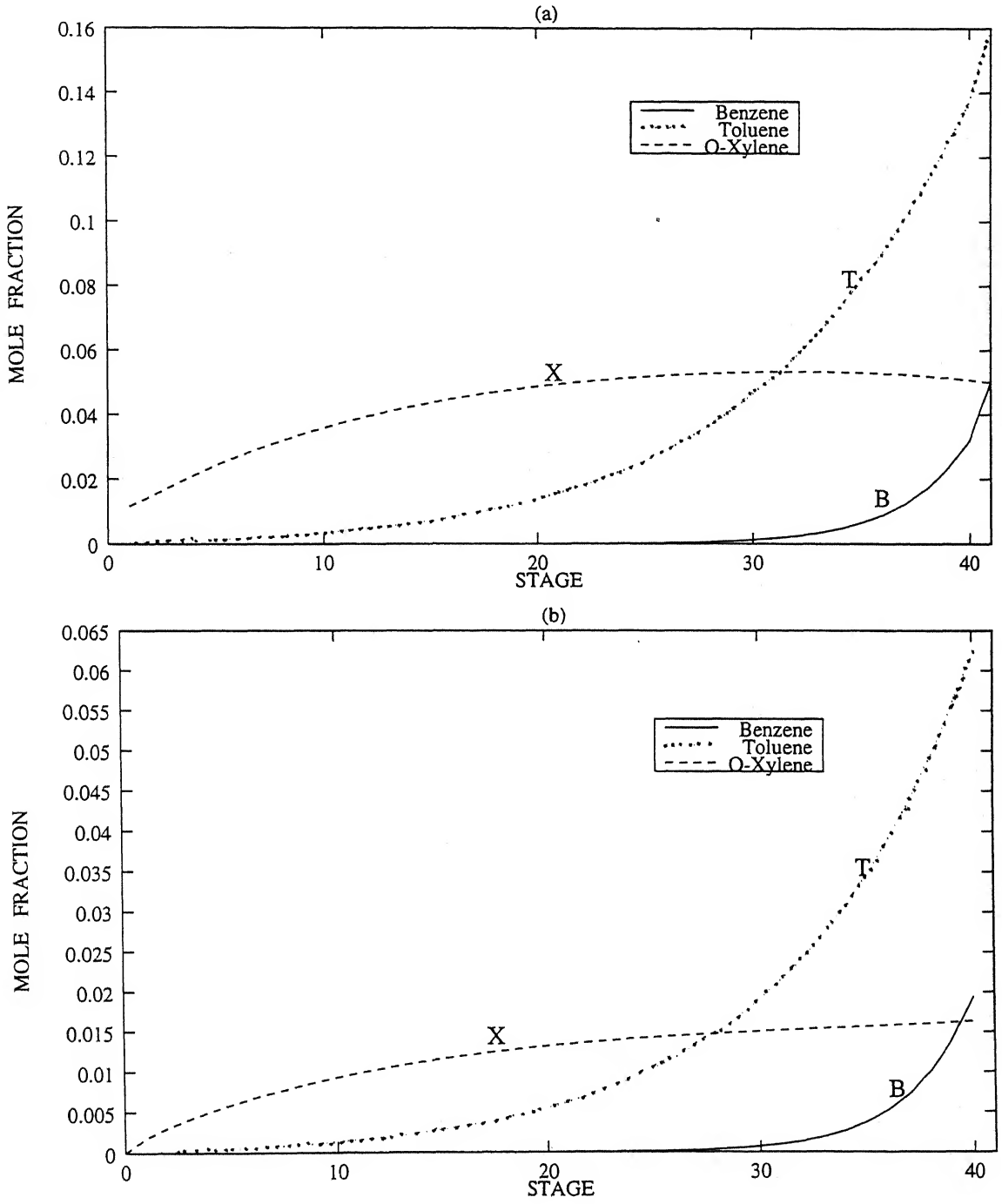

Figure 4.10: Solutes (BTX) concentration profiles (a) Continuous naphtha phase (b) Dispersed sulfolane phase. (Run 4) throughput increased

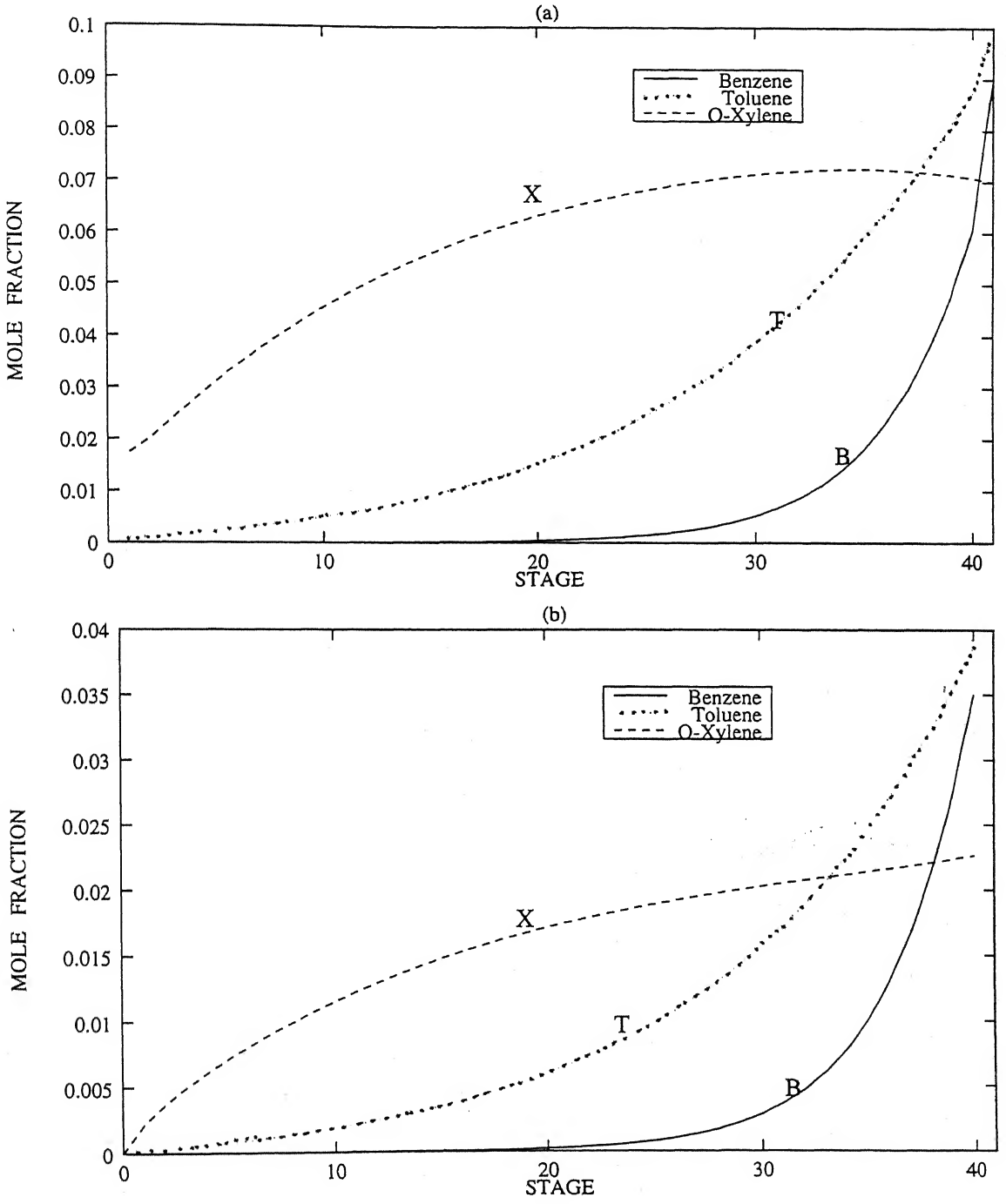

Figure 4.11: Solutes (BTX) concentration profiles (a) Continuous naphtha phase (b) Dispersed sulfolane phase. (Run 5) Inlet BTX concentration changed

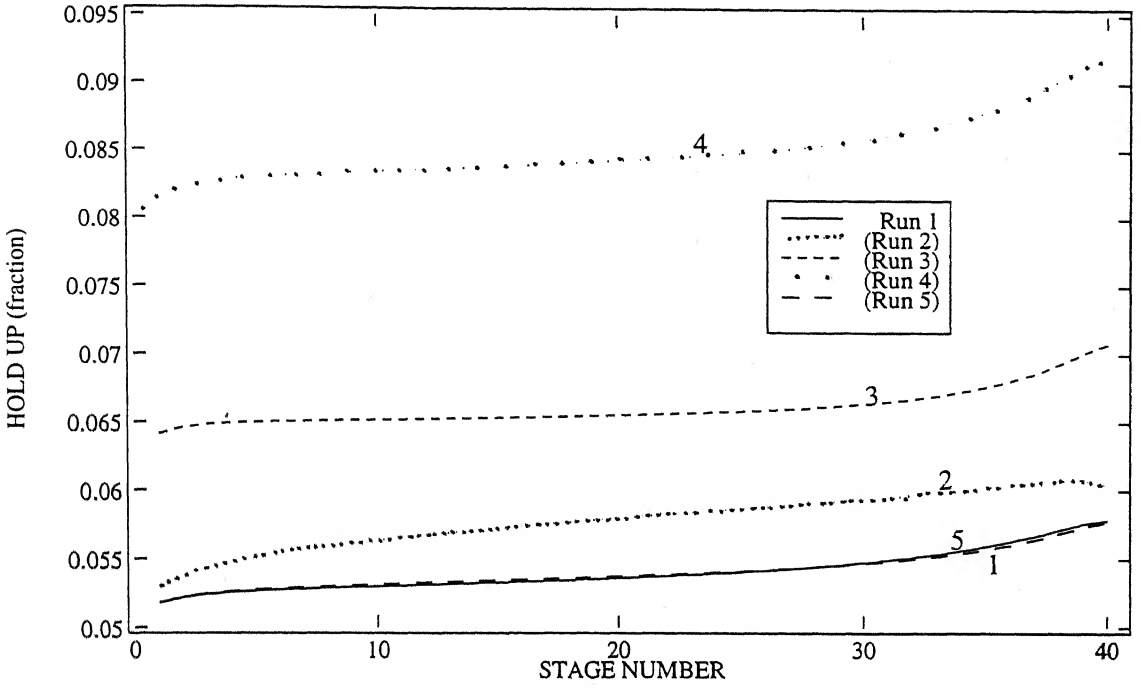

Figure 4.12: Comparative dynamic holdup profiles for simulation runs.

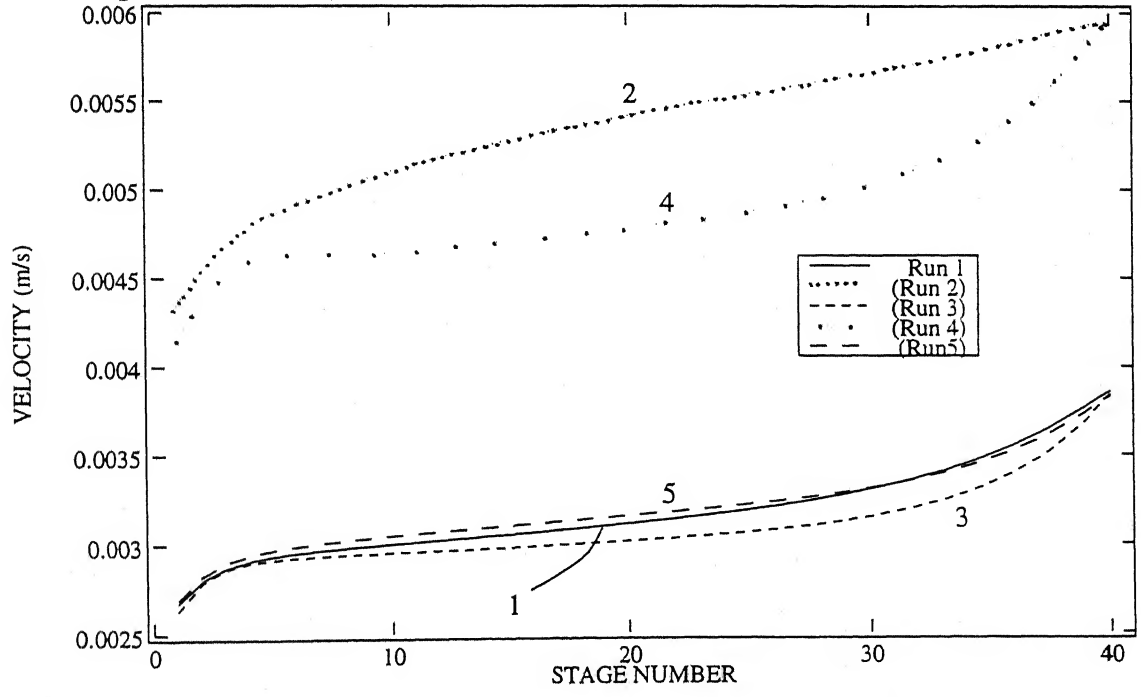

Figure 4.13: Comparative continuous phase velocity for simulation runs.

4.3 Dynamic simulation results

Test SYSTEM 1

Same system (Naphtha-BTX-Sulfolane) has been chosen for dynamic simulation testing and analysis. DASSL method has been used to solve set of 1440 DAE, formed for this system for 40 stage extraction column discussed in section 4.2. Out of 1440 equations 480 equations are differential equations and rest are algebraic equations. DASSL evaluates the derivative of independent simulation variables and the set of 1440 equations are solved by using N-R method at any instant of time; termination criteria being same as used in steady state simulation(4.2). Following results are obtained from the dynamic simulator. Four simulation runs (Run 6 to 9) have been performed to study dynamic behavior. Summary of these results is presented in Table 4.2

Table 4.2: Dynamic simulation runs

Run no.	*Total Run time*	*Perturbation/Remarks*
6.	60 minutes	at 90 seconds; Naphtha feed flow rate (U_{in}) increased from 2.0 moles/s to 3.0 moles/s
7.	90 minutes	at 90 seconds; Sulfolane feed (V_{in}) increased from 4.5 moles/s to 5.0 moles/s
8.	10 minutes	at 50 seconds; BTX concentration in naphtha feed has been disturbed from (0.05,0.16,0.05) to (0.09,0.10,0.07) i.e. keeping overall aromatics content constant.
9.	2.5 hours	at 30 seconds; U_{in} from 2.0 to 3.0 moles/s at 600 seconds; V_{in} from 4.5 to 5.0 moles/s at 1800 seconds; BTX concentration in naphtha feed changed from (0.05,0.16,0.05) to (0.09,0.10,0.07). at 3600 seconds; Unperturbed all the 3 perturbation given so far i.e. resuming feed conditions corresponding to initial state at time t=0 seconds.

Note : In all simulation runs 6 to 9, initial condition at t=0 sec has been assumed at steady state and corresponding to Run 1 (section 4.2).

Simulation run 6(for 60 minutes)(Figures 4.14 to 4.21)

Perturbation is given in the continuous phase flow rate at 90 seconds. Continuous phase flow rate increased from 2.0 moles/s (0.2 kg/s) to 3.0 moles/s (0.3 kg/s) and data are plotted against time scale for different stages selected for analysis. Although each data is available for each stage at every time instant, 3-D plots can be generated and these are discussed later. For the purpose of analysis 2-D graphs are plotted. Figures 4.14(a,b,c), represent the transient profile of concentrations of BTX respectively

in dispersed sulfolane phase. Similarly figures 4.15(a,b,c) show transient response of BTX concentrations in continuous naphtha phase. Concentration of BTX (solutes) increases with time (after 90 seconds) both in dispersed and continuous phase. Since dispersed phase flow rate is not perturbed dynamic holdup plotted in Figure 4.16 registers a slight change at different stages. Step change in continuous phase flow rate at 90 seconds, shown in Figure 4.17 affects the continuous and dispersed phase flow rates exiting from the column, as seen in Figures 4.17 and 4.18.

Simulation run 7(for 90 minutes)(Figures 4.19,4.20,4.21)

For this run perturbation in dispersed phase flow rate is given at 90 seconds. Flow rate of sulfolane phase increased from 4.5 moles/s (0.54 kg/s) to 5.0 moles/s (0.64kg/s). Transient response of solute (BTX) concentrations are plotted in figures 4.19(a,b,c) for dispersed phase and in figures 4.20(a,b,c) for continuous phase. From all these response it can be seen that benzene has been extracted in less time as compared to toluene and o-xylene by sulfolane. This is clear in Figure 4.19(a) which shows benzene concentration profile has achieved steady state faster than other two solutes concentration profile. Figure 4.21 shows the transient response of dynamic holdup at four different stages, which shows significant change in its value due to change in sulfolane flow rate.

Simulation run 8(for 10 minutes)(Figures 4.22,4.23)

For this simulation run, BTX concentration is perturbed in continuous phase feed at 50 seconds. Naphtha feed concentration changed from (0.37,0.37,0.05,0.16,0.05,0.0) to (0.37,0.37,0.09,0.10,0.07,0.0), i.e. overall aromatics (BTX) concentration is kept constant. Effects of changing concentration in feed are plotted in Figures 4.22(a,b,c) for dispersed phase and in Figures 4.23(a,b,c) for continuous phase. From all these six plots, it can be seen that change in BTX concentration significantly affect near the naptha feed point (i.e. at the bottom of the extraction column) since most of the extraction takes place at the bottom of the column. As continuous phase moves upward, change in concentration corresponding to change in feed is not very significant; this confirms the early extraction of aromatics by sulfolane. Similar studies can be carried out for various solvents and based on their response, it can be judged which solvent is best suited for a particular extraction process.

Simulation run 9(for 2.5 hours)(Figures 4.24 to 4.34)

In the absence of any real data, simulation package written must be checked by analyzing some logical tests. For validating the dynamic dynamic simulator. following

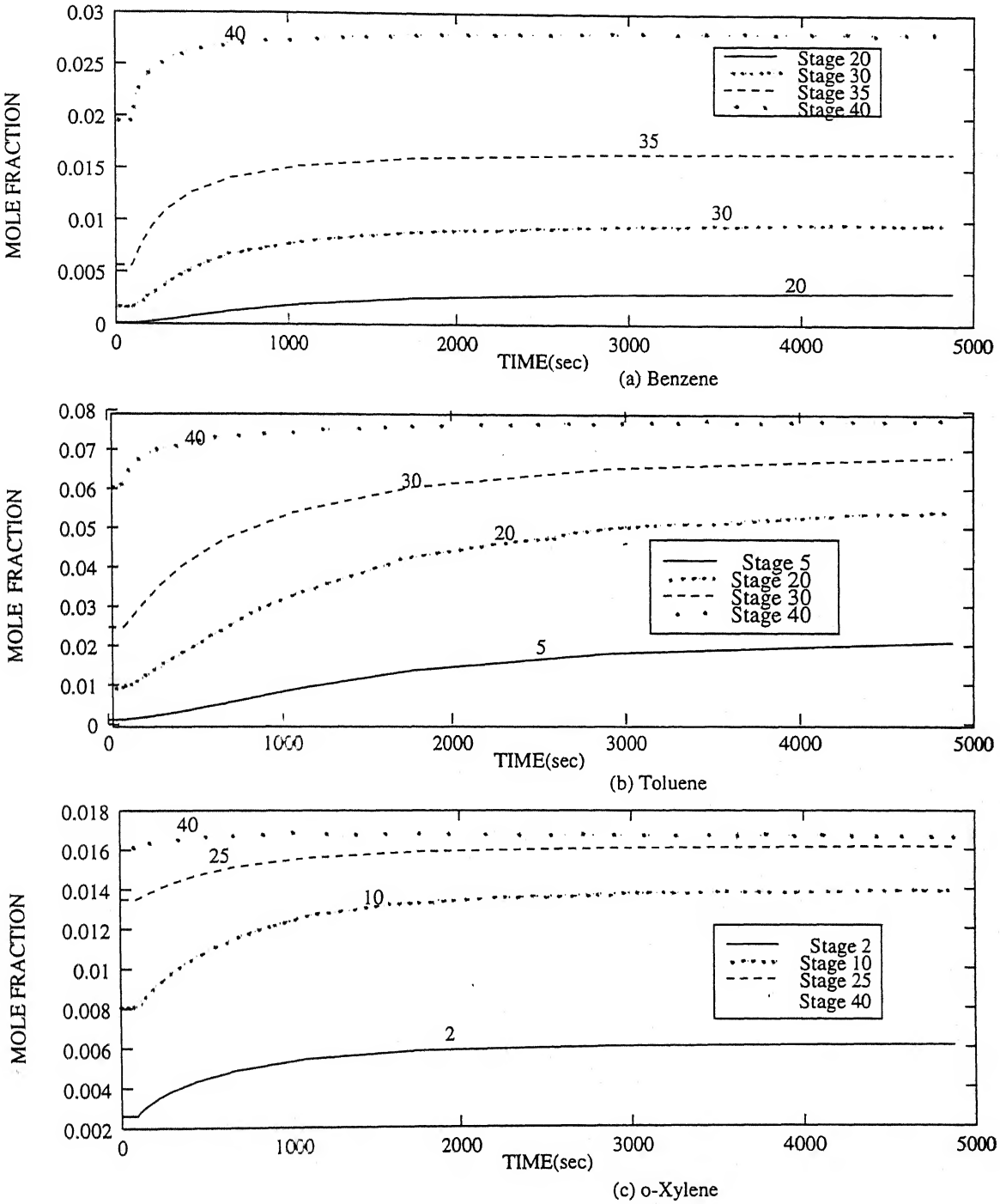

Figure 4.14: Dynamic profile of solutes (BTX) in dispersed sulfolane phase (Run 6)

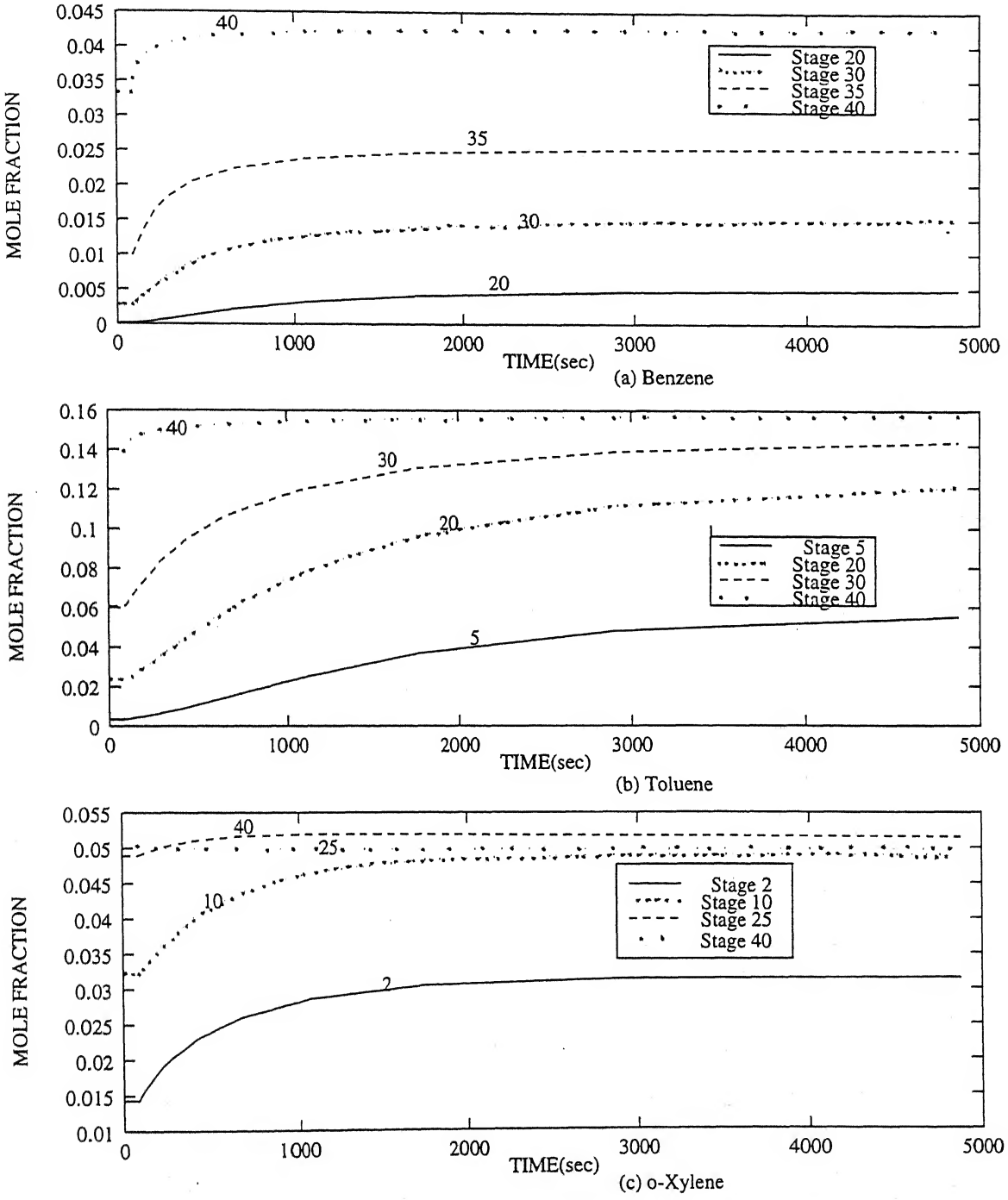

Figure 4.15: Dynamic profile of solutes (BTX) in continuous naphtha phase (Run 6)

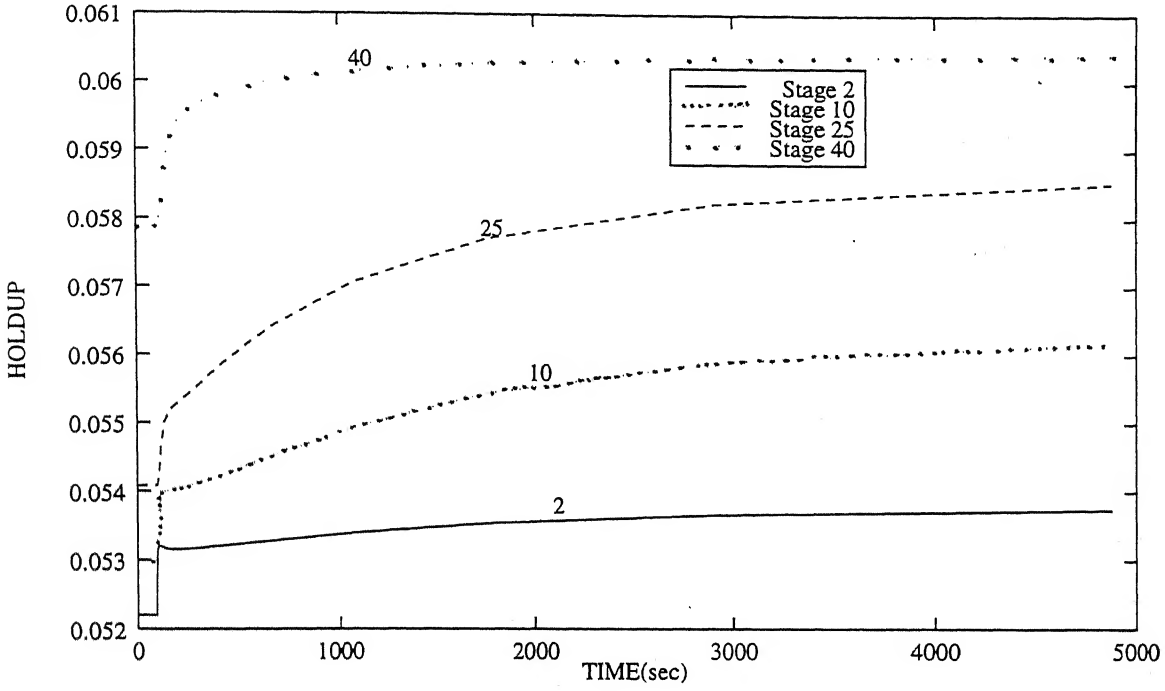

Figure 4.16: Dynamic profile of dynamic holdup (Run 6)

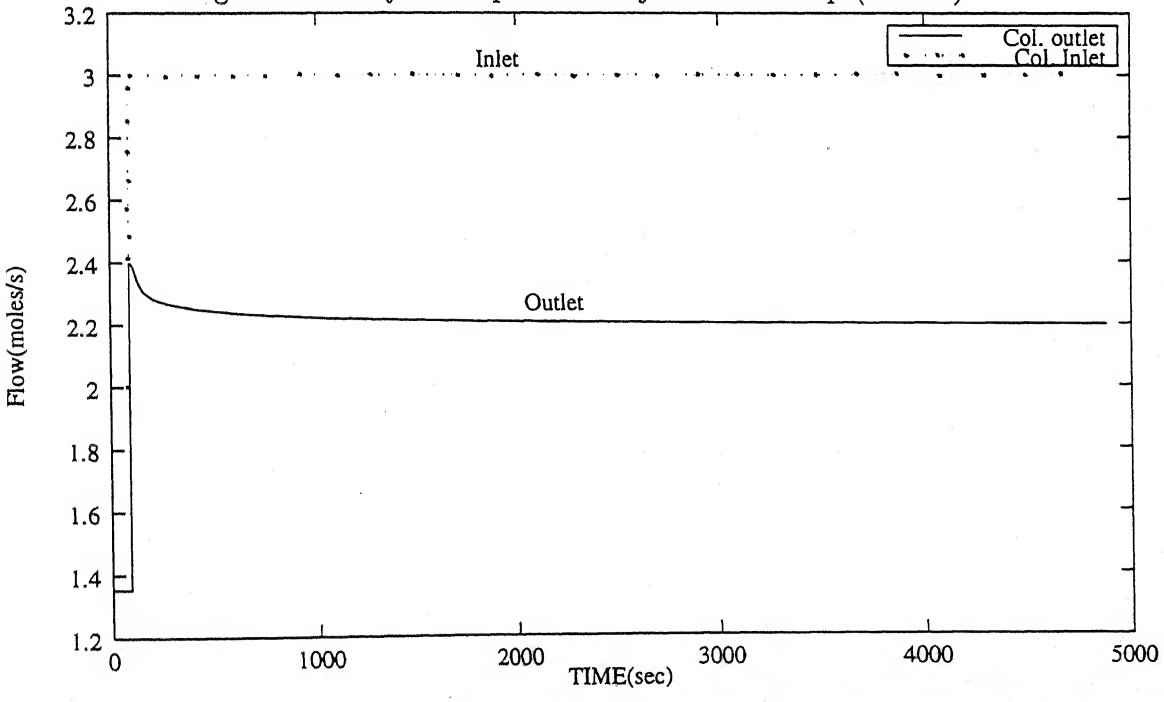

Figure 4.17: Dynamic profile of forward flow (continuous naphtha phase) (Run 6)

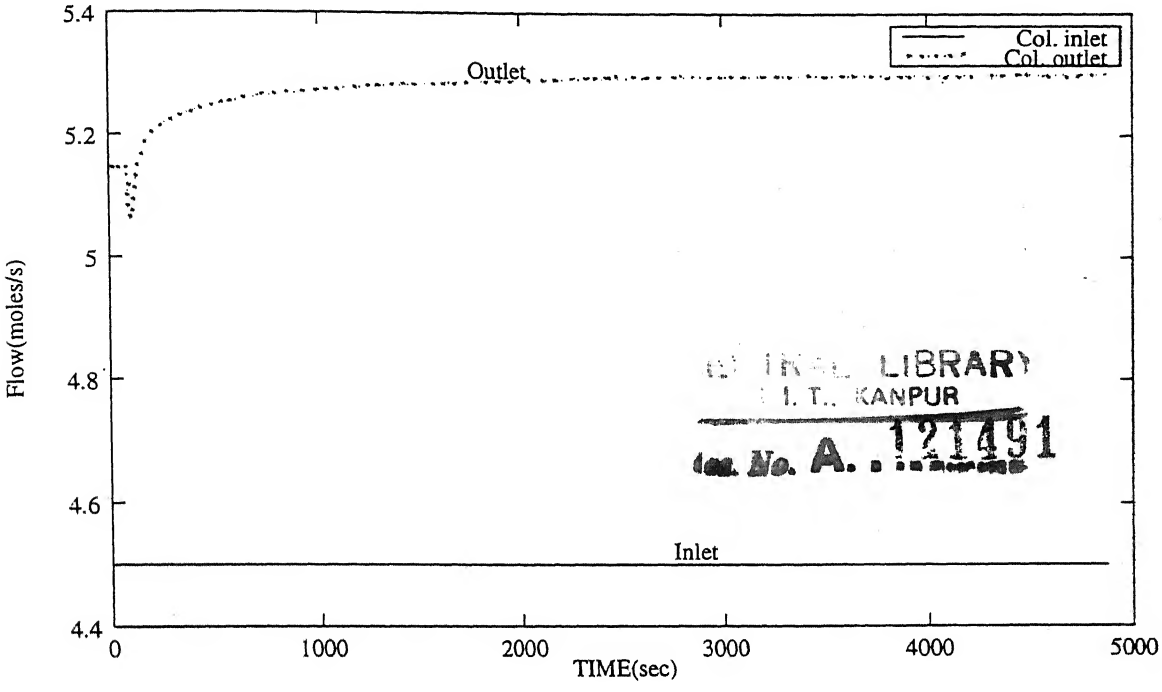

Figure 4.18: Dynamic profile of forward flow (dispersed sulfolane phase) (Run 6)

strategy is devised — three (3) perturbations given in the column feed at different times are :

1. At 30 seconds — Change in continuous phase flow rate from 2.0 moles/s (0.20 kg/s) to 3.0 moles/s (0.30 kg/s).
2. At 600 seconds — Next change in dispersed phase flow rate from 4.5 moles/s (0.54 kg/s) to 5.0 moles/s (0.6 kg/s).
3. At 1800 seconds — Next change in concentration of BTX in naphtha feed from BTX (0.05,0.16,0.05) to (0.09,0.10,0.07), keeping other concentrations constant.
4. At 3600 seconds — Unperturbed all three perturbation given so far.

These three perturbations are introduced at times mentioned and after 1800 seconds (30 minutes) simulation run is further allowed for another 1800 seconds i.e total up to 1 hour without giving any perturbation in last half hour. After 1 hour (3600 seconds), fourth perturbation is introduced in such a way which unperturbed all the previous three perturbations, thus maintaining feed conditions similar to the feed conditions at time t=0 seconds. Simulation run is further allowed for 1.5 hours i.e a total of 2.5 hours, in order to get steady state. The new steady state reached after 2.5 hours matched the initial state at time t=0 seconds (Figures 4.24 to 4.34); also intermediate behavior is as per the expectation for any extraction process. This

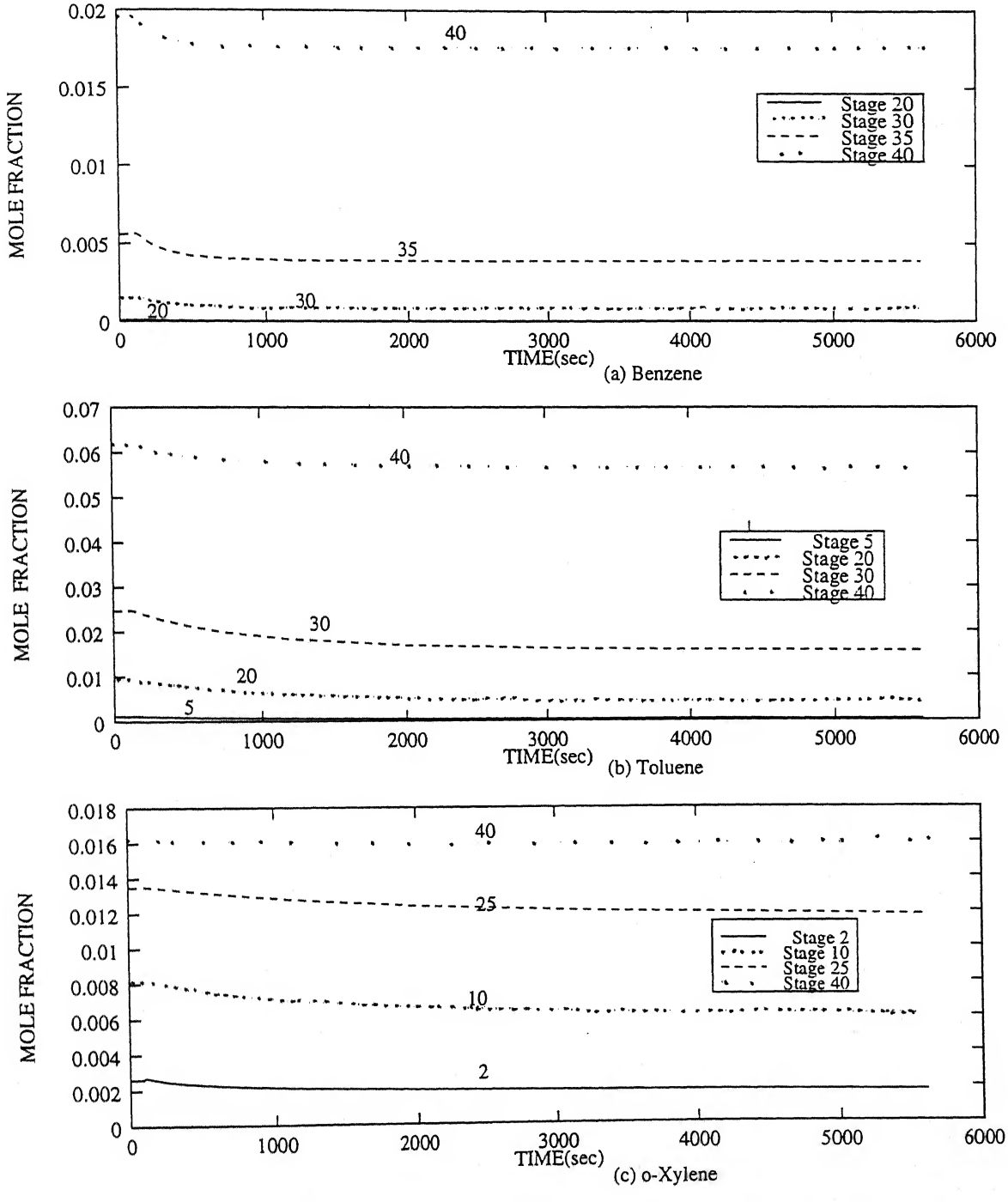

Figure 4.19: Dynamic profile of solutes (BTX) in dispersed sulfolane phase (Run 7)

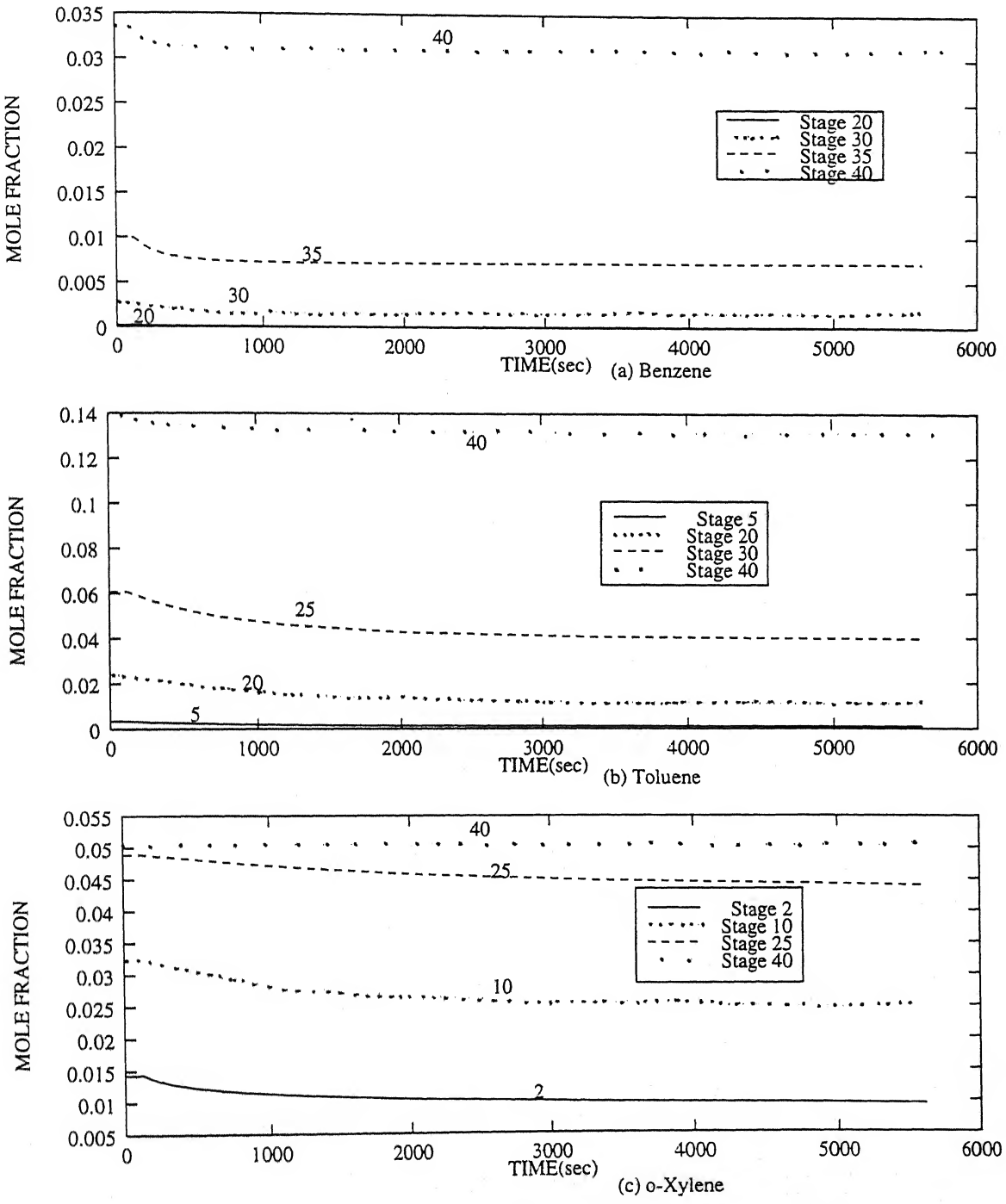

Figure 4.20: Dynamic profile of solutes (BTX) in continuous naphtha pahse (Run 7)

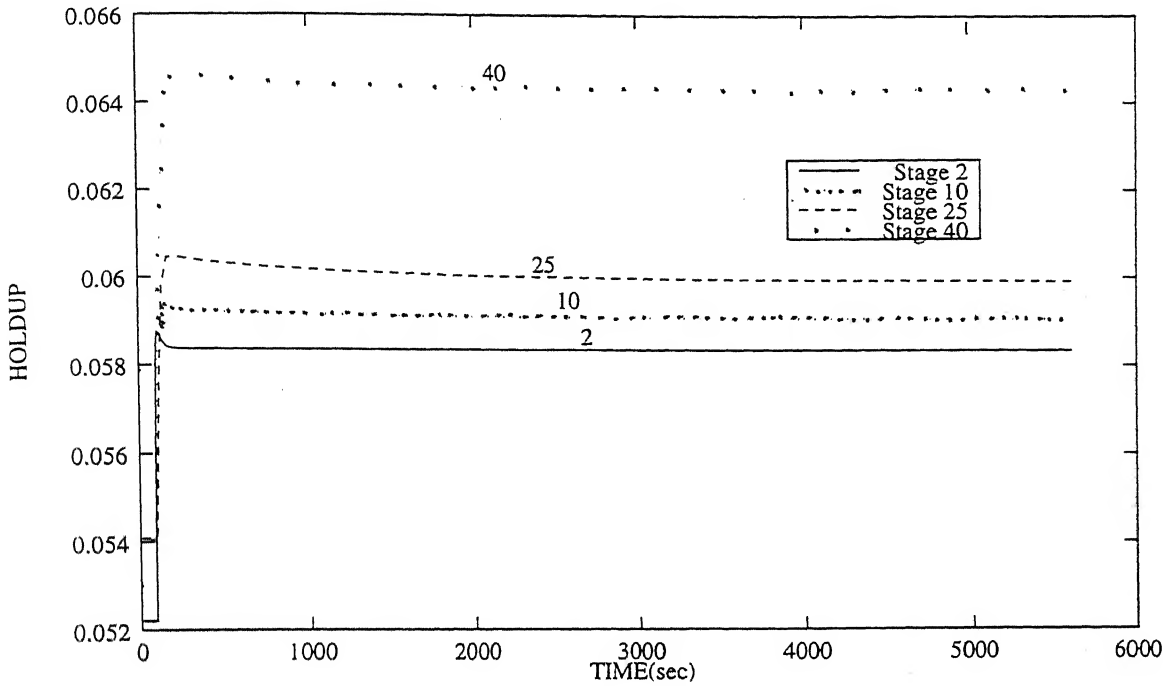

Figure 4.21: Dynamic profile of dynamic holdup (Run 7)

confirms the validity of dynamic part of the simulation code as well as DASSL code. Simulation program gives data for 3-D plots i.e. value of every variable at each time instant for every stage. From these data transient responses have been plotted. Every such plot confirms that the final steady state reached after 2.5 hours is same as initial steady state at t=0 second. Figures 4.30(a,b,c) shows transient response for BTX concentration at different stages in dispersed phase and Figures 4.31(a,b,c) in continuous phase. Figure 4.32 plots the transient response of dynamic holdup at four different stages. It can be seen that perturbations get absorbed quickly by dynamic holdup whereas concentration profiles indicate that perturbation lasts for longer time. This is due to the fact that mass transfer process is slower than physical process. Similarily perturbation lasts for lesser time in forward and backward flows of two phases inside the column. Figures 4.33 and 4.34 reflect such behavior in forward flows of continuous and dispersed phase flow.

Again dynamic simulation is tested in the absence of real plant data. which may predict different values than shown here, but will show similar trends as described here. Model parameters are yet to be fine tuned for real simulation.

Test SYSTEM 2 Similar test are performed for system 2 (water-acetone-toluene) and results are found similar to described above, which confirms the validity of model and simulation code in general (refer to Appendix D).

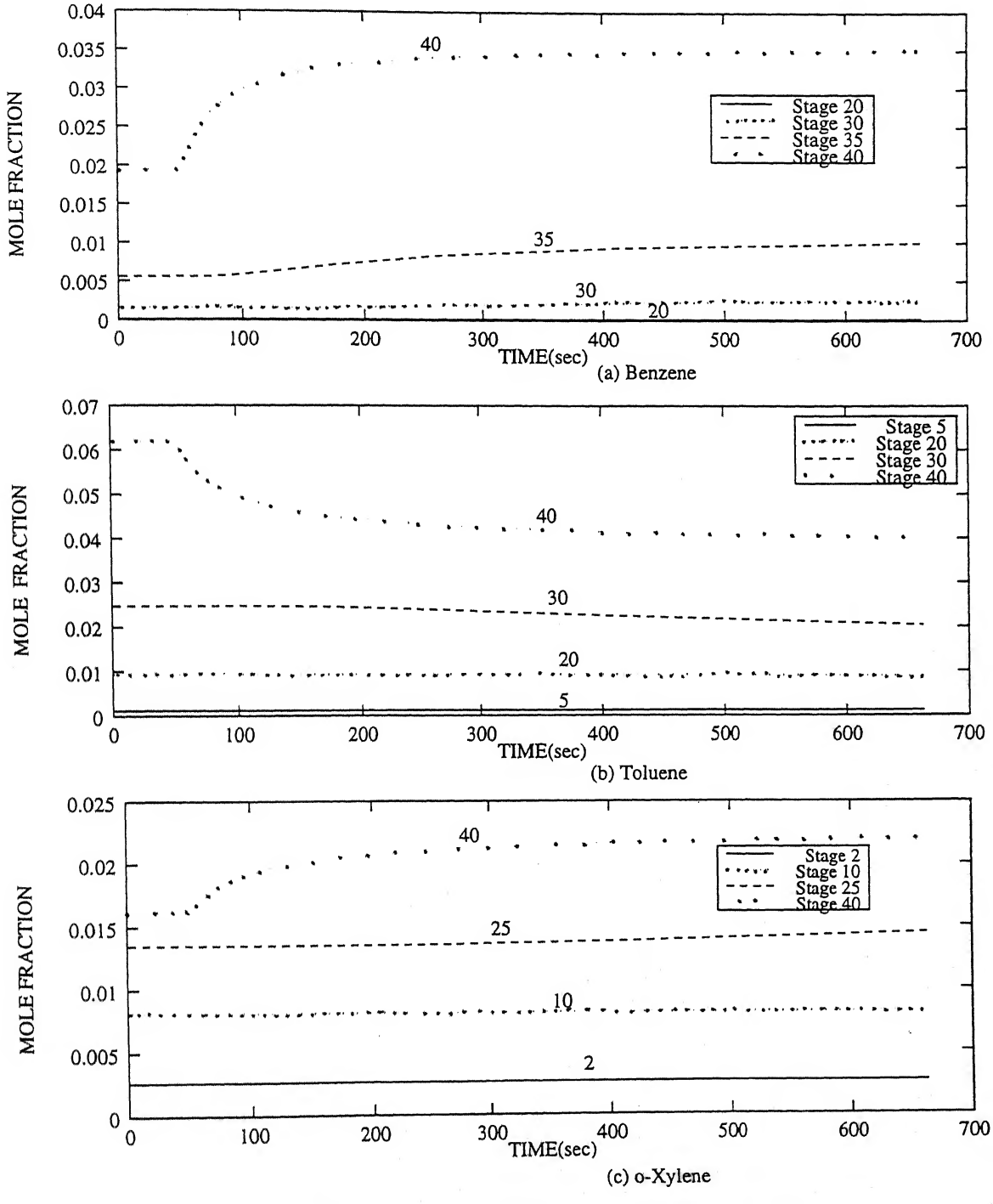

Figure 4.22: Dynamic profile of solutes (BTX) in dispersed sulfolane phase (Run 8)

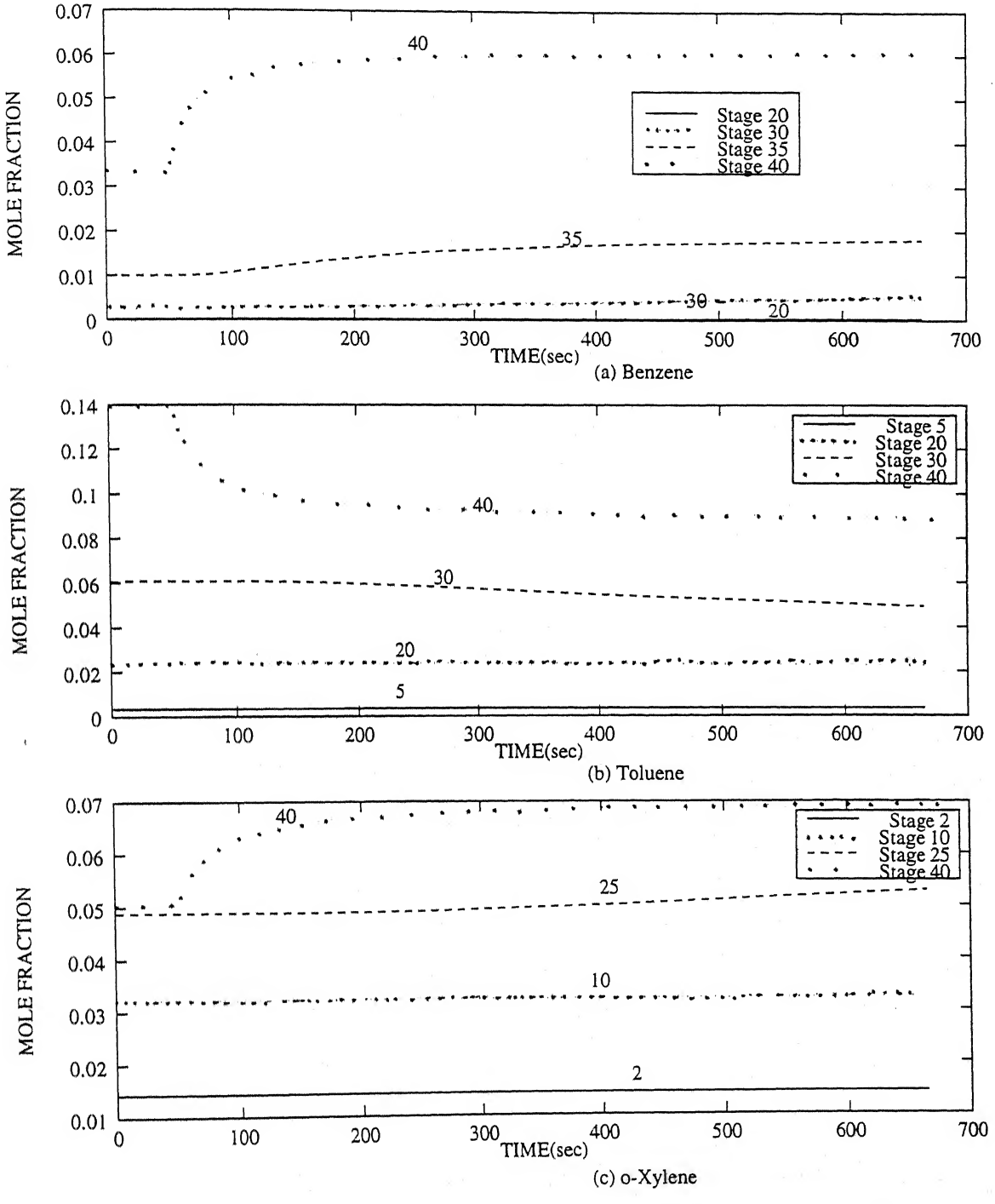

Figure 4.23: Dynamic profile of solutes (BTX) in continuous naphtha phase (run 8)

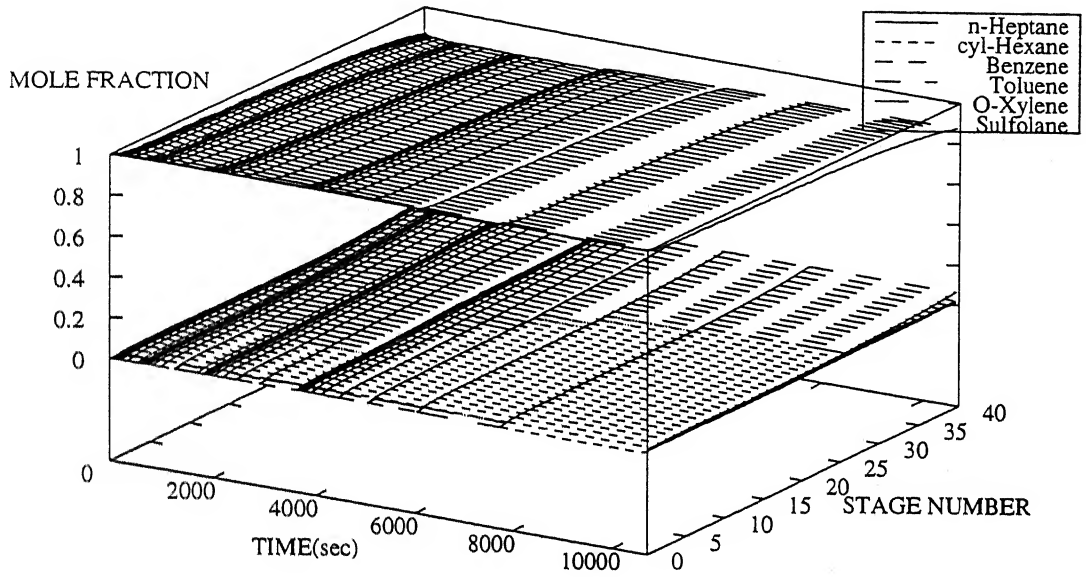

Figure 4.24: Dynamic profile concentration in dispersed sulfolane phase (Run 9)

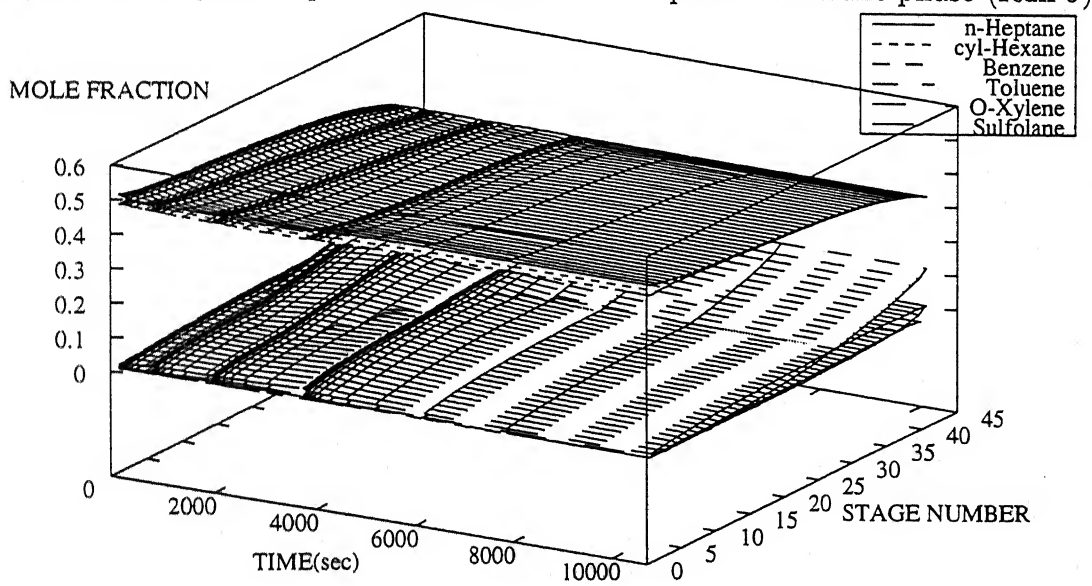

Figure 4.25: Dynamic profile concentration in continuous naphtha phase (Run 9)

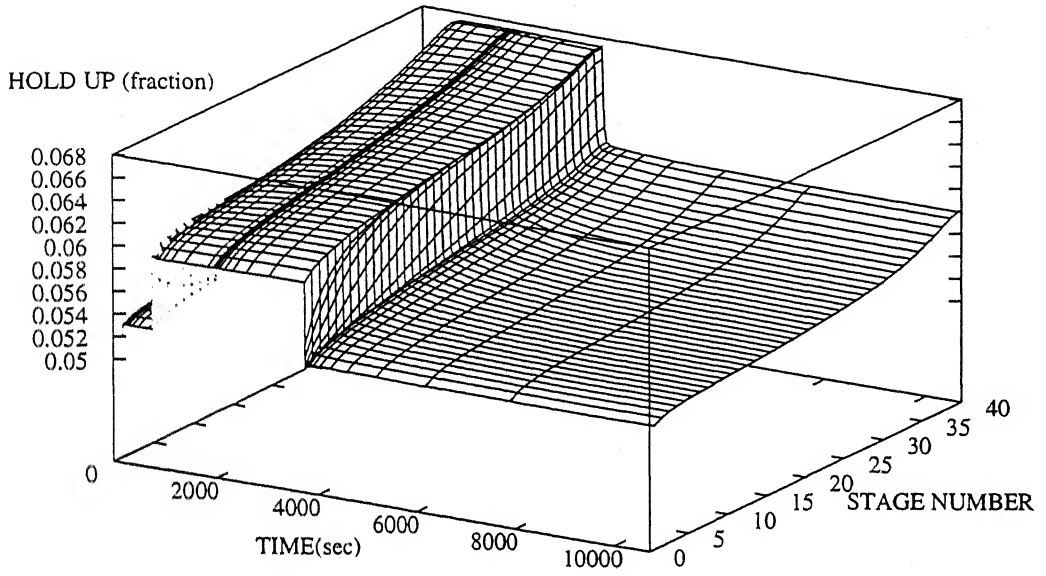

Figure 4.26: Dynamic profile of dynamic holdup (Run 9)

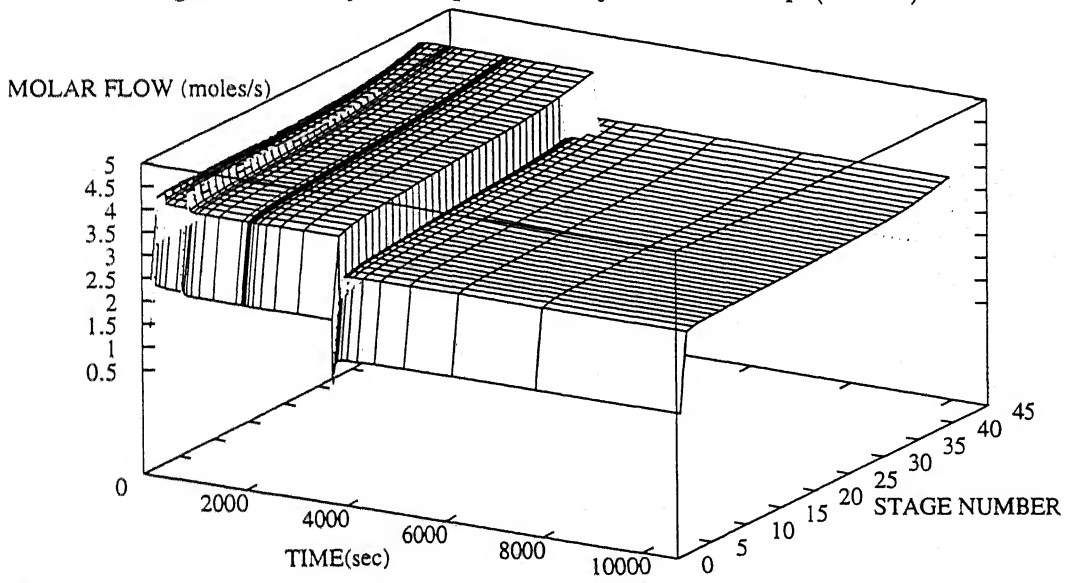

Figure 4.27: Dynamic profile of forward flow (dispersed sulfolane phase) (Run 9)

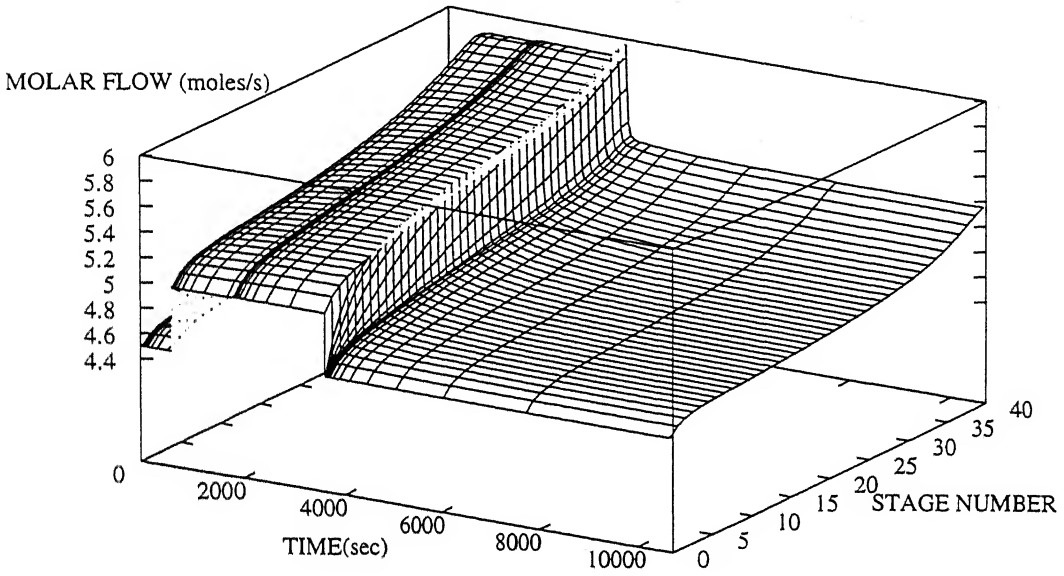

Figure 4.28: Dynamic profile of forward flow (continuous naphtha phase) (Run 9)

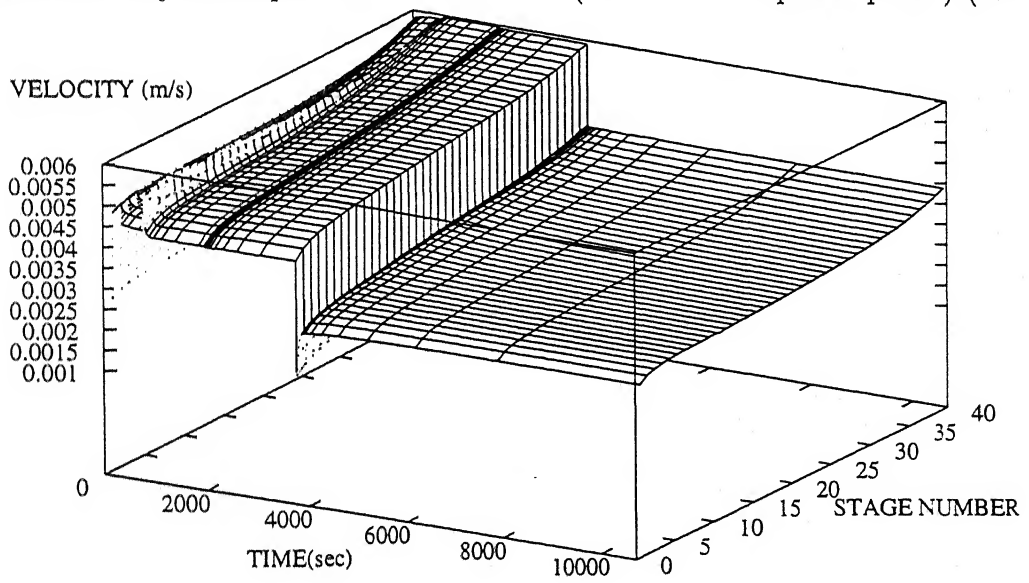

Figure 4.29: Dynamic profile continuous naphtha phase velocity (Run 9)

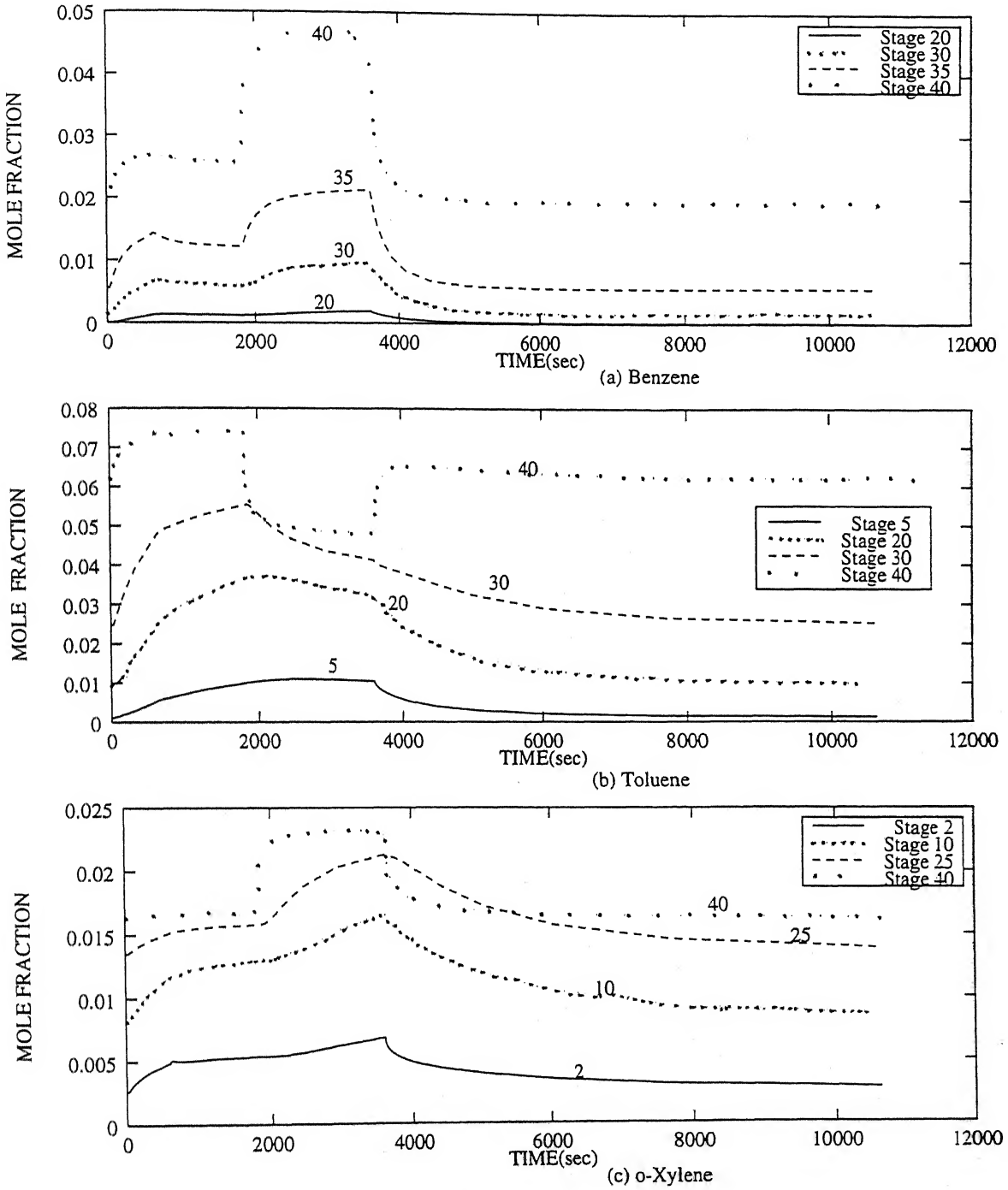

Figure 4.30: Dynamic profile of solutes (BTX) in dispersed sulfolane phase (Run 9)

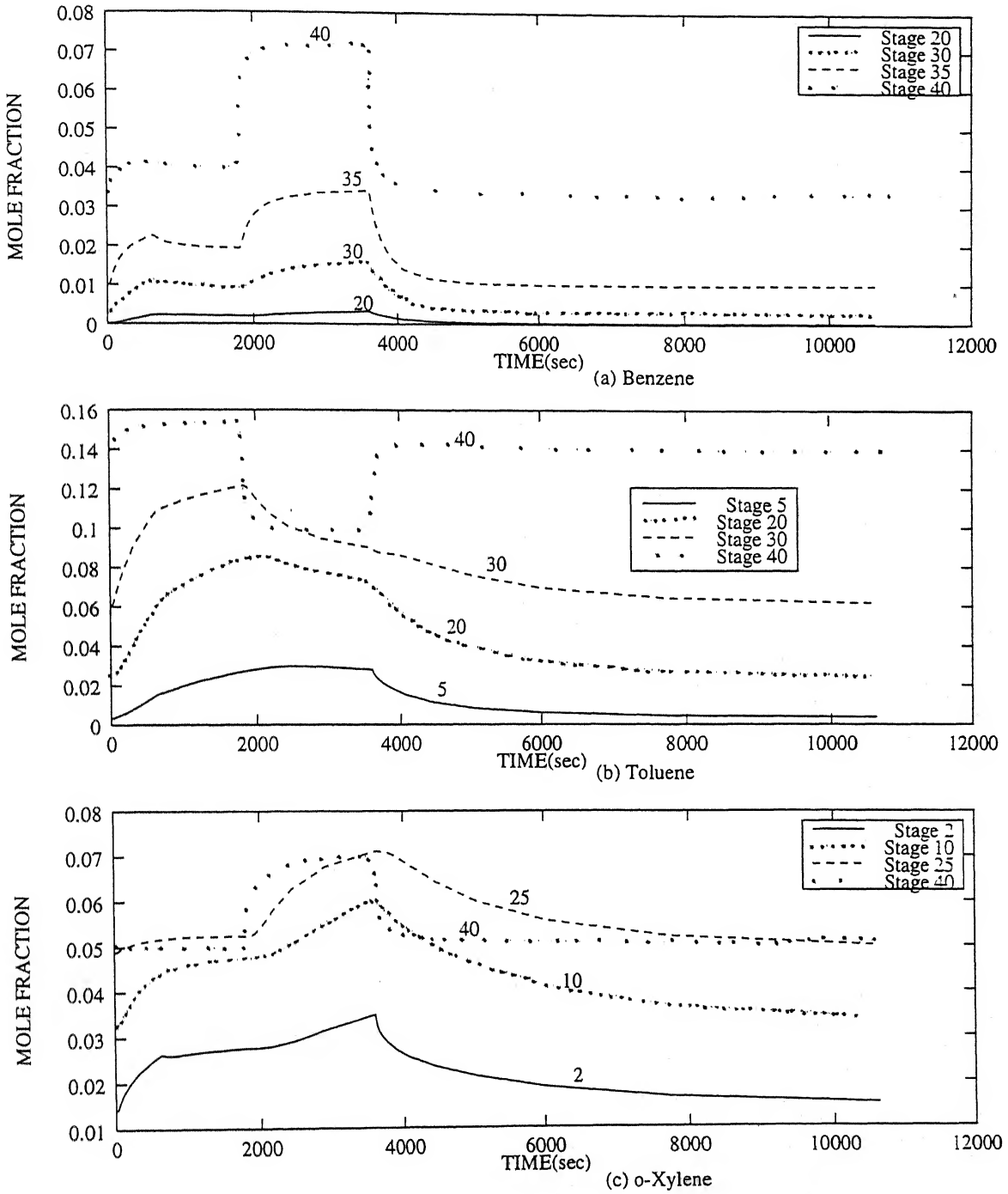

Figure 4.31: Dynamic profile of solutes (BTX) in continuous naphtha phase (Run 9)

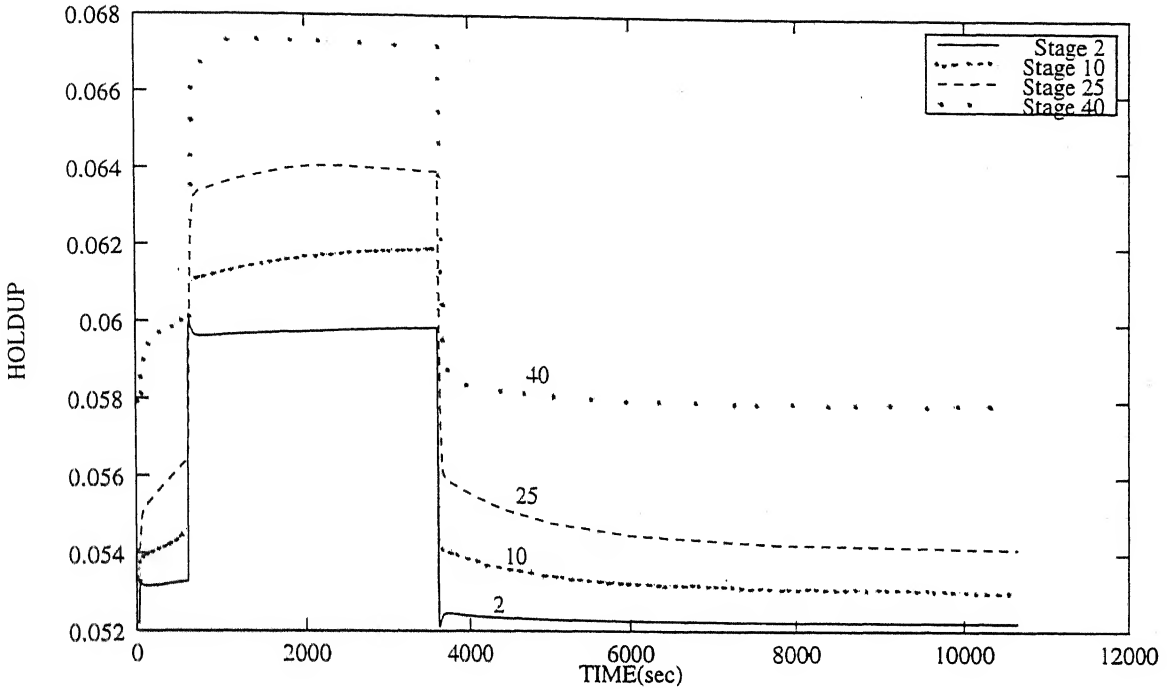

Figure 4.32: Dynamic profile of dynamic holdup (Run 9)

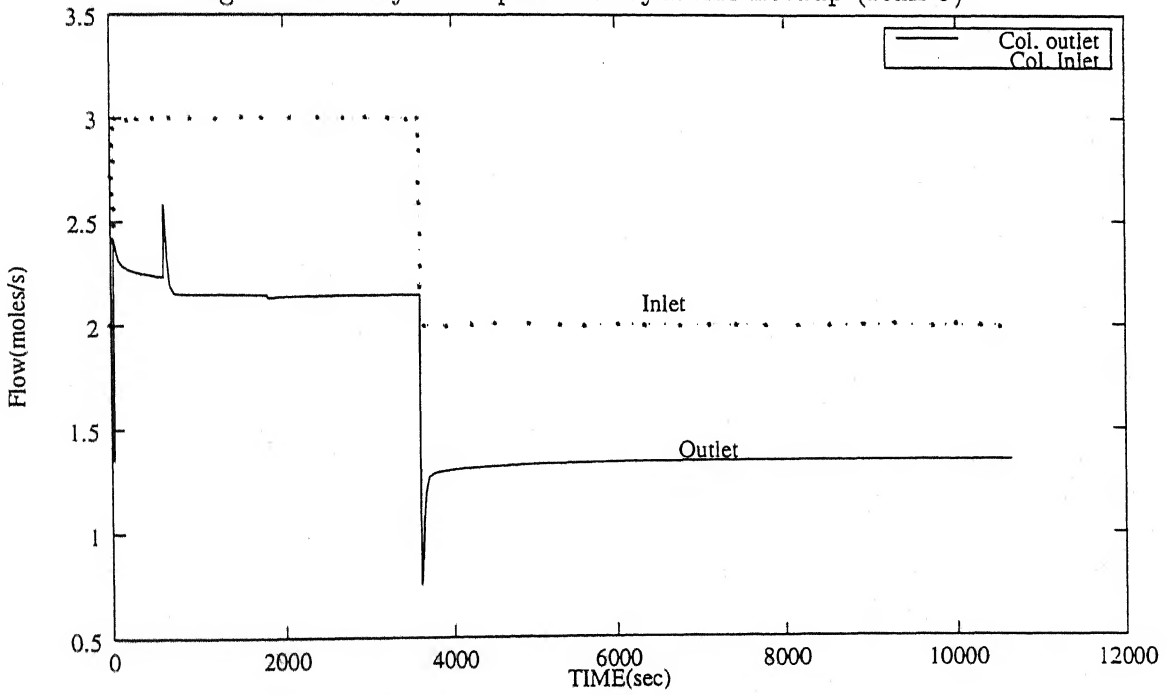

Figure 4.33: Dynamic profile of forward flow (continuous naphtha phase) (run 9)

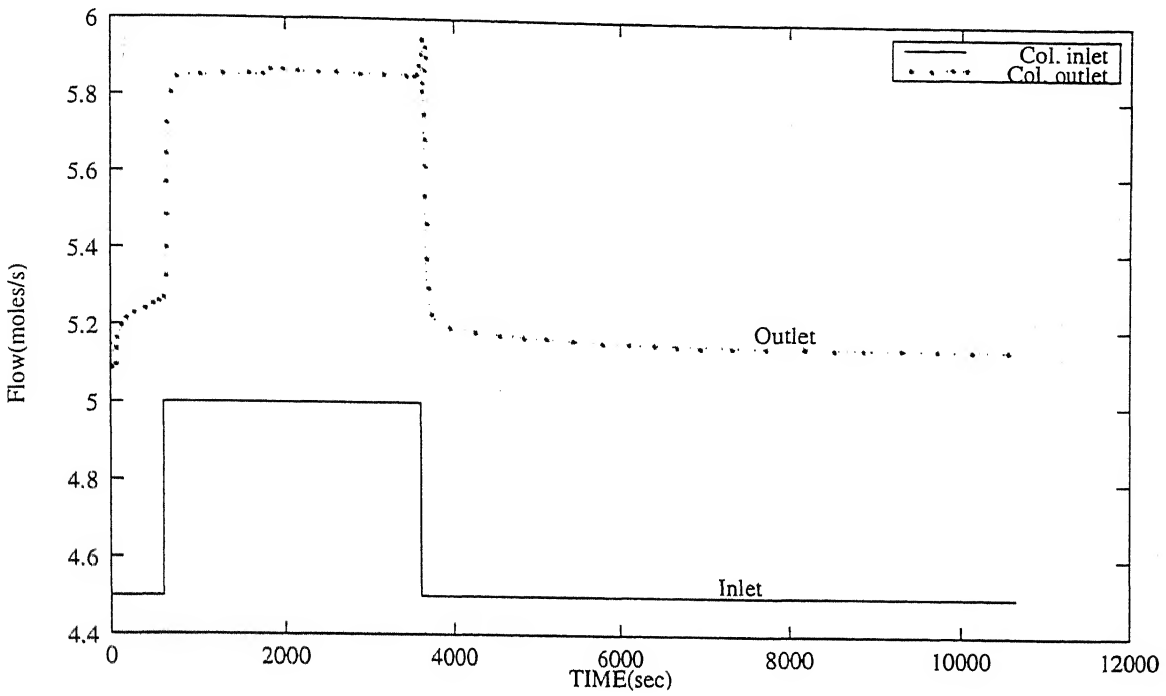

Figure 4.34: Dynamic profile of forward flow (dispersed sulfolane phase) (run 9)

4.4 Effect of axial dispersion

One of the typical phenomena in extraction process is *backmixing* in flow streams between adjacent stages. In present model this backmixing is represented by the contribution of axial dispersion which causes backward flow in both continuous and dispersed phase flow streams as presented in section 2.2.2. Extent of backmixing differs for different types of extraction columns and also depends upon size of equipment and operating conditions. The backmixing effect would be high in agitated columns such as RDC, pulsed sieve tray columns etc. , because of high turbulence. However such effects are not significant in unagitated columns such as spray columns and unagitated sieve tray column. Since we are considering an unagitated sieve tray column, backmixing is assumed only in continuous phase. Backmixing in dispersed phase is neglected completely by the fact that separated compartments of the column by sieve tray may not allow mixing of dispersed phase fluid in adjacent two compartments. Backmixing effect is represented by the axial dispersion coefficients ($\mathbf{D^c}, \mathbf{D^d}$) in model presented here[3]. Correlations of these dispersion coefficients for few types of columns are available in literature (Baird [4]) however these correlations are not well tested and reliable enough to be incorporate in this study.

Simulation run 10(for steady state)(Figures 4.35 to 4.39

[3]Axial dispersion with in stage fluid may be high enough, which supports complete mixing assumption

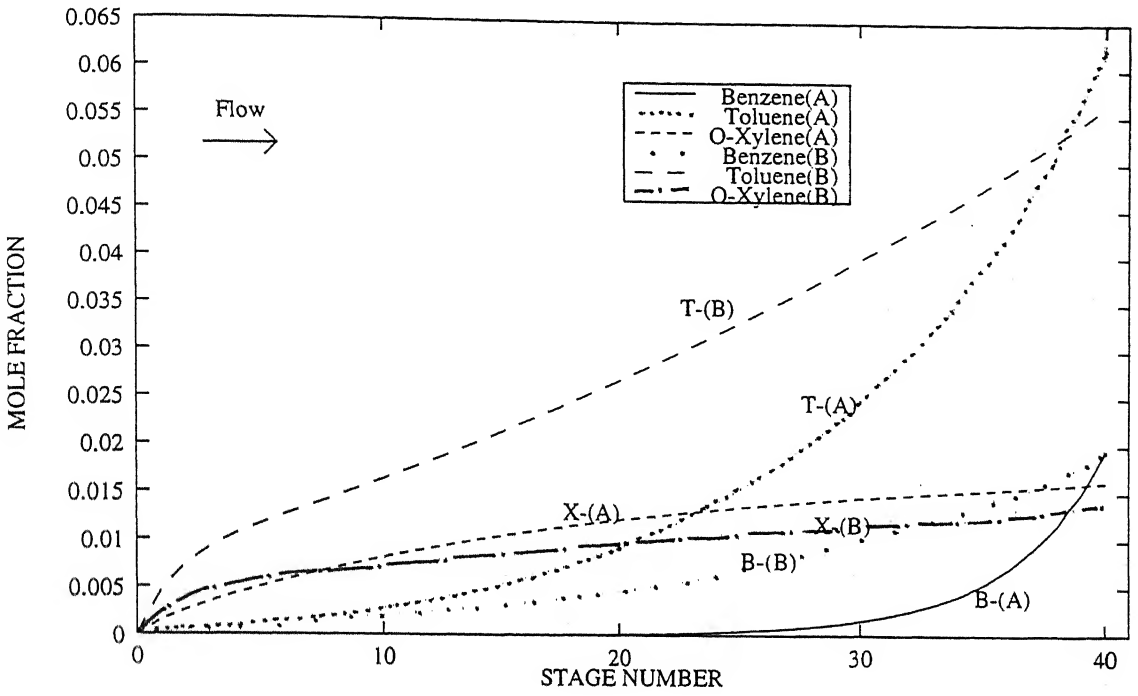

Figure 4.35: Effect of axial dispersion on solute (BTX) profile in dispersed sulfolane phase (A) $\mathbf{D^c} = 3cm^2/s$ (B) $\mathbf{D^c} = 35cm^2/s$

In order to depict axial dispersion affect on extraction process, fixed values of dispersion coefficients $\mathbf{D^c = 3.0cm^2/s}$ and $\mathbf{D^d = 0.0}$ are taken for one simulation run and $\mathbf{D^c = 35cm^2/s}$ and $\mathbf{D^d = 0.0}$ for another simulation. Results obtained from both simulations are imposed together and plotted in Figures 4.35 to 4.39. Higher axial dispersion[4], should cause loss in extraction efficiency. This fact is supported by the results obtained in Figures 4.35 and 4.36. Figure 4.36 shows less extraction from continuous phase, especially of toluene. Figure 4.37 shows the dynamic profile holdups for these two runs. Figure 4.38 shows effect of change in $\mathbf{D^c}$ value on continuous phase forward flow rate sudden change in flow rate is due to higher value of axial dispersion coefficients chosed for stages but not at the ends. Similar change is seen from Figure 4.39 for dispersed phase. These trends are matching with the results published by Zimmermann [7] for pulsed sieve tray column.

[4]means higher backmixing

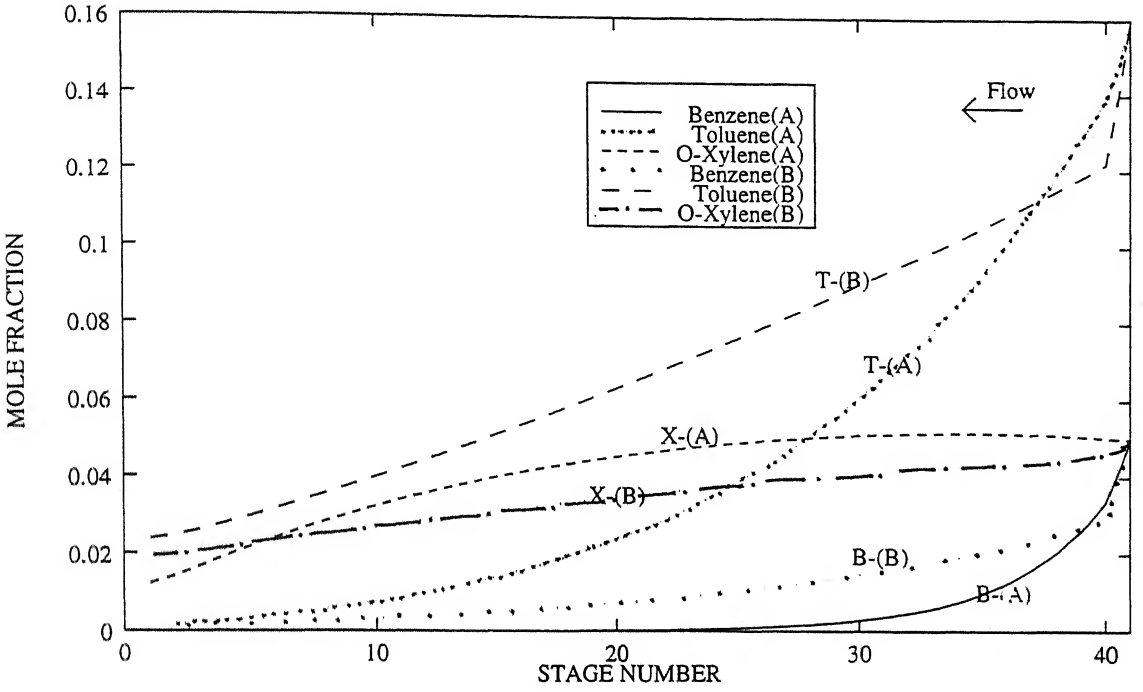

Figure 4.36: Effect of axial dispersion on solute (BTX) profile in continuous naphtha phase (A) $\mathbf{D^c} = 3cm^2/s$ (B) $\mathbf{D^c} = 35cm^2/s$

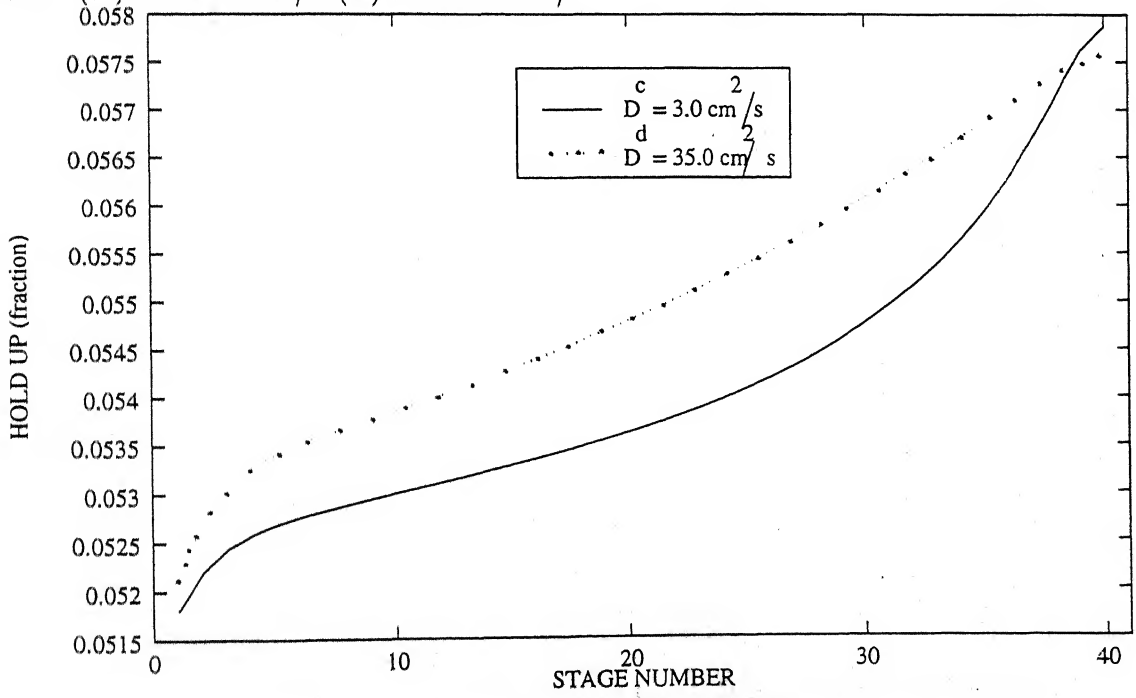

Figure 4.37: Effect of axial dispersion on dynamic holdup profile

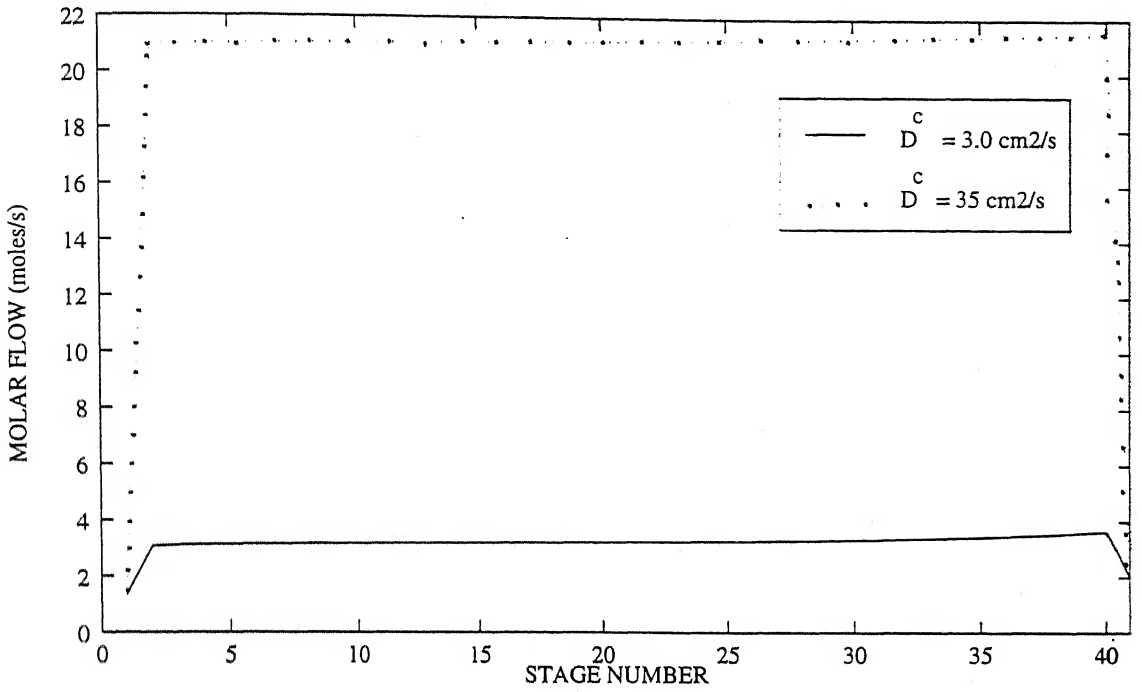

Figure 4.38: Effect of axial dispersion on forward flow (continuous phase)

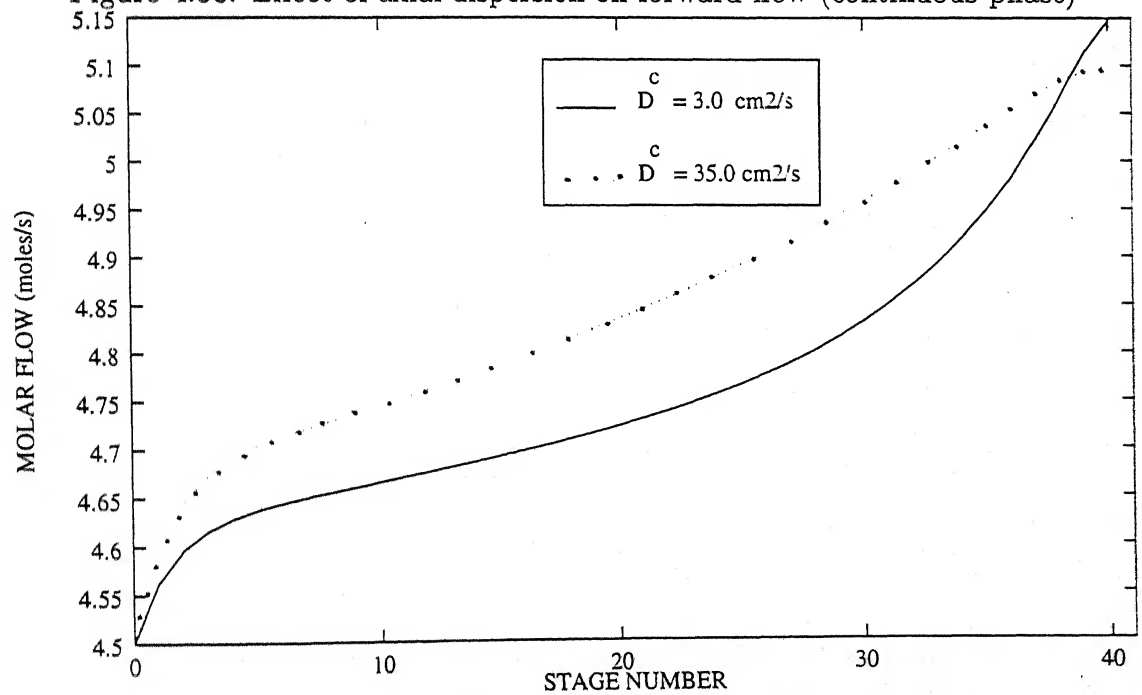

Figure 4.39: Effect of axial dispersion, forward flow (dispersed phase)

4.5 Model parameters

Before going to drop breakage and coalescence effects on extraction process, it is necessary to discuss about model parameters which have to be fine tuned by optimization against real operation data of extraction column. Model used in this study is developed incorporating maximum theoretical considerations and minimum of free parameters. But due to lack of perfect theoretical knowledge about axial dispersion, multicomponent mass transfer coefficients and drop breakage and coalescence, empirical correlations have been used to fill this gap.

For axial dispersion correlation have been developed by several authors (Baird [4, pp 323]), but they are very specific to column size and type of a column. Axial dispersion coefficients $\mathbf{D^c}$ **and** $\mathbf{D^d}$ may therefore be taken as model parameters which have to be tuned for a particular extraction column before applying present model for that column.

Correlations used for calculating dispersed phase velocity u^d and relative velocity u_r^* (see equation B.4 section B.1.2) have empirical constants. Similarly correlations used for drop breakage and coalescence such as breakage frequency, collision frequency and coalescence efficiency (see eqn. B.5 to B.9) also contain empirical constants. These should be determined by experimentation and optimization thereafter. Several attempts have been made in literature to evaluate the values of these empirical constants by carrying out independent studies[5]. The effect of mass transfer may not be significant on these empirical constants; by assuming this, same empirical constants have been used for the mass transfer model in this thesis. However if some of these empirical constants show significant change in their value when mass transfer effects are incorporated then these empirical constants should be included in the list of model parameters and must be determined simultaneously by conducting hydrodynamics cum mass transfer experimentation and optimization thereafter.

In this thesis effort has been made to evaluate mass transfer coefficients rigorously using multicomponent mass transfer theory as developed by Taylor [21]. In some previous works, such as Spencer [3] and Ricker [2], binary mass transfer coefficients have been considered as model parameters and evaluated by optimization for a particular column and extraction process. In present model if binary mass transfer coefficients are not supplied then they are calculated from empirical correlations (equations B.10 to B.13) for particular column and then interactive mass transfer coefficients are evaluated. The use of such correlation may introduce some errors in final result.

Thus only $\mathbf{D^c}$ **and** $\mathbf{D^d}$ can be taken, in the first selection as model parameters. In case of dissatisfatory results other parameters the empirical constants mentioned above may be included in the list of model parameters.

[5] generally without considering mass transfer

4.6 Effect of drop breakage and coalescence

As mentioned in the previous section correlations used for breakage frequency $g(d_j)$, collision frequency $h(d_i, d_j)$ and coalescence efficiency $\lambda(d_i, dj)$ have been tested for agitated columns in literature. Empirical constants used in these correlations have been optimized for agitated columns. Values of these constants used for our work are mentioned in Appendix B with appropriate references to the type of column they were determined for. Since same values have been used in our work for unagitated sieve tray column the results mentioned in this section may not be highly reliable. For the sake of completeness simulation runs have been performed by taking drop breakage and coalescence into account for unagitated sieve tray column.

In order to study only drop breakage and coalescence effects only 4 stage with 8 drop classes have been considered for system 1, instead of 40 stages considered in earlier sections. For unagitated sieve tray column drop spectrum (minimum to maximum diameter of drops) may not be very wide. Following 8 drop classes have selected (refer to section 2.8.2) by the simulator after discretization of drop spectrum.

Drop class	*Diameters (mm)*
(1)	1.43
(2)	1.82
(3)	2.08
(4)	2.29
(5)	2.46
(6)	2.62
(7)	2.76
(8)	2.88

Four simulation runs are carried out as

(a) With drop breakage and coalescence.

(b) With only drop breakage.

(c) With only drop coalescence.

(d) Without drop breakage and coalescence.

Holdup profiles for all the eight drop classes are indicated for these four runs in Figures 4.41(a,b,c,d). Total holdup for these four runs has been compared in Figure 4.42. Corresponding Sauter mean diameter of drop swarm in a stage are plotted in Figure 4.43. No significant effect of drop breakup and coalescence is noticed in these plots, since drop spectrum does not change much due to weak drop breakage and coalescence in unagitated sieve tray columns. Sauter mean diameter show decreasing trend for breakage but increasing trend for drop coalescence as seen in Figure 4.43.

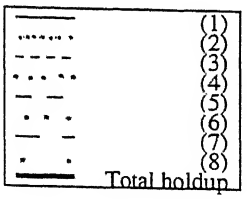

Figure 4.40: Key for Figures 4.41

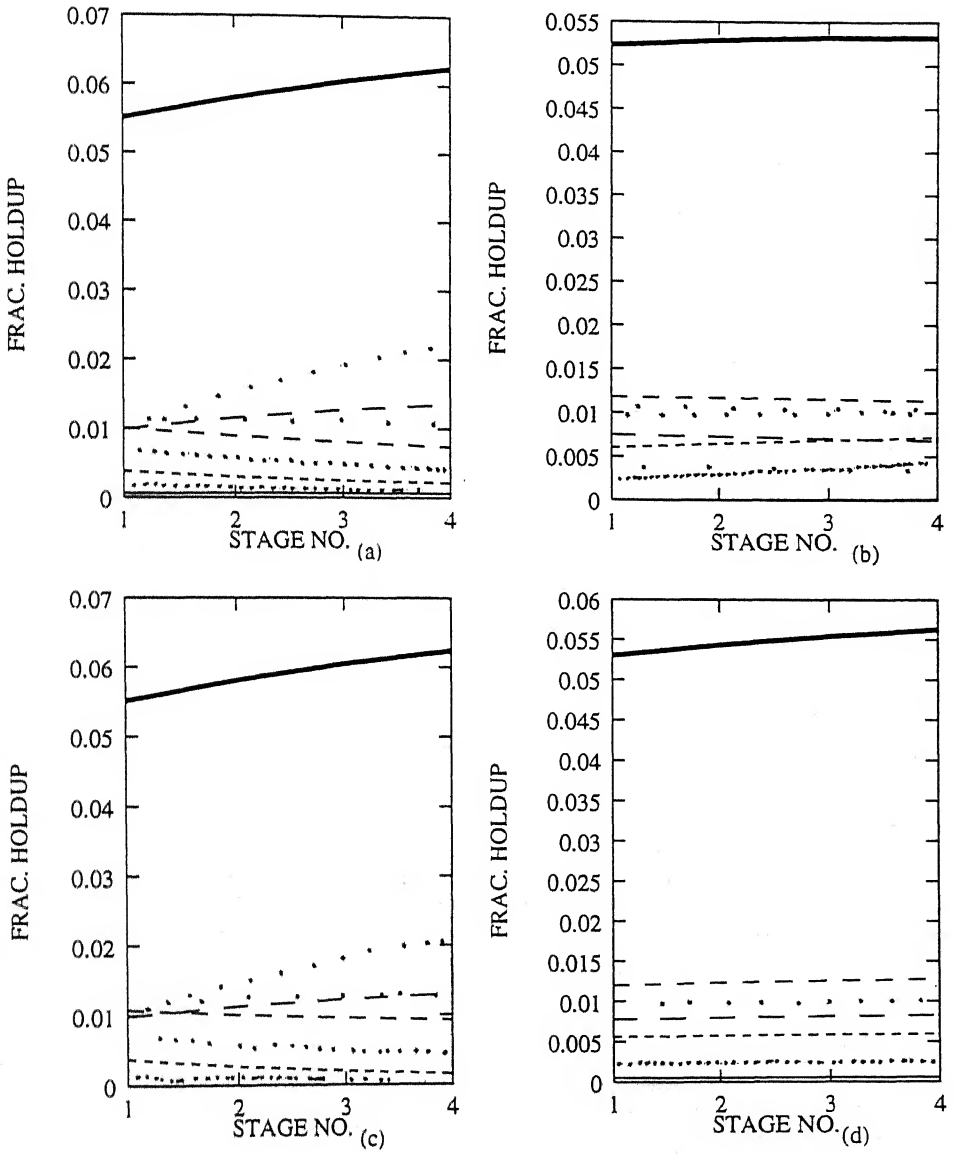

Figure 4.41: (a)With drop breakup and coalescence. (b) only drop breakage. (c) only drop coalescence. (d) without drop breakup and coalescence.

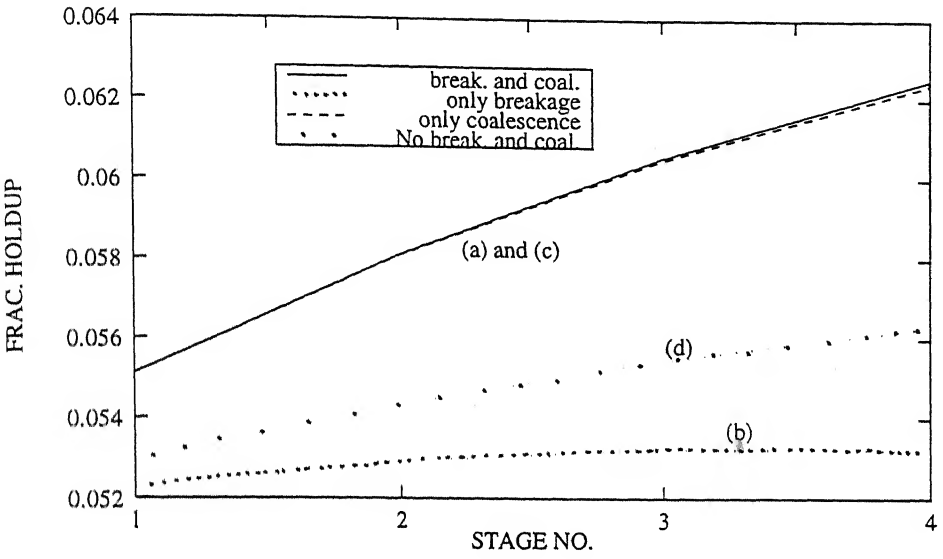

Figure 4.42: Comparison of total holdups

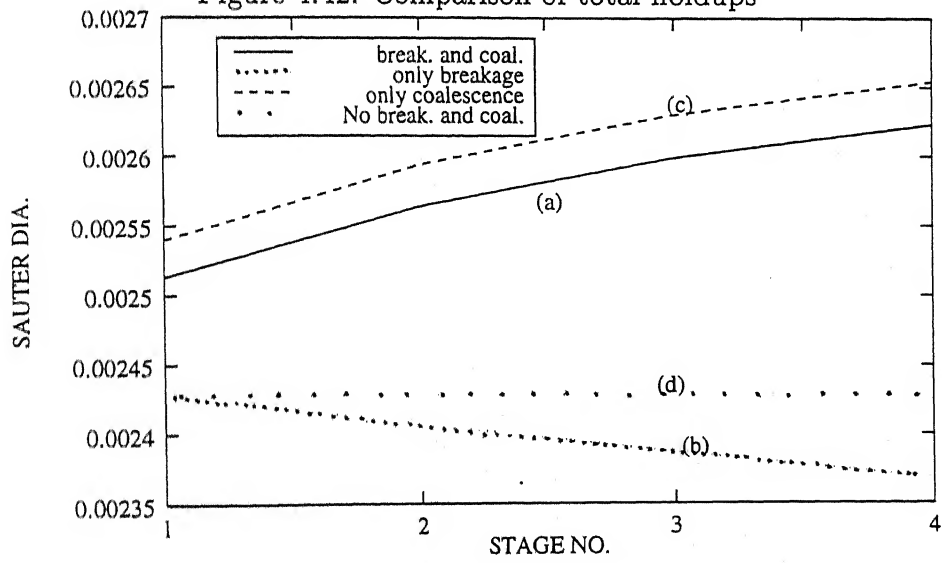

Figure 4.43: Sauter mean diameters

Chapter 5

Conclusions and Suggestions

Simulation model selected for present thesis incorporates non-equlibrium approach and drop breakage and coalescence model to describe dispersed phase behavior. The model has been extended for dynamic simulation in this thesis. In general results, predicted by the model are found satisfactory and as per the expectations. Model has been tested for two extraction systems — Aromatic extraction by sulfolane and acetone extraction by toluene.

Axial dispersion coefficients for continuous and dispersed phase are assumed as model parameters and given some suitable fixed value during simulation.

For distribution coefficient calculation UNIFAC method has been used. For LLE UNIFAC data at $25°C$ are available in literature for all of the components which have been used in this work. However extraction column described for System 1 works at an average temperature of $95°C$ [1] . This temperature difference may cause error in final results which could be corrected by taking the UNIFAC parameters at $95°C$. Modified UNIFAC method may be used which includes temperature effects also but data published in literature are limited for this method.

One of the important aspect of present model is its non-equlibrium approach to deal with interphase mass transfer and other is to incorporate drop breakage and coalescence for dispersed phase by using drop population approach. Effects such as osmotic diffusion and reverse diffusion are accounted for in the rigorous analysis used in present study to calculate interactive mass transfer coefficients. The validity of these results will definitely increase if experimental values of binary mass transfer coefficients are available; otherwise a suitable correlation can be used to predict desired estimates as in this thesis. A detailed study on interaction of species during interphase mass transfer is now possible by using such model presented here.

For unagitated column studied in this thesis drop breakage and coalescence create no significant changes in process variables. Further, the empirical constants used are

[1] Mukhopadhyay [28] has given UNIFAC data at $100°C$ but not found satisfactory with this work

those reported in literature for agitated columns. Especially coalescence efficiency is a very critical parameter which is not well understood. During steady state simulation its value has been evaluated in the range of 5-15% for correlation used for our work. Some other correlations Tsouris [17] predict even a very low value (less than 1%) of coalescence efficiency for drop diameters used in System 1. One has to take a judicious decision to select proper correlation.

The motivation behind present work is to develop a suitable model for liquid-liquid extraction which can be used for detailed study such as required for the design as well as for the control of extraction process. One of the major advantage of our formulation is that it can be applied for any type of countercurrent extraction column once sufficient information on design parameters and correlations is available for that column. For drop breakage and coalescence, models used ealier without considering mass transfer effects have been modified for mass transfer effects and included with the model presented in this work. Such an inclusion now allows study and control of physical parameters such as holdup in conjunction with mass transfer.

One of the crucial decisions in simulation is to select a robust algorithm for solving set of equations. Newton-Raphson method for solving set of nonlinear equations has been found robust in this study. Significant amount of time and computer memory saving has been obtained using Block-Thomas algorithm to solve the set of linear equations[2] in which block tridiagonal sparse matrix is formed. Smooth convergence of equation solver was also our major concern which has been achieved successfully by using N-R method. Practically, evaluation of Jacobian in every iteration takes too much time, especially evaluation of numerical derivatives. Finite difference approximation of numerical derivatives greatly increases the cost of solution because more physical properties evaluations are required; further, neglect of these derivatives may increase number of iterations or even cause failure. For dynamic simulation differential algebraic equation (DAE) set is formed. For solving DAE , DASSL which is one of the robust methods has been selected in this study. DASSL has certain advantages over other methods such as Runge-Kutte (RK) and Gear's method. Generalized RK method requires large computer memory and longer time for solving DAE problem. DASSL is a variable order and variable step size method; whereas in Gear's method using backward difference formula (BDF) formula the order is fixed. The selection of suitable order in DASSL during simulation allows large time step thus reducing time for dynamic simulation. On the other hand Gear's method having a fixed order resorts to small step size in a similar situation which slows down the simulation. Another advantage of selecting DASSL in this work is that it is simple and easy to understand; it has been found logistically convenient to incorporate DASSL with steady state simulation computer code. However for RK method or Gear's algorithm major part of the dynamic simulation problem had to be reformulated. DASSL has been tested on variety of simulation problem such as simulation of mechanical, electrical and aerodynamic systems satisfactorily.

[2]formed after linearizing, using N-R method

Present model can be studied in depth of rigorously by including several drop classes, mass transfer coefficients, drop breakage and coalescence affect and UNIFAC method. On the other hand it can be studied by neglecting or simplifying any of these details to reduce time of computation with out losing much on accuracy.

SUGGESTIONS FOR FUTURE WORK

Modeling of any chemical process is a creative exercise and success of modeling is complete only when the model is tested against real operational data. Feedback from real process may further suggest some refinement in modeling aspects which can't be envisaged just by carrying out theoretical study. It is therefore recommended that present model must be tested for a variety of extraction systems which should help to remove any bug and make the simulator versatile for study of any new extraction process. Other suggestions to make add on to the effort in this thesis, for a better success in future are :

1. Model parameters such as axial dispersion coefficients have to be tuned by optimization against real process data. Tuning of empirical constants used in correlations may be done for unagitated columns by carrying out independent experimentation as done in literature for agitated columns or they can be tuned with present model. However latter option increases the dimensionality of the optimization problem.

2. Model should be tested for agitated columns. For these columns abundance of data are already available in literature. Computer program written as a part of this thesis can be modified for such study by replacing correlations for agitated column.

3. In order to reduce CPU time[3] for solving set of non-linear equations, hybrid techniques such as Quasi-Newton method and combination of Newton and Quasi-Newton suggested by Lucia [44, 45] can be used. These methods update Jacobian without recalculation of each element – especially the Jacobian part which contains numerical derivatives is updated by the algorithm proposed by Lucia. Instability however may creep in by using such techniques.

4. In our work dynamic simulation is carried out from one steady state to another steady state i.e. DASSL is applied at initial steady state and then perturbations are introduced after some time steps. It would be useful to extended this for startup and shutdown of extraction column also. In our work time derivatives at time t=0 are taken zero ($y'(0) = 0$). DASSL can also be applied during transient state for which time derivatives have to be supplied or evaluated (see Brenan [37] for further details).

[3]One can use "prof" command in UNIX to get time consumed by each subroutine during simulation.

5. Though isothermal operation is assumed in our work, sometimes temperature profile is appled along the column height. In such case same model can be used by assuming any stage at constant temperature, however temperature difference may exist from one stage to next. Computer program has been made in a modular style keeping this factor into account. Coding of physical properties relations incorporating temperature dependence in appropriate subroutine will facilitate the non-isothermal simulation.

6. The detailed non-equilibrium dynamic model using population balance approach is not suitable as a process control model. Reduction of model by clubbing several real stages into one stage, using fixed distribution ratio (K-value) and fixed mass transfer coefficients for a range of operating conditions and avoidance of drop breakage and coalescence can be resorted to carry out modeling for control.

7. Major improvement in computation time can be achieved if some equations as well as independent variables are eliminated by substitution. For example equilibrium relations EQ_{ijk} and transport relations $MBID_{ijk}$, $MBIC_{ijk}$ can be clubbed together by substituting for either x^I_{ijk} or y^I_{ijk} from equilibrium relation into transport relations. This will reduce size of the simulation problem and memory requirement also. Such change will require reformulation of Jacobian and consequently some part of computer code also.

8. Drop breakage and coalescence study can be extended further and some useful results may be obtained for different types of column. Presently this field is under intense research in the field of liquid-liquid dispersion. Most of the related work published in literature does not include mass transfer effect. Model presented here has been modified specifically for studying drop breakage and coalescence under mass transfer conditions. A laboratory scale extraction column is recommended for such study.

Bibliography

[1] Laddha G.S. and Degaleesan T.E. *Transport Phenomena in Liquid Extraction.* Tata McGraw-Hill New-Delhi, 1976.

[2] Ricker.N.L. and King.C.J. An efficient,general method for computation of counter current separation processes with axial dispersion. *AIChE J.*, 27(2):277–284, 1981.

[3] Spencer J.L.. Steiner L., and Hartland S. Model based analysis of data from countercurrent liquid-liquid extraction data. *AIChE J.*, 27(6):1008–1016, 1981.

[4] Lo T.C., Baird M.H.I, and Hanson C. *Handbook of Solvent Extraction.* John Wiley & Sons, 1983.

[5] Krishnamurthy R. and Taylor R. A non-equilibrium stage model of multicomponent separation proceses — *I. AIChE J.*, 31(3):449–456, 1985.

[6] Krishnamurthy R. and Taylor R. A non-equilibrium stage model of multicomponent separation proceses — *II. AIChE J.*, 31(3):449–465, 1985.

[7] Zimmermann A.. Gourdon G., Joulia X., Gorak A., and Cassamatta G. Simulation of multicomponent extraction process by a non-equilibrium stage model incorporating a drop population model. *Comput. Chem. Engg.*, Supp:S403–S410, 1992.

[8] Khani S.D.A. Gourdon C., and Cassamatta G. Dynamic and steady state simulation of hydrodynamics and mass transfer in liquid-liquid extraction column. *Chem. Engg. Sci*, 44(6):1295–1305, 1989.

[9] Ramkrishna D. The status of population balance. *Rev. Chem. Engg.*, 3(1):49–95, 1985.

[10] Coulaloglou C.A. and Tavalarides L.L. Description of interaction processes in agitated liquid-liquid dispersions. *Chem. Engg. Sci*, 32:1289–1297, 1977.

[11] Sovová H. and Procházka J. Breakage and coalescence of drops in a batch stirred vessel— *I. Chem. Engg. Sci*, 36:163–171, 1981.

[12] Sovová H. A model of dispersion hydrodynamics in vibrating plate extractor. *Chem. Engg. Sci*, 38(11):1863–1872, 1983.

[13] Hsia M.A. and Tavalarides L.L. A simulation model for homogeneous dispersion in stirred tanks. *The Chemical Engg. J.*, 20:225–236, 1980.

[14] Hsia M.L. and Tavlarides L.L. Simulation analysis of drop breakage.coalescence and micromixing in liquid-liquid stirred tanks. *The Chem. Engg. J.*, 26:189–199, 1983.

[15] Rubio L.M., Kumar A., and Hartland S. Drop size distribution and average drop size in a *Wirz* extraction column. *Trans IChemE.*, 72(A):493–502, 1994.

[16] Tsouris C. *Modelling and Control of Extraction Column.* PhD thesis, Syracuse University, May 1992.

[17] Tsouris C. and Tavalarides L.L. Breakage and coalescence models for drops in turbulent dispersions — *I. AIChE J.*, 40(3):395–406, 1994.

[18] Tsouris C., Kirou V.I., and Tavalarides L.L. Drop size distribution and holdup profiles in a multistage extraction column — *II. AIChE J.*, 40(3):407–417, 1994.

[19] Jiřičný V. and Krătký. Counter-current flow of dispersed and continuous phase— *I. Chem. Engg. Sci*, 34:1141–1149, 1979.

[20] Stewart W.E and Probber R. Matrix calculation of multicomponent mass transfer in isothermal system. *Ind. Engg. Chem. Fund.*, 3(3):224–235, 1964.

[21] Taylor R. and Krishna R. *Multicomponent Mass Transfer.* John Wiley & Sons Inc., 1993.

[22] Smith L.W. and Taylor R. Film model for multicomponent mass transfer : A statistical comparison. *Ind. Engg. Chem. Fund.*, 22:97–104, 1983.

[23] Fredenslund A., Jones R.L., and Prausnitz J.M. Group contribution estimation of activity coefficients in non-ideal liquid mixtures. *AIChE J.*, 21(6):1086–1098, 1975.

[24] Magnussen T. and Fredenslund A. *UNIFAC* parameter table for prediction of liquid-liquid equilibria. *Ind. Engg. Chem. Proc. Des. Dev.*, 20:331–339, 1981.

[25] Sorensen.J.M. *DECHEMA, chemistry data series-part I,II,III.* Frankfurt, 1979,1980. LLE data collection.

[26] Larsen B.L., Rasmussen P., and Fredenslund A. A modified *UNIFAC* group-contribution model for prediction of phase equilibria and heat of mixing. *Ind. Engg. Chem. Res.*, 26:2274–2286, 1987.

[27] Mehrotra, M.O.Garg, and S.J.Chopra. Liquid liquid phase equilibria for dearomatisation of *ATF* fraction. *Fluid Ph. Eql.*, 32:17–25, 1986.

[28] Mukhopadhyay M. and Dongaonkar K.R. Prediction of liquid-liquid equilibrium in multicomponent aromatics extraction systems by use of the *UNIFAC* group contribution model. *Ind. Engg. Chem. Proc. Des. Dev.*, 22:521–532, 1983.

[29] Hooper H.H., Michel S., and Prausnitz J.M. Correlation of liquid-liquid equilibria for some water-organic liquid systems in the region 20-250 ^{o}C. *Ind. Engg. Chem. Res.*, 27:2182–2187, 1988.

[30] Rousseau R.W. *Handbook Of Separation Process Technology.* John-Wiley & Sons, 1987.

[31] Gani R. and Cameron I.T. Modelling for dynamic simulation of chemical processes:the index problem. *Chem. Engg. Sci*, 47(5):1311–1315, 1992. Shorter Communication:Rev art.

[32] Gani R. Modelling of dynamic simulation of chemical processes. *Chem. Engg. Sci*, 47(5):561–563, 1992.

[33] Gani.R. A generalized dynamic model for distillation column-i. *Comput. Chem. Engg.*, 10:181–198, 1986.

[34] Gear.C.W. Simultaneous numerical solution of differential-algebraic equations. *IEEE Trans. on Circuit Theory.*, CT-18(1):89–95, 1971.

[35] Gear.C.W and Petzold.L.R. *ODE* methods for the solution of differential-algebraic system. *SIAM J. Numer. Anal.*, 21(4):716–728, 1984.

[36] Petzold.L.R. Differential-algebraic equation are not *ODE*s. *SIAM J. Sci. Stat. Comput.*, 3:367–384. 1982.

[37] Brenan K.E, Campbell S.L, and Petzold L.R. *Numerical Solution of Initial-Value Problems in Differential-Algebraic Equations.* North-Holland, 1989.

[38] Henley E.J. and Seader J.D. *Equilibrium Stage Separation Operations in Chemical Engineering.* John-Wiley & Sons, 1981.

[39] Kennard.E.H. *Kinetic Theory Of Gases.* McGraw Hill NY., 1938.

[40] Bird R.B, Stewart W.E., and Lightfoot E.N. *Transport Phenomena.* Wiley NY, 1960.

[41] Treybal R.E. *Liquid Extarction, 2nd ed.* McGraw Hill New York, 1963.

[42] Reid R.C. and Sherwood T.K. *The properties of Gases and Liquid.* McGraw-Hill Book Co., 1966.

[43] Seader J. D. Rate based modelling for staged separation. *Chem. Engg. Prog.*, 41(9), 1989.

[44] Lucia.A and Macchietlo. A new approach to the approximation of quantities involving physical properties derivatives in equation oriented process design. *AIChE J.*, 29:705–713, 1983.

[45] Lucia.A. Low cost solutions to multistage,multicomponent separation problem by hybrid fixed point algorythm. *Found. of Computer Aided Process Design,2nd ed*, 1983.

[46] Mecklenbergi and Hartland. Design of differential countercurrent extractor with backmixing. *Cand. J. Chem. Engg.*, 47:453–459, 1969.

[47] Liang. Effect of surfactant on drop formation. *Chem. Engg. Sci*, 45(1):97–103, 1990.

[48] Kirou and Tavlarides. Flooding,holdup and drop size measurement in multistage column. *AIChE J.*, 34(283):843–848, 1988.

[49] Korchinsky.W.J. Stagewise model of continuous liquid-liquid extraction. *Chem. Engg. Sci*, 31:871–875, 1976.

[50] Garg.M.O and Pratt.H.R.C. Drop coalescence and breakage in extraction column. *AIChE J.*, pages 432–443, 1984.

[51] Pantelides. The mathematical modelling of transient system using *DAE. Comput. Chem. Engg.*, 12:449–454, 1988.

[52] Moler.C and Loan Van C. The exponential os a matrix. *SIAM REV.*, pages 808–811, 1978.

[53] Kehat.E and Ghitis B. Simulation of an extraction column. *Comput. Chem. Engg.*, 5(3):171–180, 1981.

[54] Holland C.D. *Fundamentals of Multicomponent Distillation.* McGraw-Hill Book Com., 1981.

Appendix A

DASSL: *Differential Algebraic System SoLver*

This section describes briefly about DASSL formulation and its implementation in this study. Details of this method and some useful definitions commonly used for solving *Differential Algebraic Equation* (DAE) can be seen from Brenan,Campbell & Petzold [37, 1989]. DASSL is a very robust tool for solving DAE of index[1] 0 and 1. It also solves the equation set of semi-implicit type of DAE (as is in this study) very well. DASSL requires the equation set to be solved in the form of

$$F\left(t_{n+1}, y_{n+1}, y'_{n+1}\right) = 0 \tag{A.1}$$

with
$y(t_0) = y_0$
$y'(t_0) = y'_0$
where $h_{n+1} = t_{n+1} - t_n$ step size at current step (n−1). The non-linear set of equations A.1 is then solved by using multivariable Newton-Raphson method. In this study $y'(t_0)$ is evaluated by assuming steady state at time t=0, i.e. $y'(t_0) = y'_0 = 0$ is taken. This is true for one steady state to next steady state but may not be true for startup/shutdown problem. DASSL approximates the derivative y'_{n+1} using the k^{th} order backward differentiation formula (BDF), where k ranges from 1 to 5 (suggested by Brenan [37, pp 118]). DASSL is a variable order and variable step size method which makes it most robust and powerful to solve even steep differential equations. Detailed derivation can be seen from Brenan [37]. Here a brief formulation of DASSL is given :

[1]Index of DAE defined as number of times differentiation required to convert DAE into ODE set.

A.1 Intermediate parameters used in DASSL formulation

Some intermediate parameters used for DASSL are :

$$\psi_i(n+1) = h_{n+1} + h_n + \cdots + h_{n+2-i} = t_{n+1} - t_{n+1-i} \ , \quad i \geq 1 \tag{A.2}$$

$$\alpha_i(n+1) = h_{n+1}/\psi_i(n+1) \tag{A.3}$$

$$\beta_1(n+1) = 1 \tag{A.4}$$

$$\beta_i(n+1) = \frac{\psi_1(n+1)\psi_2(n+1)\cdots\psi_{i-1}(n+1)}{\psi_1(n)\psi_2(n)\cdots\psi_{i-1}(n)} \ , \quad i > 1 \tag{A.5}$$

$$\phi_1(n) = y_n \tag{A.6}$$

$$\phi_i(n) = \psi_1(n)\psi_2(n)\cdots\psi_{i-1}(n)\ [y_n, y_{n-1}, \ldots, y_{n-i+1}] \ , \quad i > 1 \tag{A.7}$$

$$\phi_i^*(n) = \beta_i(n+1)\phi_i(n) \ , \quad i \geq 1 \tag{A.8}$$

$$\sigma_1(n+1) = 1 \tag{A.9}$$

$$\sigma_i(n+1) = \frac{h_{n+1}^i\ (i-1)!}{\psi_1(n+1)\psi_2(n+1)\cdots\psi_i(n+1)} \ , \quad i > 1 \tag{A.10}$$

$$\gamma_1(n+1) = 0 \tag{A.11}$$

$$\gamma_i(n+1) = \gamma_{i-1}(n+1) + \alpha_{i-1}(n+1)/h_{n+1} \ , \quad i > 1 \tag{A.12}$$

$$\alpha_s = -\sum_{j=1}^{k} \frac{1}{j} \tag{A.13}$$

$$\alpha^0(n+1) = -\sum_{j=1}^{k} \alpha_j(n+1) \tag{A.14}$$

The divided difference[2] $[y_n, y_{n-1}, \ldots, y_{n-i+1}]$ formula can be seen from any standard numerical method text.

A.2 DASSL formula for time derivatives y'_{n+1}

DASSL formula for time derivative of variable is given as :

$$\mathrm{y'_{n+1}} = \mathrm{y_{n+1}^{'(0)}} - \frac{\alpha_s}{\mathrm{h_{n+1}}}(\mathrm{y_{n+1}} - \mathrm{y_{n+1}^0}) \tag{A.15}$$

where,

$$y_{n+1}^0 = \sum_{i=1}^{k+1} \phi_i^*(n) \tag{A.16}$$

and

$$y_{n+1}^{'(0)} = \sum_{i=1}^{k+1} \gamma_i(n+1)\phi_i^*(n) \tag{A.17}$$

[2] eg: $[y_1, y_0] = \frac{y_1 - y0}{t_1 - t0}$

A.3 Step size selection

In this study following strategy is adopted to decide the correct step size. At any step, for correct step size and order, solution of DAE must satisfy following error condition.

$$ERR = M\|y_{n+1} - y^0_{n+1}\| \leq 1.0, \tag{A.18}$$

where

$$M = max\left(\alpha_{k+1}(n+1)\ ,\ |\ \alpha_{k+1}(n+1) + \alpha_s - \alpha^0(n+1)\ |\right) \tag{A.19}$$

- At step=1, using $h_0 = 10^{-3} \times (TOUT - 0)$ as previous step size for time step 1. Here TOUT is the time for which simulator has to be run.
- Take successful step size of previous step, raise the step size in next step, if it can be doubled[3], h_{n+1}=$2h_n$, solve DAE and check error condition A.18
- If raised step size is not accepted then use previous successful step size, h_{n+1}=h_n.
- If above two steps failed then step size is to be decreased,follow the sequence if this decrease is called for.
  1. Step size is decreased at least by a factor r=0.9 i.e. (h_{n+1}=rh_n) and at most r=0.5 and see where it could be accepted; if not, call it failure no. 1.
  2. If failure 1 occur, then take r again from 0.9 to 0.25 and multiply by the step evolved after failure no. 1; keep on checking error condition after every new step selected; if not satisfied, call this as failure no. 2.
  3. After failure no. 2 the step size is reduced by one quarter (1/4), based on the philosophy that such a high step is not trusted.
- Keep on counting the numbers of failure in above operation. After a large step size decrease (i.e. too many failure), the BDF formula is most accurate at order one. Therefore reduce current order to 1 and keep on trying again; after each failure reduce step size by 1/4 till [$t + h \approx t$], where it is declared that DASSL **FAILED**.

A.4 Order selection for next step

Initially order is kept at 1, and step is increased as described in section A.3. After that the order is raised or lowered depending upon whether error estimates of Taylor series - TERKM2,TERKM1,TERK and TERKP1 form an increasing or decreasing

[3]Sometimes this doubling may give severe instability problem in equation solver so vary this factor from 1.5 to 2.0,try to keep as high as (upto 2.0) possible

sequence. If an increasing sequence is formed then order is reduced and if a decreasing sequence is formed than order is increased. The error estimates are given below.

$$TERKM2 = \|(k-1)\sigma_{k-1}(n+1)\phi_k(n+1)\| \quad \text{(A.20)}$$

$$TERKM1 = \|k\sigma_k(n+1)\phi_{k+1}(n+1)\| \quad \text{(A.21)}$$

$$TERK = \|(k+1)\sigma_{k+1}(n+1)\phi_{k+2}(n+1)\| \quad \text{(A.22)}$$

$$TERKP1 = \|(k+2)\sigma_{k+2}(n+1)\phi_{k+3}(n+1)\| \quad \text{(A.23)}$$

The DASSL technique is still under refinement, Hence in case of failure some suitable strategy has to be adopted based on intuition, which may be specific to the problem. If process behavior or its estimate is available a priori some time step saving steps could be adopted. In this study continuing with DASSL, if any perturbation is given to the process then simulator (computer program) integrates DAE first up to the time of perturbation. After that very small step size is taken (irrespective of what DASSL suggest) to introduce perturbation and finally DASSL is again allowed to implement step size and order as described in sections A.3 and A.4.

Appendix B

Correlations Used

The model described in this study is general and could be used for agitated as well as unagitated multicomponent countercurrent extraction column . However, in this study it is tested for *Unagitated Sieve Tray* extraction column. For other columns same computer code can be used with modifications in the correlations used. Following sections present the correlations used to test the model for unagitated sieve tray column.

B.1 Design parameters

B.1.1 Drop diameters

- **Maximum stable drop diameter d_{max}**
  taken from (Baird [4],pp 129, eqn. 17)

$$d_{max} = C_1 \left(\frac{g_c \gamma}{\rho_c} \right)^{0.6} (\epsilon)^{-0.4} \tag{B.1}$$

  where C_1 is a constant depending upon system properties and type of the column. For RDC value of $C_1 = 0.72$ is reported. For this study its value is taken as 0.8 considering the fact that in an unagitated column larger drop diameter may exist.
  ϵ is power dissipated per unit mass of fluid phase. Relationships of ϵ for some contactors are given in (Baird [4], pp 130, Table 1). For our work ϵ relation for spray column, which is assumed to be applicable for each compartment of unagitated sieve tray, is taken :

$$\epsilon = u_d g \frac{\Delta\rho}{\rho_c} \tag{B.2}$$

  u_d is a superficial velocity of dispersed phase.

- **Mean diameter** d_{mean} *or* d_{32} *or* d_{vs}
  Several reliable correlations are available for mean drop diameters possible in any contactor. Various authors call it by various names such as d_{32} , vediyan mean drop correlation d_{vs} etc. The correlation proposed by Vediyan (Laddha [1], pp 308, eqn. 6.53) has been used for unagitated sieve tray column :

$$\frac{d_{vs}}{(\gamma/\Delta\rho g)} = 1.592 \left(\frac{U_n^2}{2gd_n}\right)^{-0.0665} \tag{B.3}$$

  where U_n and d_n are jet velocity and nozzle (hole) diameter respectively.

B.1.2 Characteristic velocity u_r^*

Various author have published several correlations. The correlation proposed by Vediyan (Laddha [1], pp 313, eqn. 6.54) is used here.

$$\frac{u_r^*}{(\gamma\Delta\rho g/\rho_c^2)^{\frac{1}{4}}} = 1.088 \left(\frac{U_n^2}{2g\ d_n}\right)^{-0.0818} \tag{B.4}$$

Other correlations are also available from Baird [4], Khani [8].

B.1.3 Static holdup, Jet velocity, Jet diameter ...

These are used in design calculations. All these calculations are referred from (Laddha [1], Chapter 11- Perforated Plate Towers). These calculations are specific to perforated towers only and therefore not valid for other types of column.

B.2 Drop breakage and Coalescence

B.2.1 Breakage frequency $g(d_j)$

Mechanistic model (which includes the physical properties of the system ,the geometry and energy provided to the dispersion) was first proposed by Coulaloglou [10] in 1977 for agitated columns. Relations cited by (Tsouris and Tavlarides [17], pp 396, eqn. 4) are used here :

$$g(d_j) = k_1 \frac{\epsilon^{\frac{1}{3}}}{(1+\phi)d_j^{\frac{2}{3}}} exp\left[-k_2 \frac{\gamma(1+\phi)^2}{\rho_d \epsilon^{\frac{1}{3}} d_j^{\frac{5}{3}}}\right] \tag{B.5}$$

where k_1, k_2 are empirical constants, evaluated by experimentation and optimization for a particular column. Hsia [13] evaluated these parameters for dispersion in stirred

tank. In the absence of any information of these data for unagitated sieve tray column, same values of these parameters have been used for this study also. It has been assumed that order of these parameters may be same for other columns. However experimentation is necessary in order to validate results for drop breakage and coalescence for other extraction columns. Typical values are $k_1 = 0.00481$ and $k_2 = 0.0551$ taken from Hsia [13].

B.2.2 Daughter drop distribution $\beta(d_i, d_j)$

After breakage of any drop the produced drops are called as daughter drop. It is assumed that father drop after breaking gives certain spectrum of daughter drops. The probability density of this spectrum is called as daughter drop density function represented by $\beta(d_i, d_j)$. It represents the probability density of daughter drop of diameter d_j due to breakage of father drop of diameter d_i. For convenience sometimes it is represented as $\beta(i, j)$ or $\beta(v_i, v_j)$ also. The distribution used in PhD thesis of (Tsouris [16], PhD thesis, pp42, eqn. 4.20) is used here :

$$\beta(v, v') = \frac{\alpha\left(v - \frac{v'}{2}\right)^2}{\int_{v_{min}}^{v'}\left(v - \frac{v'}{2}\right)^2 dv} + \frac{1-\alpha}{v' - v_{min}} \tag{B.6}$$

where α is given by

$$\alpha = exp\left[-c_2\frac{d - d_{min}}{d_{min}}\right] \tag{B.7}$$

Above c_2 is a constant the optimum value of which has been found to be 0.75. Critical or minimum drop diameter d_{min} is taken as 0.0 for present study. The value of parameter α lies between 0 and 1, which are its extreme values.

B.2.3 Collision frequency

Theoretical formulation can be seen from Kennard [39, 1938.pp 103-114], in where collision frequency formula has been developed for gas molecules. The formulation used here is developed by (Tsouris [17],pp 401, eqn. 50).

$$h(d_i, d_j) = \frac{\pi}{4}(d_i + d_j)^2(\overline{u_i^2} + \overline{u_j^2})^{\frac{1}{2}} n_i n_j \tag{B.8}$$

where mean velocity is given by $\overline{u^2} = 1.07\epsilon^{\frac{2}{3}}d^{\frac{2}{3}}$. ϵ here used for spray column as in equation B.2.

B.2.4 Coalescence efficiency

This is not well understood in the literature published so far. Some definition favour higher efficiency for smaller drops and some for larger drops . For present, work model

proposed in PhD thesis by Tsouris [16] is used.

$$\lambda(d_i, d_j) = exp\left[-\frac{c_3\mu_c}{\rho_c\epsilon^{\frac{1}{3}}(d_i + d_j)^{\frac{4}{3}}}\right] \tag{B.9}$$

where optimum value of constant c_3 has been found to be 8.0×10^2 for a column used in Tsouris' thesis. In the absence of any data same value is used here. Typically coalescence efficiency ranges between 5-15 % using above formula.

B.3 Binary mass transfer coefficient

Although it is preferd to use experimental values of binary mass transfer coefficient, in the absence of such data, correlations have to be used for calculations. These correlations are geometry dependent and are the basic inputs for the theoretical rigorous calculation of interactive mass transfer coefficient matrix used in $MBID_{ijk}$ *and* $MBIC_{ijk}$ equations sets. For present study, correlations Tables published in (Baird [4], pp 324-326, Tables 1,2) are referred for binary mass transfer coefficients. The simulator has been tested using the following two correlations for continuous and dispersed phases respectively.

$$k'_d = 0.0432\frac{d}{t}\left(\frac{\rho_d}{M_d}\right)_{av}\left(\frac{U_n^2}{dg}\right)^{0.089}\left(\frac{d^2}{t\mathcal{D}_d}\right)^{-0.034}\left(\frac{\mu_d}{\sqrt{\rho_d d\gamma}}\right)^{0.601} \tag{B.10}$$

$$k'_c = 0.386\left(\frac{\rho_c}{M_c}\right)_{av}\left(\frac{\mathcal{D}_c}{t}\right)^{0.5}\left(\frac{\rho_c\gamma}{\Delta\rho g t\mu_c}\right)^{0.407}\left(\frac{gt^2}{d}\right)^{0.148} \tag{B.11}$$

These are used for mass transfer coefficients prediction at the time of drop detachment from sieve tray. Rise time t is given by

$$t = \frac{n_o(\pi/6)d^3}{Q_d} \tag{B.12}$$

Further $\left(\frac{\rho_d}{M_d}\right)_{av}$ and $\left(\frac{\rho_c}{M_c}\right)_{av}$ are equvivalent to molar densities c^d and c^c respectively. For diffusivity calculation famous empirical correlation by Wilke-Chang (1955) is used see (Taylor [21], pp 91, eqn 4.2.18,4.1.8) or (Reid [42], pp 549, eqn 11-45) and is given below.

$$\mathcal{D}_{im} = 7.4 \times 10^{-8}\left(\frac{(\phi_m M_m)^{1/2}T}{\mu_(m)\mathcal{V}_i^{0.6}}\right) \tag{B.13}$$

where
$\mathcal{D}_{im}$ = mutual diffusivity of solute i into m (cm^2/sec)
M_m = molecular weight.
T = temperature K
μ_m = viscosity (centipoise)
$\mathcal{V}_i$ = molal volume at normal boiling point. $(cm^3/g\ mole)$
ϕ_m = association parameter.

Appendix C

Computer program and data

A stand alone computer code written in "C" language for simulating multicomponent, countercurrent staged extraction process. The program simulates for both *steady state and dynamic simulation.* Complete simulation package contains 19 computer files with 12,000 lines of "C" code. This program has been tested on UNIX machines like DEC 2000 αXP and HP9000/850. Following is the list of the files and brief description about each file.

Table C.1: Computer files in simulation package developed.

S.no	*Computer file*	*Brief description*
1	simuldefs.h	Definition file; Declares and define all functions and definitions used in whole simulation code.
2	main.c	Startup file, contains main program
3	simulation.c	Selects steady state or dynamic simulation options and sets appropriate flags.
4	step.c	Comprises main simulation loop. It calls various other functions like initial guess settings, conditioning input, N-R method step size optimization etc.
5	DASSL.c*	Main body of DASSL code and formulation of dynamic simulation. It also calls various functions from simulfun03.c
6	change.c*	It reads perturbations from file supplied by user which stores pertutbation during simulation. This file also made some checks before applying any perturbation.

7	block.c	The functions stored in this file are called by file step.c frequently for calculation of A,B abd C blocks of Jacobian.
8	vector.c	Similar as block.c , but call for function vector (residuals) D vector.
9	a_minor.c	Calculates 30 different minors A(0,0) to A(4,5), for A block.
10	b_minor.c	Calculates 30 different minors B(0,0) to B(4,5), for B block.
11	c_minor.c	Calculates 30 different minors C(0,0) to C(4,5), for C block.
12	d_vector.c	Calculates 5 different subvectors D(0) to D(4), for D vector.
13	simulfun01.c	Stored various functions which are used for calculating expressions such as average mol. wt., axial dispersion coefficients, molar density etc.
14	simulfun02.c	Extension of simulfun01.c, but stored most of the correlations also.
15	simulfun03.c	Similar to simulfun02.c, extensively used for dynamic simulation only.
16	break_coal.c	This stores functions for drop breakage and coalescence calculations.
17	thermo_model.c	Stores about UNIFAC method.
18	mtc.c	For mass transfer calculations.
19	simutils.c	General utility function file, for programming point of view. Functions stored here are general in nature and may be used with any other "C" program.

[*] Are the files, used only for Dynamic simulation, never by steady state simulation.

A computer flowsheet of whole simulation package is shown in Figure C.1 both for steady state and dynamic simulation.

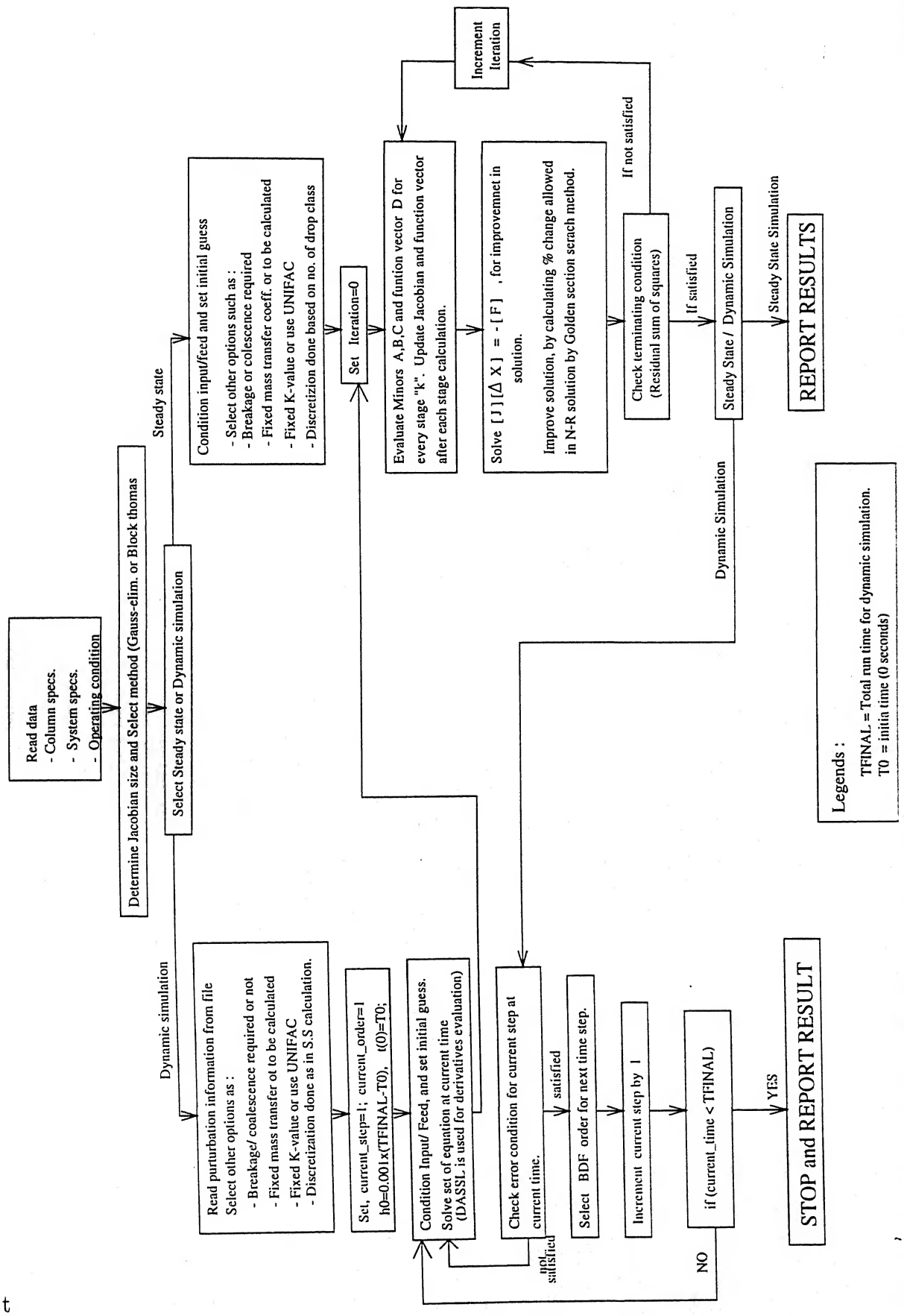

t

Figure C.1: Flow sheet of computer program for simulating extraction column

Following are the sample data files for simulation run no. 1, described in chapter 4.

Table C.2: Column 1 specification

Line no.	*Data in computer file*	*Description*
1.	0.300000	Column diameter (m)
2.	0.100000	Tray spacing (m)
3.	40	No. of real stages
4.	0.003175	Hole diameter (m)
5.	0.010000 t	Pitch and type of pitch (triangular)
6.	384	No. of holes/plate

Table C.3: System 1 specification

Line no.	*Data in computer file*	*Description*
1.	6	No. of components
2.	100.20 98.18 78.11 92.13 106.16 120.00	Mol. wt. of each *component**
3.	1	No. of drop class
4.	0.007500	Interfacial tension
5.	0.000320 0.003000	Viscosity of continuous & dispersed phase
6.	750.0 1260.0	Density of continuous & dispersed phase
7.	0.000209 0.000240 0.000260 0.000290 0.000345 0.003000	Viscosity of each component
8.	0.000162 0.000140 0.000097 0.000119 0.000140 0.000120	Molar volume of each component
9.	1.000000 1.000000 1.000000 1.000000 1.000000 1.000000	Association parameter of each component
	DATA ARE IN SI UNITS	

(*) n-Heptane(1), cyl-Hexane(2), Benzene(3), Toluene(4), o-Xylene(5) and Sulfolane(6).

Table C.4: Operating condition

Line no.	*Data in computer file*	*Description*
1.	500000.0	Operating pressure (N/m^2)
2.	368.15	Operating temperature (K)
3.	2.0	Molar feed flow, continuous phase (moles/s)
4.	0.37 0.37 0.05 0.16 0.05 0.00	Composition (mole fraction) feed Naphtha
5.	4.5	Molar feed flow, dispersed phase (moles/s)
6.	0.00 0.00 0.00 0.00 0.00 1.00	Composition (mole fraction) feed Sulfolane
	Next two data lines will be entered for each stage side streams, if they are not present enter 0.0 for data. First these lines are entered for continuous phase (for all 40 stage) and then same exercise repeated for dispersed phase side streams.	
7. 8	0.00 0.00 0.00 0.00 0.00 0.00 0.00	Side feed to stage 1 (flow rate) its composition (mole fraction)
9. 10.	.. ..	
11.	so on ..	

Table C, list parameters used for UNIFAC model, which are supplied as a separate file. For system 1, 6 UNIFAC groups (Magnussen [24]) are identified as :
— CH_3, — CH_2, — CH, — ACH, — $ACCH_3$ and — TMS (Separate group for Sulfolane).

```
------------------------------------------------------------------------
TABLE C.5 : UNIFAC parameters
------------------------------------------------------------------------
LINE(1)     ==>(no-group)  Total Number Of Groups
LINE(2)     ==>(Rk)  Volume parameters(Rk) for groups (In Particular order )
LINE(3)     ==>(Qk)  Surface Area parameters(Qk) for groups (In same order)
LINE(4-9)   ==>(nu(k,i))  No. Of Groups Of Type "k" in Molecule "i".
                  Enter In one LINE for One specie(molecule), as

                        nu(1,1) nu(2,1) ........  nu(no-group,1)
                           .                          .
                           .                          .
```

Line no.	*Data*
1.	6
2.	0.9011 0.6744 0.4469 0.5313 1.2663 4.0358
3.	0.8480 0.5400 0.2280 0.4000 0.9680 3.2000
4.	2 5 0 0 0 0
5.	1 5 1 0 0 0
6.	0 0 0 6 0 0
7.	0 0 0 5 1 0
8.	0 0 0 4 2 0
9.	0 0 0 0 0 1
10.	0.0000 0.0000 0.0000 -114.8 -115.7 561.40
11.	0.0000 0.0000 0.0000 -114.8 -115.7 561.40
12.	0.0000 0.0000 0.0000 -114.8 -115.7 561.40
13.	156.50 156.50 156.50 0.0000 167.00 21.970
14.	104.40 104.40 104.40 -146.8 0.0000 238.00
15.	67.840 67.840 67.840 59.160 26.590 0.0000

(This data set are taken from Magnussen [24].

```
                    nu(1,no-spicie) ..... nu(no-group,no-spicie)

LINE(10-15)  ==>(a(m,n))  Interaction parameters,. "m" to "n". as

                    a(1,1) a(1,2) .....      a(1,no-group)
                       .                          .
                       .                          .
                    a(no-group,1) .....      a(no-group,no-group)
```

All these data files are also supplied for dynamic simulation also. Apart from these a perturbation file is also supplied to computer program in case of dynamic simulation, which stores perturbation information to be applied during dynamic simulation. This sample computer file for simulation run 6 (see section 4.3)is reported here as it is.

```
-------------------------------------------------------------------------
  Perturbation file (Simulation run 6) for dynamic simulation
-------------------------------------------------------------------------
#Read These INSTRUCTIONS CAREFULLY !!!
#[1] Try Not to  Edit Any Text or Insert any Text line in this file,Use .
#[2] If required, Use # character in first column to ignore that line
#[3] Enter Data Change Only(in place of * ),If Particular variable is not
#    Changing write * (star) in place of that
#[4] DO NOT REMOVE ANY LINE OR CHANGE DATA SEQUENCE
#Example Entry :
```

```
#
# Change No.=   5   , At Time =  45.0  seconds
# Uin =   0.95
# Vin =   *
#
#Indicates at perturbation no 5,time 45.0 seconds ,Uin changes from prev.
#to 0.95,Vin remain same
# Only blanks and TABS are allowed between  =  and data value or *
################################################################################
#


Total No. Of Changes(perturbation) proposed  =    1

Change No.=    1     ,    At Time = 90.000000 seconds
Uin =    3.0
yin[1] =    *
yin[2] =    *
yin[3] =    *
yin[4] =    *
yin[5] =    *
yin[6] =    *
Vin =    *
xin[1] =    *
xin[2] =    *
xin[3] =    *
xin[4] =    *
xin[5] =    *
xin[6] =    *
Fc[1] =    *
yf[1][1] =    *
yf[2][1] =    *
yf[3][1] =    *
yf[4][1] =    *
yf[5][1] =    *
yf[6][1] =    *
Fd_in[1] =    *
xf[1][1] =    *
xf[2][1] =    *
xf[3][1] =    *
xf[4][1] =    *
xf[5][1] =    *
xf[6][1] =    *
    .
    .
```

```
.
.
Fc[40] =    *
yf[1][40] =    *
yf[2][40] =    *
yf[3][40] =    *
yf[4][40] =    *
yf[5][40] =    *
yf[6][40] =    *
Fd_in[40] =    *
xf[1][40] =    *
xf[2][40] =    *
xf[3][40] =    *
xf[4][40] =    *
xf[5][40] =    *
xf[6][40] =    *
```

Appendix D

Results for System 2

This Appendix list the results obtained for system 2 i.e. (Water(1), Acetone(2), Toluene(3).

Appendix D

Results for System 2

This Appendix gives the results obtained for system 2 i.e. (Water(1), Acetone(2), Toluene(3). This system is recommended for the lab experiments in which Toluene as a solvent (dispersed phase) enters from bottom of a 4 stage unagitated sieve tray column, which extracts Acetone from Water. Continuous phase feed enters from top of the column. Specifications are in Table D.1.

Table D.1: Specifications for for Test System 2

Column 2 data (as in Table C.2)
0.076200 0.250000 4 0.003000 0.010000 t 28
System 2 physical properties data (as in Table C.3)
3 18.000000 58.000000 92.000000 1 0.022000 0.001000 0.000530 989.000000 853.000000 0.001000 0.000292 0.000587 0.000019 0.000077 0.000119 2.600000 1.000000 1.000000
(1)Water, (2)Acetone, (3)Toluene
Operating condition (as in Table C.4)
200000.00 298.15 0.65 0.90 0.10 0.00 0.32 0.000 0.000 1.000 0.00 0.00 0.00 0.00 . . . . 0.00 0.00 0.00 0.00

Table D.1 Contd..
UNIFAC data (as in Table C.5)
5 0.5313 1.2663 1.6724 0.9011 0.9200 0.4000 0.9680 1.4880 0.8480 1.4000 5 1 0 0 0 0 0 1 1 0 0 0 0 0 1 0.0000 167.20 593.70 156.50 859.40 -146.8 0.0000 917.70 104.40 5695.0 -78.31 -73.87 0.0000 66.560 634.80 -114.8 -115.7 472.60 0.0000 1300.0 372.80 203.70 -171.8 342.40 0.0000
Five UNIFAC groups identified as : $-ACH$, $-ACCH_3$, $-CH_3CO$, $-CH_3$ and $-H_2O$ Data Source : Magnussen [24]

Simulation Runs System 2

Feed conditions for steady state run (Run A) and perturbations for dynamic state (Run B) are listed in Table D.2. For dynamic simulation initial feed conditions has been taken corresponding to Run A at time t=0 seconds.

Table D.2: Simulation Runs System 2

Run	Remark	Feed condition/Perturbation
A.	Steady State Fig D.1 to D.6	S=0.32 moles/s, F=0.65 moles/s, S/F=2.3 w/w Aq. feed conc.(0.90, 0.10, 0.00)
B.	Dynamic Fig D.7 to D.11	(1) t=0 sec– feed condition as in Run A. (2) t=30 sec– F increased from 0.65 to 0.75 moles/s (3) t=400 sec– S increased from 0.32 to 0.42 moles/s (4) t=800 sec– Aqueous feed concentration changes from (0.90,0.10,0.0) to (0.8,0.2,0.0). (5) t=1600 sec– Unperturbed all three perturbation (above) given so far. Allow simulation for 1 hour.

S=Solvent phase (Toluene) feed rate (Average molecular weight = 92)
F=Aqueous phase feed rate (Average molecular weight = 20)
S/F= Solvent to feed ratio

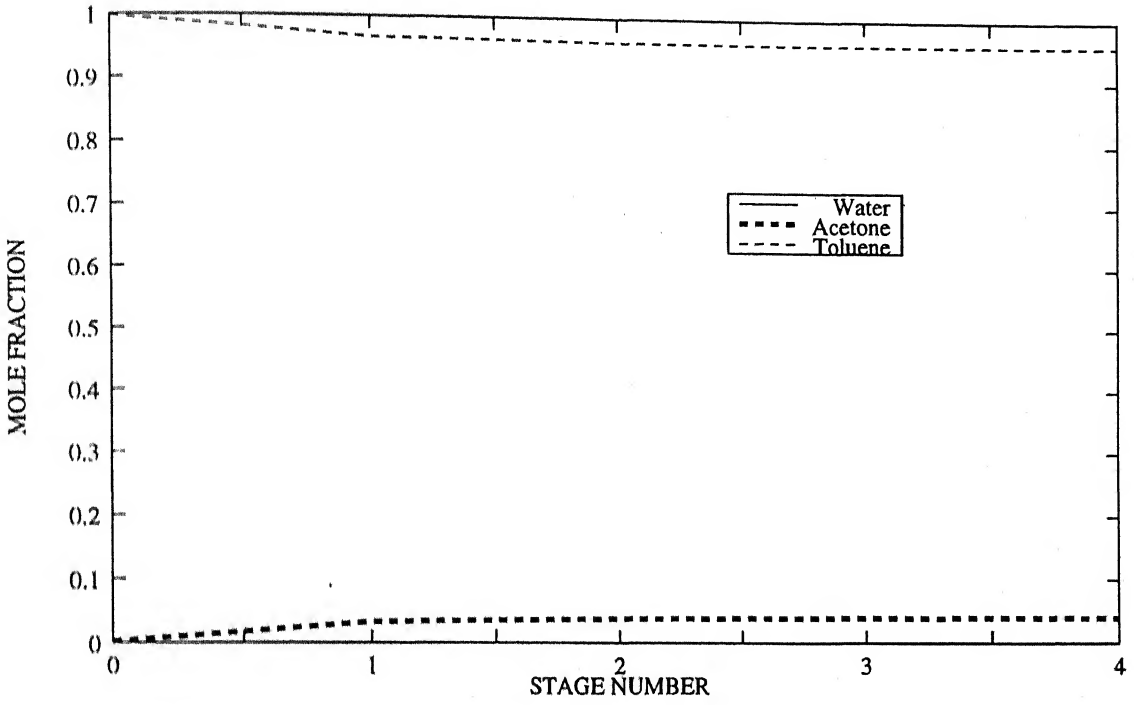

Figure D.1: Concentration profile for dispersed (Toluene) phase (Run A)

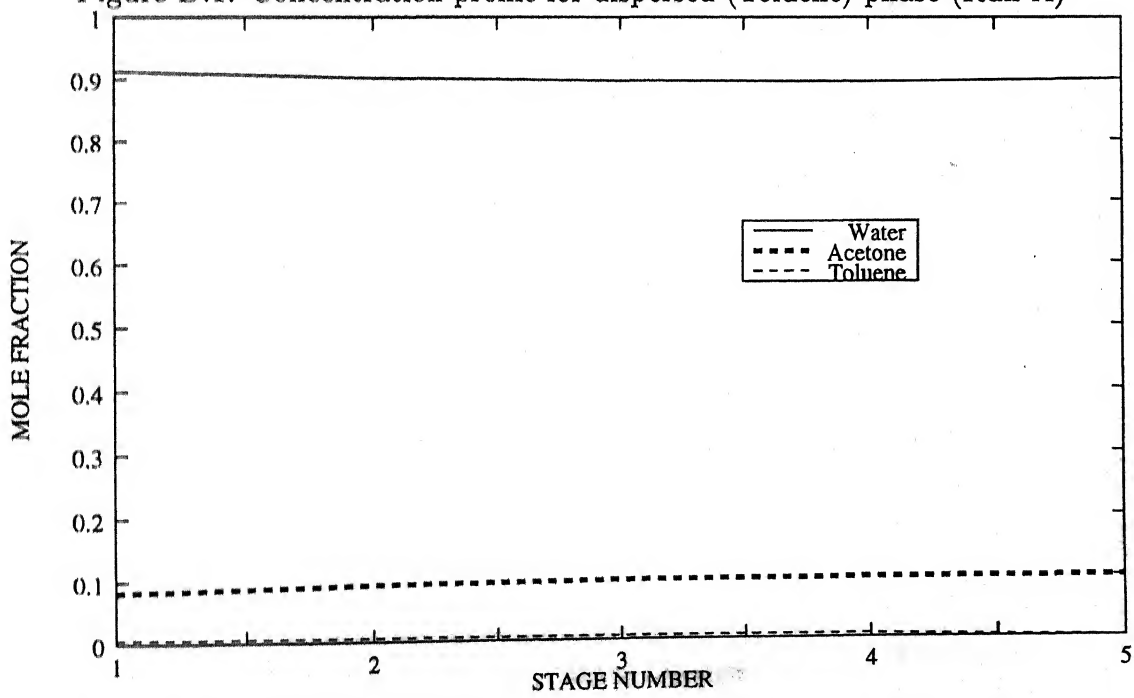

Figure D.2: Concentration profile for continuous (Aqueous) phase (Run A)

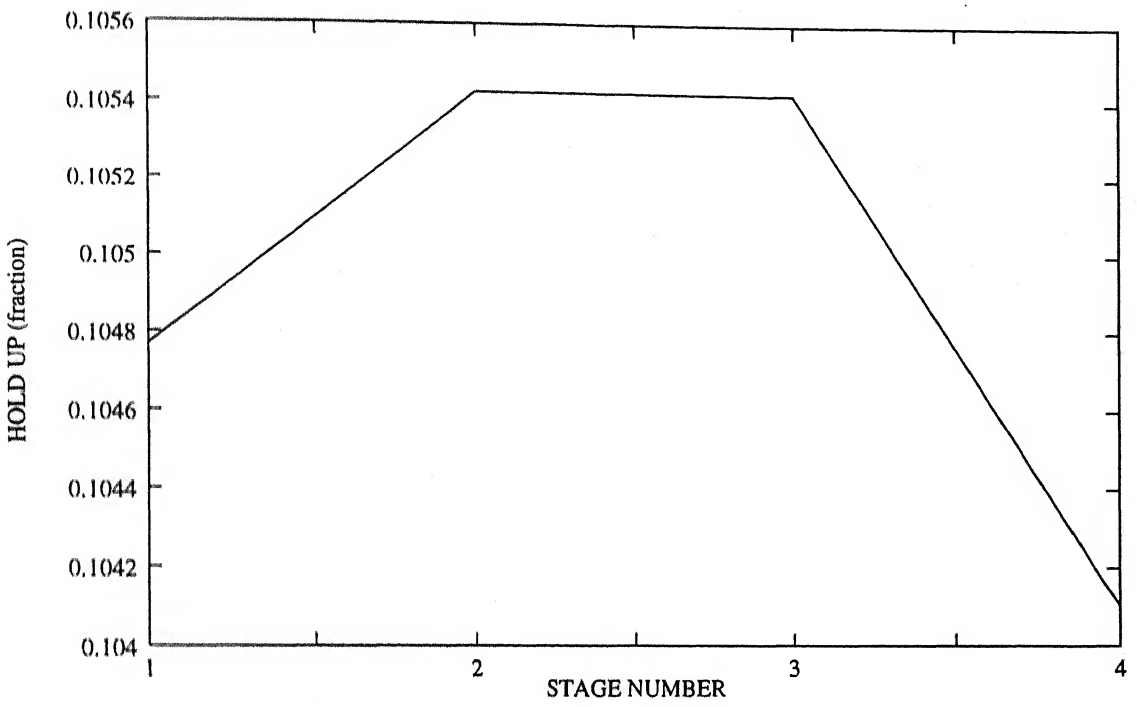

Figure D.3: Dynamic holdup profile (Run A)

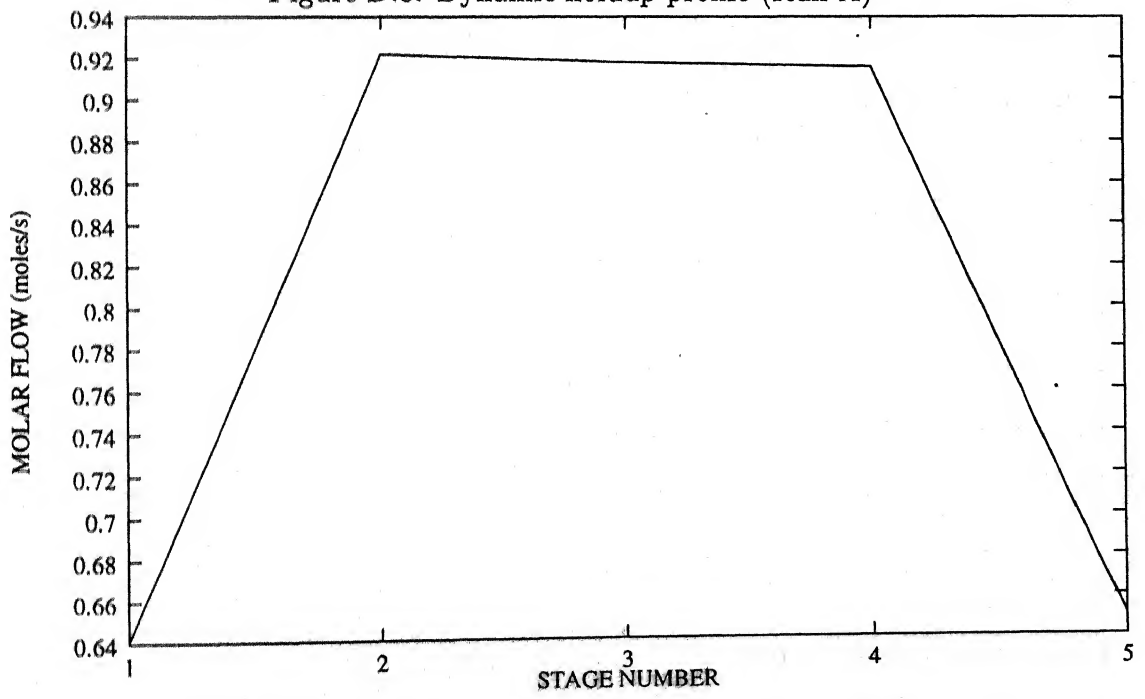

Figure D.4: Forward flow (continuous aqueous phase)(Run A)

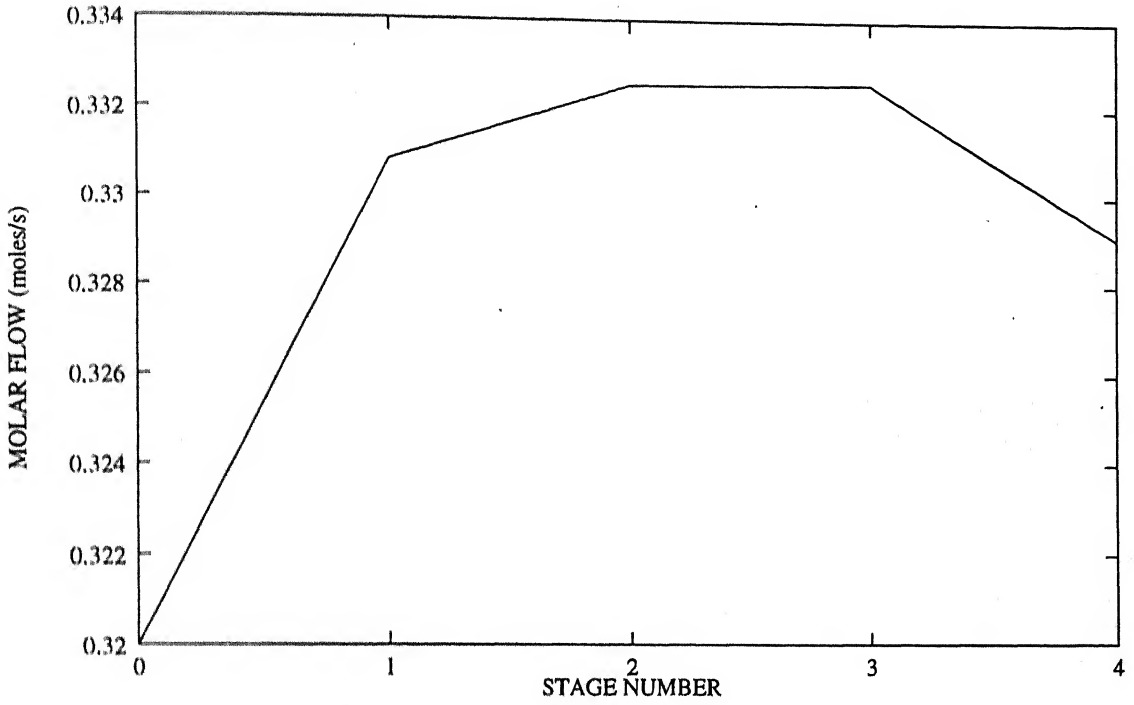

Figure D.5: Forward flow (dispersed toluene phase)(Run A)

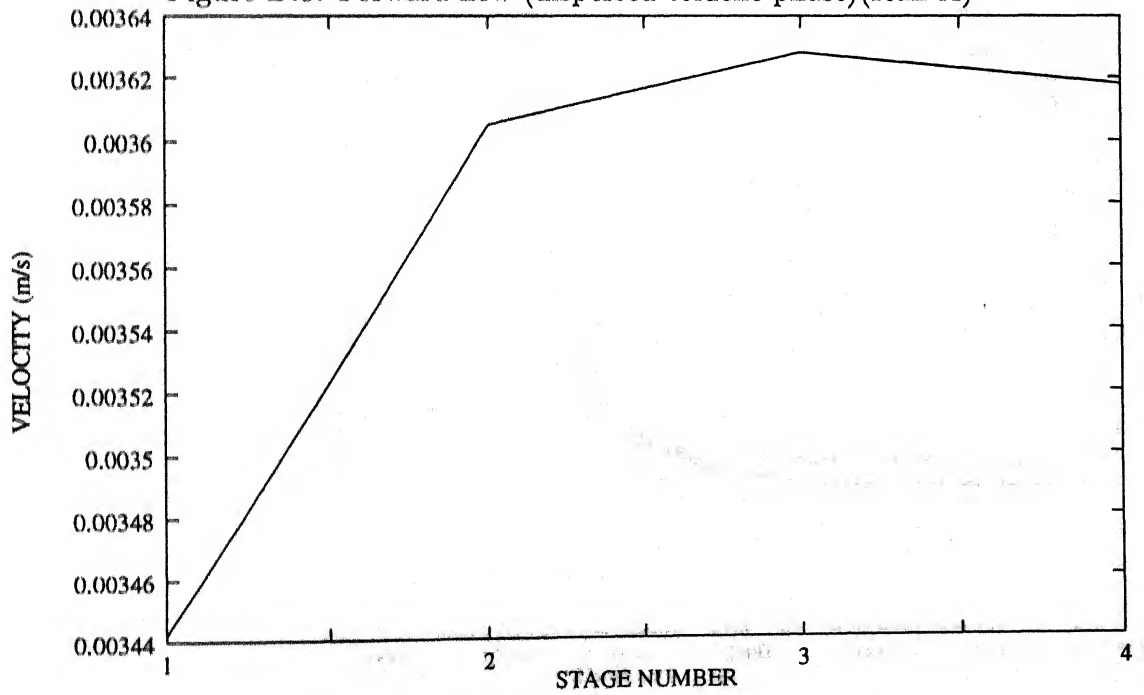

Figure D.6: Continuous phase velocity (Run A)

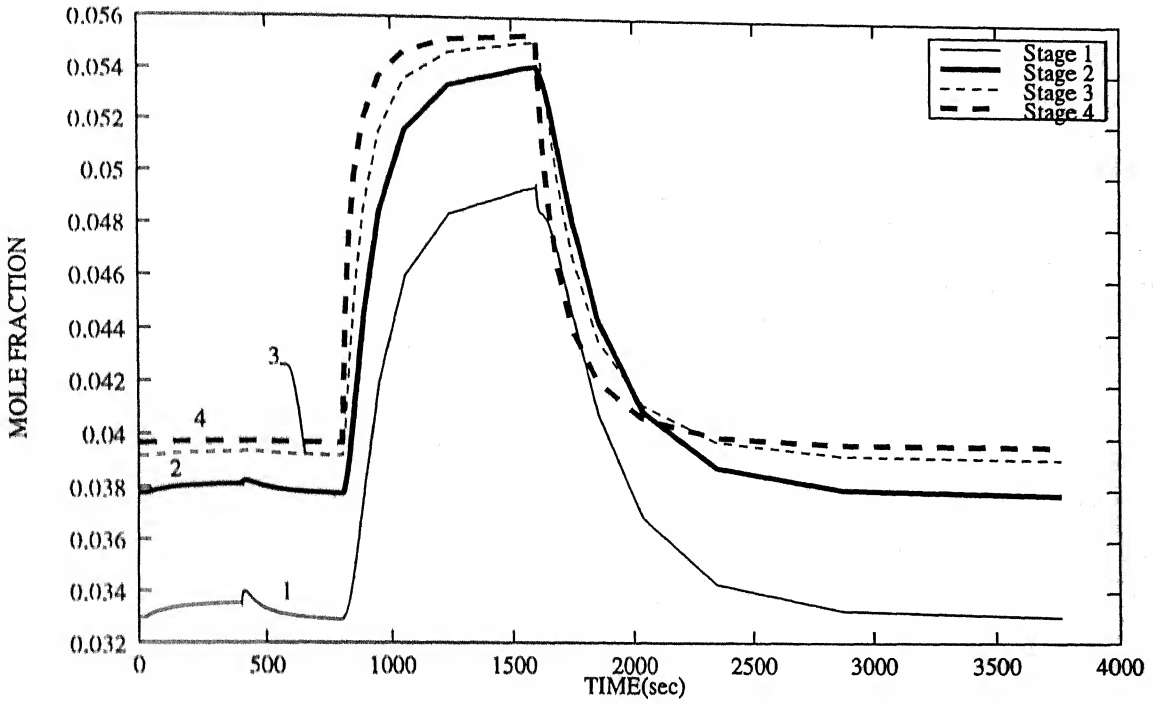

Figure D.7: Transient profile for Acetone concentration in dispersed (Toluene) phase (Run B)

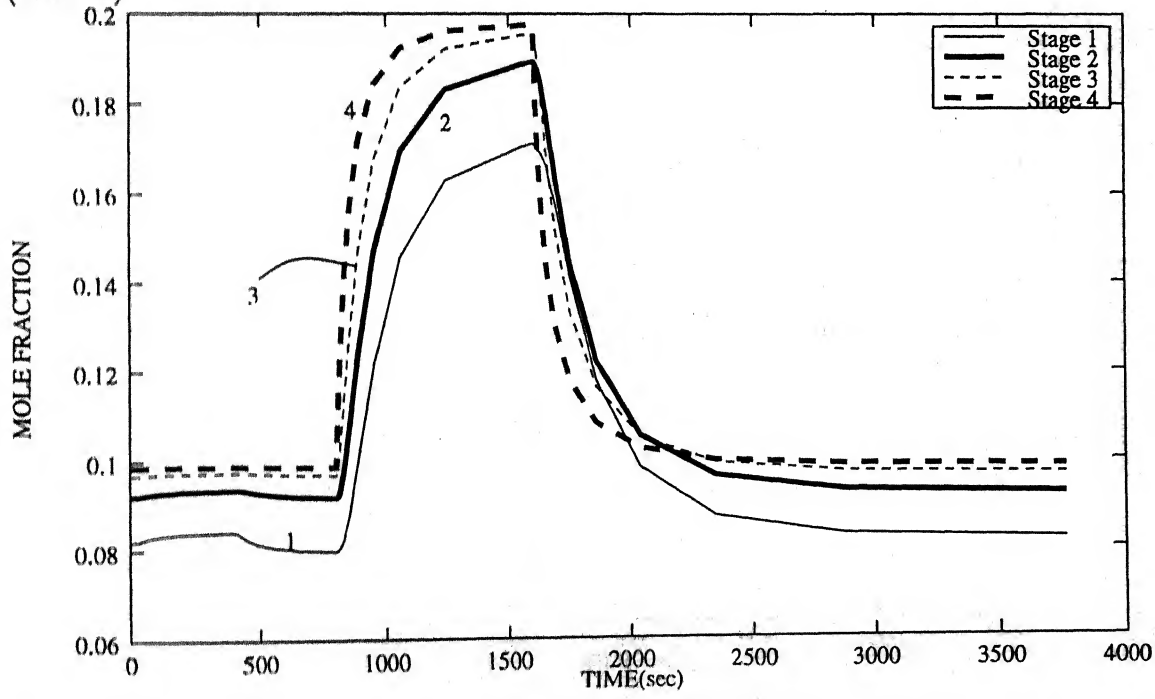

Figure D.8: Transient profile for Acetone concentration in continuous (Aqueous) phase (Run B)

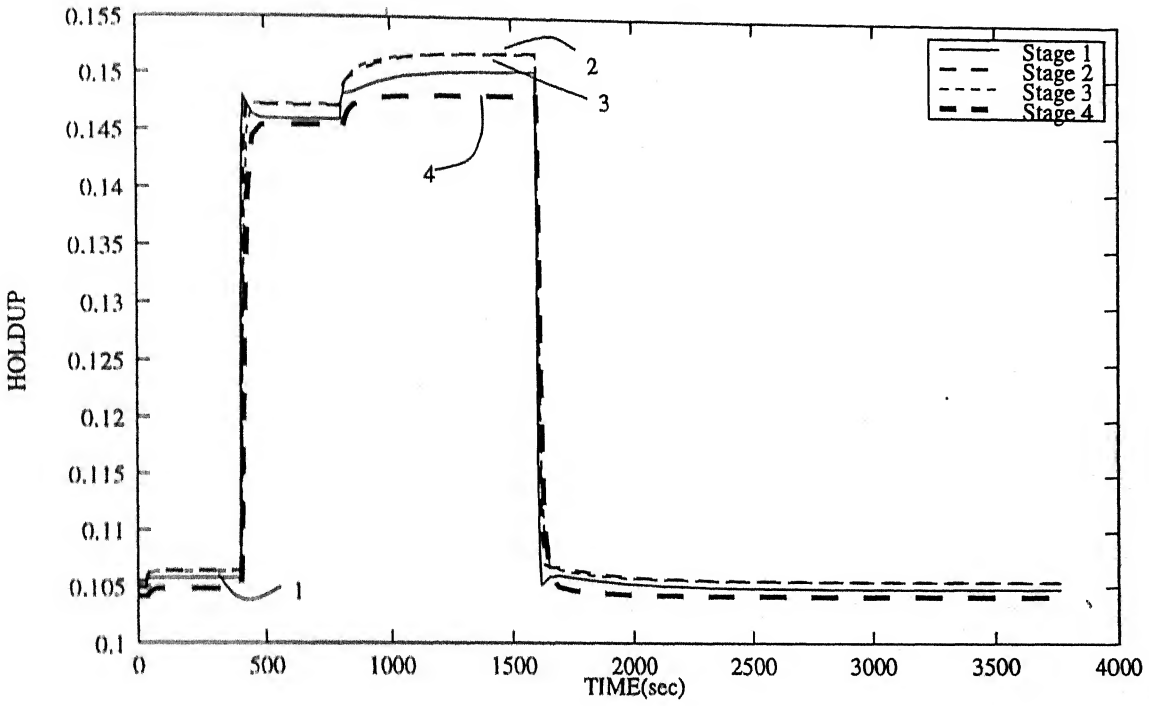

Figure D.9: Forward flow (Transient profile for dynamic holdup (Run B)

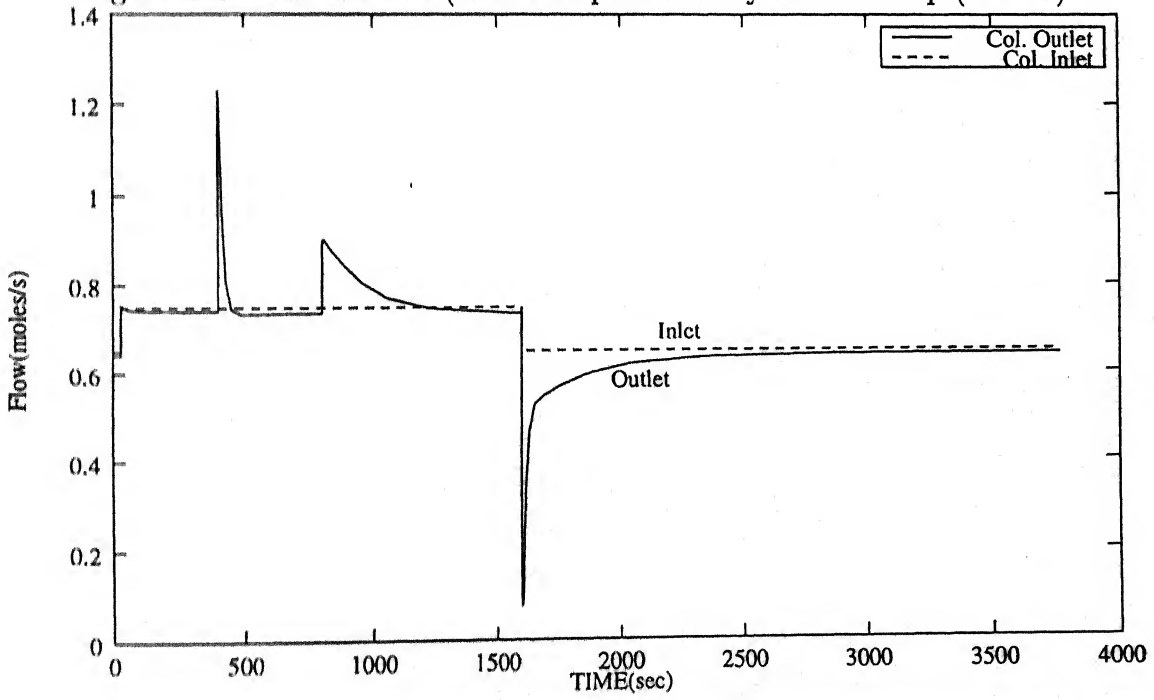

Figure D.10: Transient profile for forward flow of continuous (Aqueous) phase (Run B)

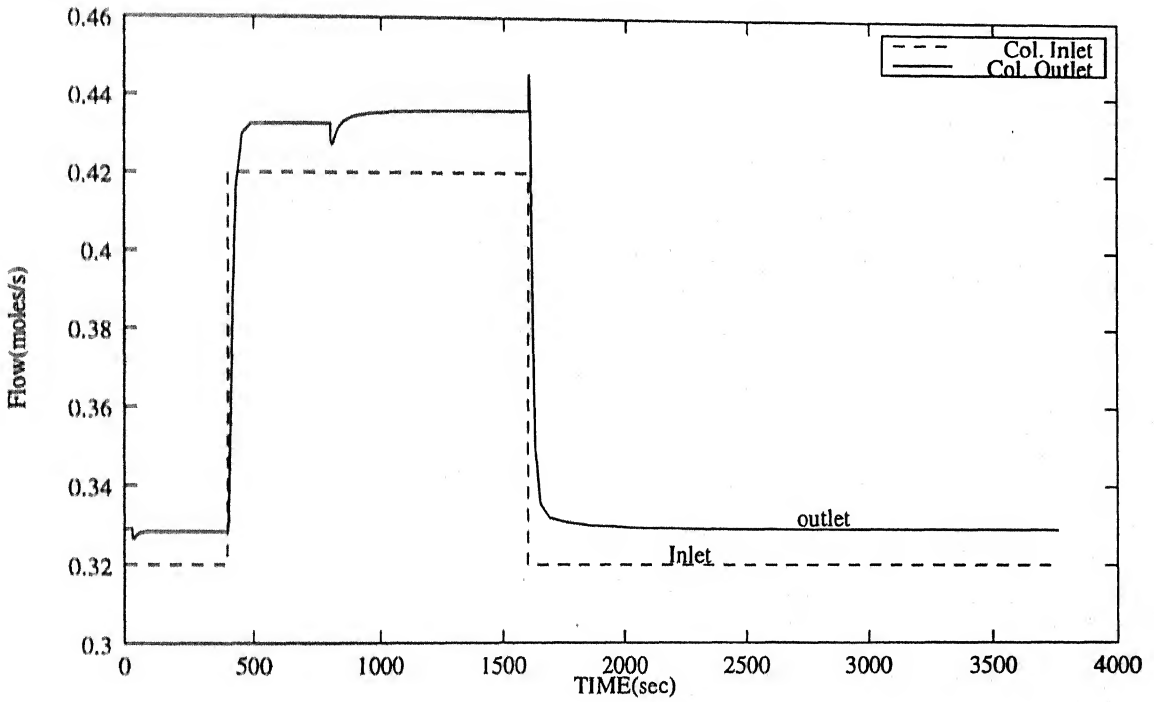

Figure D.11: Transient profile for forward flow of dispersed (Toluene) phase (Run B)

Appendix E

Elements of Jacobian

This section gives elements of Jacobian shown in Figure 3.1. The Jacobian is highly sparse in nature so only non-zero elements are written in this section. Arrangements of the elements for any matrix block (A,B or C) has been shown in Figure 3.2. Each element represents the partial derivative of model equation (shown as rows in Figure 3.2) with respect to independent variable (shown as column in Figure 3.2). Partial derivative which have not been given in this section are zero.

$$\frac{\partial MBD_{ijk}}{\partial V^{+}_{j'k'}} = -x_{ij'k'}; \quad for\ (j' = j, k' = k)$$

$$= x_{ij'k'}; \quad for\ (j = j', k' = k-1)$$

$$\frac{\partial MBD_{ijk}}{\partial V^{-}_{j'k'}} = -x_{ij'k'}; \quad for\ (j' = j, k' = k)$$

$$= x_{ij'k'}; \quad for\ (j' = j, k' = k+1)$$

$$\frac{\partial MBD_{ijk}}{\partial x_{i'j'k'}} = -(V^{+}_{j'k'} + V^{-}_{j'k'}) + \frac{\partial \Pi_{ijk}}{\partial x_{i'j'k'}}; \quad for\ (i' = i, j' = j, k' = k)$$

$$= \frac{\partial \Pi_{ijk}}{\partial x_{i'j'k'}}; \quad for\ (i' \neq i, k' = k)$$

$$= V^{+}_{j'k'}; \quad for\ (j' = j, k' = k-1)$$

$$= V^{-}_{j'k'}; \quad for\ (j' = j, k' = k+1)$$

$$\frac{\partial MBD_{ijk}}{\partial N_{i'j'k'}} = 1.0; \quad for\ (i' = i, j' = j, k' = k)$$

$$\frac{\partial MBD_{ijk}}{\partial P_{j'k'}} = \frac{\partial \Pi_{ijk}}{\partial P_{j'k'}}; \quad for\ (k' = k)$$

$$\frac{\partial MBC_{ijk}}{\partial U^{+}_{k'}} = -y_{i'k'}; \quad for\ (i'=i, k'=k)$$

$$= y_{j'k'}; \quad for\ (i'=i, k'=k-1)$$

$$\frac{\partial MBC_{ijk}}{\partial U^{-}_{k'}} = -y_{i'k'}; \quad for\ (i'=i, k'=k)$$

$$= y_{j'k'}; \quad for\ (i'=i, k'=k+1)$$

$$\frac{\partial MBC_{ijk}}{\partial y_{i'k'}} = -(U^{+}_{k'} + U^{-}_{k'}); \quad for\ (i'=i, k'=k)$$

$$= -U^{+}_{k'}; \quad for\ (i'=i, k'=k-1)$$

$$= -U^{-}_{k'}; \quad for\ (i'=i, k'=k+1)$$

$$\frac{\partial MBCijk}{\partial N_{i'j'k'}} = -1.0; \quad for\ (i'=i, k'=k)$$

$$\frac{\partial VP_{jk}}{\partial V^{+}_{j'k'}} = 1.0; \quad for\ (j'=j, k'=k)$$

$$\frac{\partial VP_{jk}}{\partial x_{i'j'k'}} = -\left(u^{D}_{j'k'} + \frac{\mathbf{D^D}_{k'}}{\Delta h_{k'}}\right) P_{j'k'} S \frac{\partial c^{D}_{jk}}{\partial x_{i'j'k'}}; \quad for\ (j'=j, k'=k)$$

$$\frac{\partial VP_{jk}}{\partial P_{j'k'}} = -\left[P_{j'k'} c^{D}_{j'k'} S \frac{\partial uD_{jk}}{\partial P_{j'k'}} + \left(u^{D}_{j'k'} + \frac{\mathbf{D^D}_{k'}}{\Delta h_{k'}}\right) c^{D}_{j'k'} S\right]; \quad for\ (j'=j, k'=k)$$

$$\frac{\partial VP_{jk}}{\partial u^{c}k'} = P_{j'k'} c^{D}_{j'k'} S; \quad for\ (k'=k)$$

$$\frac{\partial VM_{jk}}{\partial V^{-}_{j'k'}} = 1.0; \quad for\ (j'=j, k'=k)$$

$$\frac{\partial VM_{jk}}{\partial x_{i'j'k'}} = -\left(\frac{\mathbf{D^D}_{k-1}}{\Delta h_{k-1}}\right) P_{j'k'} S \frac{\partial c^{D}_{j'k'}}{\partial x_{i'j'k'}}; \quad for\ (j'=j, k'=k)$$

$$\frac{\partial VM_{jk}}{\partial P_{j'k'}} = -\left[\frac{\mathbf{D^D}_{k-1}}{\Delta h_{k-1}} c^{D}_{jk} S\right]; \quad for\ (k'=k)$$

$$\frac{\partial UP_k}{\partial U^+_{k'}} = 1.0; for\ (k' = k)$$

$$\frac{\partial UP_k}{\partial y_{j'k'}} = -\left(\frac{\mathbf{D^D}_k}{\Delta h_{k'}}\right)(1-\phi_{k'})S\frac{\partial c^C_k}{\partial y_{i'k'}};\quad for\ (k' = k)$$

$$\frac{\partial UP_K}{\partial P_{j'k'}} = \frac{\mathbf{D^C}_k}{\Delta h_{k'}}c^C_{k'}S;\qquad for\ (k' = k)$$

$$\frac{\partial UM_k}{\partial U^-_{k'}} = 1.0;\qquad for\ (k' = k)$$

$$\frac{\partial UM_k}{\partial y_{i'k'}} = -\left(u^C_k + \frac{\mathbf{D^C}_{k-1}}{\Delta h_{k-1}}\right)(1-\phi_k)S\frac{\partial c^C_k}{\partial y_{i'k'}};\quad for\ (k' = k)$$

$$\frac{\partial UM_k}{\partial P_{j'k'}} = \left(u^C_k + \frac{\mathbf{D^C}_{k-1}}{\Delta h_{k-1}}\right)c^C_k S;\qquad for\ (k' = k)$$

$$\frac{\partial UM_k}{\partial u^C k'} = -(1-\phi_k)c^C_k S;\qquad for\ (k' = k)$$

$$\frac{\partial MBIC_{ijk}}{\partial y_{i'j'k'}} = -\sum_{m=1}^{NC} N_{ijk} - a_{j'k'}K^C_{ii'jk};\qquad for\ (i' = i, j' = j, k' = k)$$

$$= -a_{j'k'}K^C_{ii'jk};\qquad for\ (i' \neq i, j' = j, k' = k)$$

$$\frac{\partial MBIC_{ijk}}{\partial y^I_{i'j'k'}} = a_{jk}K^C_{ii'jk};\qquad for\ (j' = j, k' = k)$$

$$\frac{\partial MBIC_{ijk}}{\partial N_{i'j'k'}} = (1-y_{ik});\ for\ (i' =, j' = j, k' = k)$$

$$= -y_{ik};\ for\ (i' \neq i, j' = j, k' = k)$$

$$\frac{\partial MBIC_{ijk}}{\partial P_{j'k'}} = -\frac{a_{jk}}{P_{jk}}\sum_{m=1}^{(NC-1)} K^C_{imjk}(y_{mj}k - y^I_{mjk});\quad for\ (i' = i, j' = j, k' = k)$$

$$\frac{\partial MBID_{ijk}}{\partial x_{i'j'k'}} = -\sum_{m=1}^{NC} N_{ijk} - a_{j'k'}K^D_{ii'jk};\qquad for\ (i' = i, j' = j, k' = k)$$

$$= -a_{j'k'}K^D_{ii'jk};\qquad for\ (i' \neq i, j' = j, k' = k)$$

$$\frac{\partial MBID_{ijk}}{\partial x^I_{i'j'k'}} = a_{jk}K^C_{ii'jk}; \quad for\ (j'=j, k'=k)$$

$$\frac{\partial MBID_{ijk}}{\partial N_{i'j'k'}} = (1-x_{ijk});\ for\ (i'=, j'=j, k'=k)$$
$$= -x_{ijk};\ for\ (i'\neq i, j'=j, k'=k)$$

$$\frac{\partial MBID_{ijk}}{\partial P_{j'k'}} = -\frac{a_{jk}}{P_{jk}}\sum_{m=1}^{(NC-1)} K^D_{imjk}(x^I_{mjk}-x_{mjk}); \quad for\ (i'=i, j'=j, k'=k)$$

$$\frac{\partial EQ_{ijk}}{\partial x^I_{i'j'k'}} = -K_{ijk} - x^I_{ijk}\frac{\partial K_{ijk}}{\partial x^I_{i'j'k'}} \quad for\ (i'=i, j'=j, k'=k)$$
$$= x^I_{ijk}\frac{\partial K_{ijk}}{\partial x^I_{i'j'k'}} \quad for\ (i'\neq i, j'=j, k'=k)$$

$$\frac{\partial EQ_{ijk}}{\partial y^I_{i'j'k'}} = 1 - x^I_{ijk}\frac{\partial K_{ijk}}{\partial y^I_{i'j'k'}} \quad for\ (i'=i, j'=j, k'=k)$$
$$= -x^I_{ijk}\frac{\partial K_{ijk}}{\partial y^I_{i'j'k'}} \quad for\ (i'\neq i, j'=j, k'=k)$$

$$\frac{\partial NDI_{jk}}{\partial x^I_{i'j'k'}} = 1.0; \quad for\ (j'=j, k'=k)$$

$$\frac{\partial NCI_{jk}}{\partial y^I_{i'j'k'}} = 1.0; \quad for\ (j'=j, k'=k)$$

$$\frac{\partial ND_{jk}}{\partial x_{i'j'k'}} = 1.0; \quad for\ (j'=j, k'=k)$$

$$\frac{\partial NC_k}{\partial y_{i'k'}} = 1.0; \quad for\ (k'=k)$$